Electrolysers, Fuel Cells and Batteries : Analytical modelling

J.W. Haverkort

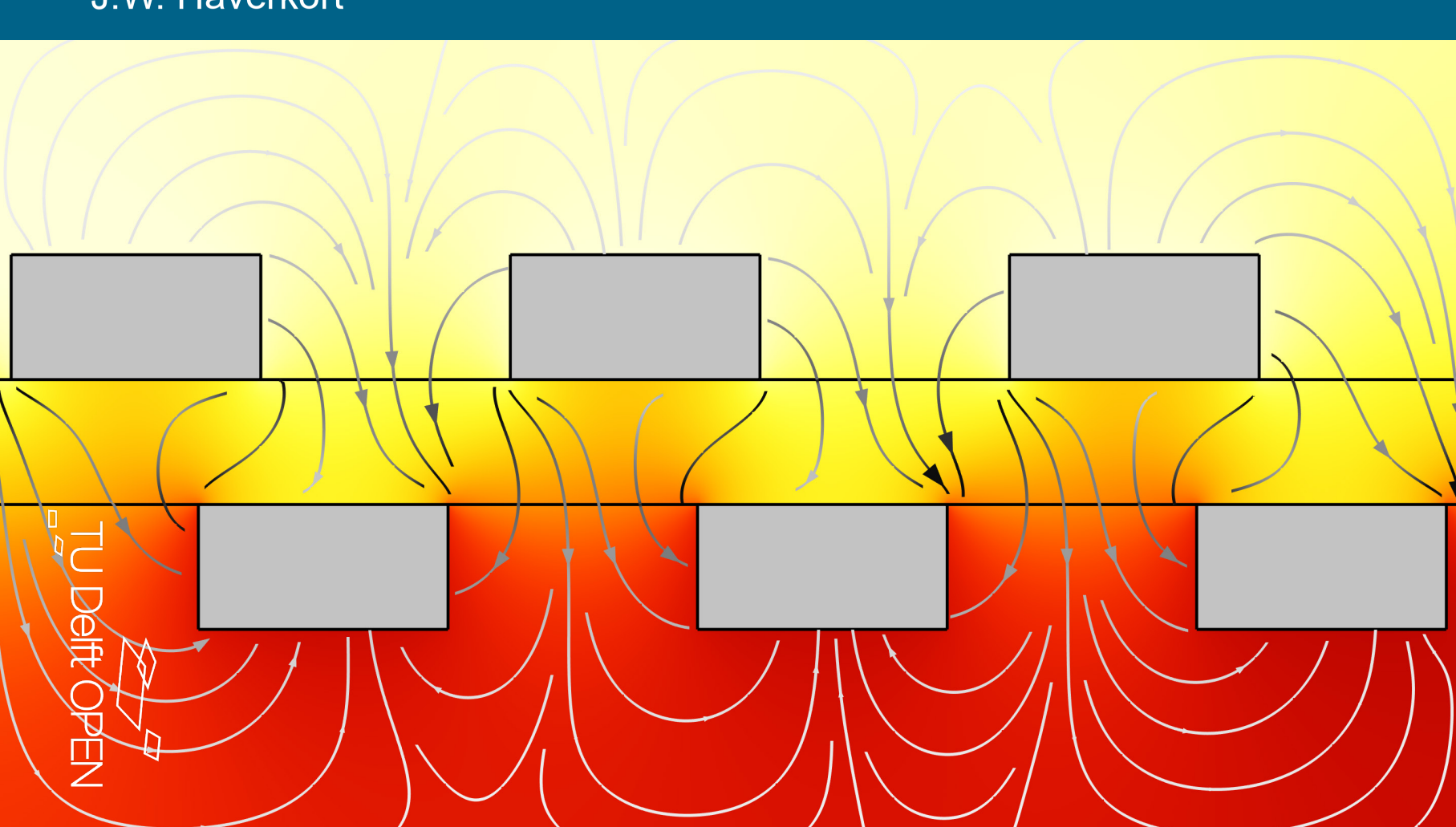

TU Delft OPEN

Electrolysers, Fuel Cells and Batteries

analytical modelling

J.W. Haverkort

Title Open Textbook: Electrolysers, Fuel Cells and Batteries: analytical modelling
Author: J.W. Haverkort
Publisher: TU Delft OPEN Publishing
Year of publication: 2024
This edition: 2025, v1.2 (minor corrections compared to original edition)
ISBN (softback/paperback): 978-94-6366-853-8
ISBN (E-book): 978-94-6366-855-2
DOI: https://doi.org/10.59490/tb.93
Attribution cover image: made using COMSOL Multiphysics® by W.L. v.d. Does

Preface

Prerequisites

This book was written to accompany the lectures of the M.Sc. course ME45203: Electrolysers, Fuel Cells and Batteries at Delft University of Technology. Its main aim is to create an understanding of the mathematical description of the relationship between current and voltage in electrochemical devices. A solid background in physical transport phenomena is assumed, while some training in electrochemistry, batteries or fuel cells is highly beneficial. Reading and re-reading the first chapter before continuing with the other chapters may be advisable when this is lacking.

Reader guidelines

Important equations will be boxed

$$\boxed{j_\perp = j_* \left(\mathrm{e}^{\eta/b_\mathrm{a}} - \mathrm{e}^{-\eta/b_\mathrm{c}} \right).} \tag{1}$$

We will indicate logical steps that are important but perhaps not immediately obvious, and may require one or a few lines of derivation, with the blue "exercise figure": . The student is encouraged to work out these steps independently. Footnotes, appendices, and sections denoted with * are optional additional reading material and are not part of the curriculum of ME45203.

Content

The first three chapters of the book explore the fundamental concepts related to electrochemistry, transport, and porous electrodes, respectively. The final four chapters are named after particular applications: batteries, fuel cells, electrolysers, and redox flow batteries, respectively. However, from the perspective of analytical modelling, there are more similarities than differences between these devices, so these chapters focus on those aspects that are distinctively associated with these applications. For batteries, treated in chapter 4, a distinctive feature is that their porous electrodes are involved in the reaction as products or reactants. Chapter 5 on fuel cells focuses on the management of water produced in the reaction. This includes how to model the

multiphase flow in diffusion layers or gas diffusion electrodes and inside a flooded catalyst layer. While these aspects are perhaps most often associated with fuel cells, they can be equally important for proton exchange membrane electrolysers or CO_2 electrolysers, for example. In chapter 6 on electrolysers we examine the effects of gas bubbles. Contrary to the previous chapters, the direction normal to the current is modelled here. Finally, in chapter 7 on redox flow batteries, both directions parallel and normal to the current are considered in a quasi-two-dimensional model that considers the flow of reactants through a flow field.

Acknowledgements

This textbook reports on knowledge developed over decades and centuries. Because it would be impossible to exhaustively credit all authors of works that have been relevant in creating this book, only a very limited number of references are included. I would like to thank the many people who contributed to this work by providing their lecture notes, proofreading, and correcting many of the mistakes and things that were unclear. In particular, I want to mention the keen observations of Hadi Rajeai, Aviral Rajora, Sohan Phadke, Joe Blake, Wouter van der Does, Nico Valle Marchante, Jelmer Postma, Nikhilesh Kodur Venkatesh, Remco Hartkamp, Emile Craye, and last but not least Gilles Deiters. I am also grateful for the professional support received from Saskia Roselaar in editing, great help from Isis Verhaag with the figures, and Jacqueline Michielen-van de Riet for help in the publishing process. I would be most grateful if readers could let me know of mistakes or suggestions by sending an e-mail to J.W.Haverkort@tudelft.nl.

Delft, April 2024 J.W. (Willem) Haverkort

Contents

Nomenclature

Dimensionless variables

$\bar{c}$	Concentration c/c_0
$\mathcal{B}$	Bruggeman's coefficient in $\tau^2 \approx \epsilon^{-\mathcal{B}}$
$\mathcal{E}$	Electrode effectiveness factor
$\bar{\phi}$	Electrolyte potential $F\phi/\mathcal{R}T$
r	Reaction order
s	Liquid water saturation
S	Transfer coefficient, inverse mass transfer resistance
$\mathrm{S_{oC}}$	State of charge
t_i	transference/transport number of ion i
X	Conversion $(c_{\mathrm{in}} - c_{\mathrm{out}})/c_{\mathrm{in}}$
z	Ion charge number

Constants

e	Elementary charge $1.602176634 \cdot 10^{-19}$	[C]
F	Faraday constant 96485.3329	[C/mol]
k_{B}	Boltzmann constant $1.38064852 \cdot 10^{-21}$	[J/K]
N_{A}	Avagadro constant $6.02214076 \cdot 10^{23}$	[-]
$\mathcal{R}$	Gas constant 8.31446	$[\mathrm{J/mol_g/K}]$

Dimensionless numbers

Gz	Graetz number $\langle w \rangle l^2/hD$
M	Thiele modulus $1/\mathcal{E} \rightarrow 0$
Pe	Péclet number $\langle w \rangle l/D$
Re	Reynolds number wl/ν

Sh	Sherwood number $Nl/D\Delta c$	

Greek variables

α	Charge transfer coefficient	[-]
δ	Boundary layer thickness	[m]
ϵ	Porosity	[-]
η	Activation overpotential $\Phi - \phi - \left(\Phi - \phi\right)_{\mathrm{eq}}$	[V]
γ	Surface tension	[N/m]
κ	Effective electrolyte conductivity	[S/m]
λ	Pore size distribution parameter	[-]
μ	Dynamic viscosity	[Pa s]
ν	Kinematic viscosity	[m^2/s]
Φ	Electrostatic potential in electrode	[V]
ϕ	Electrostatic potential in electrolyte	[V]
ρ	Density	[kg/m^3]
ρ_q	Charge density	[C/m^3]
σ	Effective electrode conductivity	[S/m]
τ	Tortuosity	[-]
ε	Gas fraction	[$\mathrm{m}_{\mathrm{g}}^3/\mathrm{m}^3$]
φ_{e}	Voltage efficiency	[-]

Lower case roman

a	Volumetric surface area	[$\mathrm{m}_{\mathrm{s}}^2/\mathrm{m}^3$]
b	Tafel slope $RT/\alpha F$	[V]
c	Concentration	[$\mathrm{mol\ m}^{-3}$]
c_{m}	Cup mixing concentration $\frac{1}{\langle w \rangle l}\int_0^l wcdx$	[$\mathrm{mol\ m}^{-3}$]
h	Flow channel height	[m]
j	Magnitude of total current density	[A/m^2]
j_*	Superficial exchange current density	[$\mathrm{A}/\mathrm{m}_{\mathrm{s}}^2$]
k	Areal reaction rate constant	[$\mathrm{mol}^{1-r}\ \mathrm{s}^{-1}\ \mathrm{m}^{3r-2}$]
n	Electrons per reactant/product molecule	[$\mathrm{mol}_{\mathrm{e}^-}/\mathrm{mol}$]
p	Pressure	[Pa]
q	Electric charge	[C]
r	Pore radius [m]	

t	Time	[s]
x	Coordinate in the direction of the main current	[m]
y	Coordinate normal to x and z	[m]
z	Coordinate parallel to flow, normal to main current	[m]
$\varkappa$	Charge number q/e	[-]

Mathematical operators

$\cosh x$	Hyperbolic cosine $\frac{1}{2}(\mathrm{e}^{x} + \mathrm{e}^{-x})$
$\ln x$	Natural logarithm $\mathrm{e}^{\ln x} = x$
$\sinh x$	Hyperbolic sine $\frac{1}{2}(\mathrm{e}^{x} - \mathrm{e}^{-x})$
$\tanh x$	Hyperbolic tangent $\sinh x / \cosh x$

Notation

$'$	A spatial derivative d/dx ($d/d\bar{x}$ dimensionless)
$\bar{}$	Overbars denote dimensionless quantities
Δ	Difference right minus left, or after minus before
$\hat{\boldsymbol{n}}$	Unit vector, normal to a surface into the fluid
$\langle . \rangle$	Spatial average, $\frac{1}{x}\int_0^x .dx$ or $\frac{1}{z}\int_0^z .dz$ in one dimension
D/Dt	Material derivative $\frac{\partial}{\partial t} + \boldsymbol{u} \cdot \nabla$
opt	Optimised for energy efficiency

Subscripts

$\perp$	Normal to a surface, into the fluid
$\parallel$	Parallel to particle/parcel trajectory
i	Species index
x, y, z	Vector component in the x- y- or z-direction
+	Positively charged ions, cations
-	Negatively charged ions, anions
0,L	At $x = 0$ or $x = L$
a	Anode
c	Cathode
cap	Capillary
d	Discharge/discharged
diff	Diffusion (superscript)
eq	Equilibrium

fl	Fluid
g	Gas
in,out	At the inlet $z = 0$ or outlet $z = h$, respectively
l	Liquid
lim	Limiting
lin	Linear
m	Molecular / material
mig	Migration (superscript)
O	Oxidation
opt	Optimal with respect to energy efficiency
R	Reduction
ref	Reference
s	Solid/Surface
tn	Thermoneutral
tot	Total

Upper case roman

A	Projected electrode area	$[\mathrm{m}^2]$
AR	Areal resistance	$[\Omega\mathrm{m}^2]$
C_p	Heat capacity, at constant pressure	$[\mathrm{J\ kg^{-1}\ K^{-1}}]$
D	Effective diffusion coefficient	$[\mathrm{m^2\ s^{-1}}]$
E	Electrode potential	[V]
$\mathcal{E}_\mathrm{a}$	Activation energy	[J]
G	Gibbs free energy	[J/mol]
I	Current	[A]
J_*	Total superficial exchange current density aLj_*	$[\mathrm{A/m^2}]$
J_κ	Characteristic current density $b\kappa/L$	$[\mathrm{A/m^2}]$
l	Flow channel thickness	[m]
L	Electrode thickness	[m]
$\mathcal{M}$	Mobility, u/F in equilibrium	[s/kg]
M	Molar mass	$[\mathrm{kg\ mol^{-1}}]$
N	Molar flux	$[\mathrm{mol\ m^{-2}\ s^{-1}}]$
R	Radius of a particle or bubble	[m]
S	Source term	$[\mathrm{something/m^3/s}]$

T	Temperature	[K]
$\mathcal{U}$	Potential energy	[J]
V	Voltage	[V]
$\mathcal{V}$	Volume	[m^3]
$\mathcal{V}_m$	Molar volume M/ρ	[m^3/mol]

Vectors

$\boldsymbol{A}$	Area, normal to surface	[m^2]
$\boldsymbol{E}$	Electric field	[V/m]
$\boldsymbol{F}$	Force	[N]
$\boldsymbol{I}$	Current	[A]
$\boldsymbol{i}$	Electronic current density	[A m^{-2}]
$\boldsymbol{j}$	Ionic current density	[A m^{-2}]
$\boldsymbol{N}$	Molar flux	[mol m^{-2} s^{-1}]
$\boldsymbol{U}$	Superficial velocity with components U, V, W	[m/s]
$\boldsymbol{u}$	Interstitial velocity with components u, v, w	[m/s]

Other conventions

1. The cathode is the electrode at which the reduction occurs, and oxidation occurs at the anode.
2. Cell potentials are that of the cathode minus that of the anode $E_{cell} = E_c - E_a$, so positive for Galvanic cells and negative for electrolytic cells.
3. We will draw the cathode on the right and the anode on the left.
4. Surface local fluxes $N_\perp$ and $j_\perp$ are always directed from the solid surface into the electrolyte, so $j_\perp$ is positive on the anode and negative on the cathode.
5. Since anodic currents are positive, the overpotential will also be positive on the anode, and negative on the cathode.
6. Tafel slopes b will be used on an e-folding basis, rather than per decade.
7. The number of electrons $n > 0$ transferred in the reaction O + $n e^- \rightarrow$R; per number of reactant or product molecules as indicated.

Chapter 1

Electrochemistry

This introductory chapter constitutes a refresher of the basic electrochemical terminology and notation necessary for the subsequent chapters. In this chapter, the basic foundations are laid in terms of electrostatics, equilibrium thermodynamics, and electrochemical kinetics culminating in a simplified cell model.

1.1 Electrostatics

An electric charge q [C] in an electric field $\boldsymbol{E}$ [V/m] experiences an electrostatic force

$$\boldsymbol{F} = q\boldsymbol{E}. \tag{1.1}$$

Since this is a conservative force, the electric field can be expressed in terms of an electrostatic potential ϕ as

$$\boldsymbol{E} = -\nabla\phi. \tag{1.2}$$

Combining these two equations, we get $\boldsymbol{F} = -q\nabla\phi$, where we see that a positive charge moves down along a potential gradient while a negative charge moves up in potential. The electric potential energy of a charge is the negative of the work done by an electric field in moving the charge within such a field

$$\mathcal{U} = -\int \boldsymbol{F} \cdot d\boldsymbol{x} = q\Delta\phi, \tag{1.3}$$

where $\Delta\phi$ is ϕ at the end minus the start of the path that the charged particle traverses. Positively charged particles thus increase their potential energy when the potential increases, while negatively charged particles increase their potential energy when the potential decreases. Note that in all these equations only *differences* in potential, termed *voltages*, are physically relevant.

1.2 Current and resistance

When thinking of conduction and current we usually think about the movement of electrons. While this is most relevant inside metals, electrochemistry is also concerned with the flow of charged molecules, or ions. Media that conduct ions are called electrolytes. In general, we can define current as the flow of *charge*, regardless of whether the *charge carriers* are electrons, ions, or other charged particles. The movement of ion charge in the form of a current I [C/s=A] through an area A constitutes a current density i [A/m^2]

$$i = \frac{I}{A}. \tag{1.4}$$

Since the flow of ions is not constrained to any preferential direction, in general, the ionic current density $\boldsymbol{i}$ is a vector field that can have a different direction and magnitude at each location.

Often, there is an approximate proportionality between the current density $\boldsymbol{i}$ and the electric field, expressed through[1]

$$\boxed{\boldsymbol{i} = \kappa \boldsymbol{E}.} \tag{1.5}$$

In the next chapter, we will get into why this is often the case and also when it does not hold. The constant of proportionality is the *conductivity* κ [S/m = Ω^{-1}m^{-1}], which is the inverse of the *resistivity*. These material properties depend strongly on the charge carrier and physical parameters, such as temperature, and can differ widely between materials. Metals, for example, typically conduct electrons very well. Aqueous salt solutions, on the other hand, are typically insulating for electrons but conduct ions well. We will refer to such ionic conductivity with the symbol κ, while reserving the symbol σ for the conductivity of a material towards electrons. When speaking of conductivity, it is therefore important to specify with respect to what particle. We will also use a different symbol $\boldsymbol{j}$ for the electronic current density so that Ohm's law for electrons reads $\boldsymbol{j} = \sigma \boldsymbol{E}$. Since the ionic current is converted to electronic at the electrode, charge conservation gives $j = I/A$ as well. We will typically use the symbol j for the current density unless explicitly referring to the current density magnitude inside the electrolyte.

Referring to Figure 1.1, we consider the case in which there is a difference in potential $\Delta\phi \equiv \phi(L) - \phi(0) < 0$ between the back and front of a block of material of thickness L. The average electric field strength in the x-direction is obtained by integrating Eq. (1.2) to give $E_x = -\Delta\phi/L$, which after inserting in Eq. (1.5) gives the positive current density in the x-direction,

$$i_x = -\frac{\kappa \Delta\phi}{L} \tag{1.6}$$

[1] This is the continuum formulation of Ohm's law.

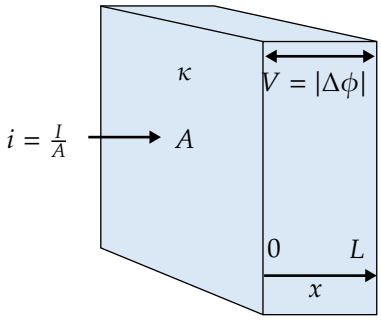

Figure 1.1: *A schematic to illustrate Ohm's law $V = IR$ and Pouillet's law $R = L/\kappa A$ in a planar domain with ion conductivity κ.*

Multiplying with the area A and taking the absolute value with $I = |i_x|A$ and $V = |\Delta\phi|$ we obtain

$$I = \frac{V}{R}, \quad \text{where } R = \frac{L}{A\kappa}. \tag{1.7}$$

The first of these equations is **Ohm's law**, while the second is referred to as **Pouillet's law**. The latter relates resistance to geometry and the material property κ in a logical way. The larger the distance ions have to travel or the lower the electrolyte conductivity, the larger the resistance. The area appears only because we introduced the current. Dividing Eq. (1.7) by the area A, we obtain an expression for the current density magnitude:

$$i = \frac{V}{AR}, \quad \text{where } AR = \frac{L}{\kappa} \tag{1.8}$$

Here the *area-specific resistance* (ASR) AR [Ωm^2] may be viewed as a separate new symbol or as the product of area and resistance.

Since the rate at which a desirable product is made in an electrochemical device scales with the current I, and the cost of electrodes, membranes, etcetera scale with area A the ratio $j = I/A$, the current density, is a good performance metric. Electrochemical processes are usually only commercially attractive above a certain current density. A high current density allows for a large amount of product to be made per unit area of the cell components used.

On the other hand, the potential drop V has to be maintained by a power source, for which the power consumption is given by $P = IV$ [W].

Often, a balance has to be found between maximising the current density i and minimising the required potential drop V. From Eq. (1.8), minimising the area-specific resistance is therefore crucial. This means that the distance L that the charge has to travel has to be as small as possible, through a medium with conductivity as large as possible. Therefore, electrodes have to be positioned as close together as

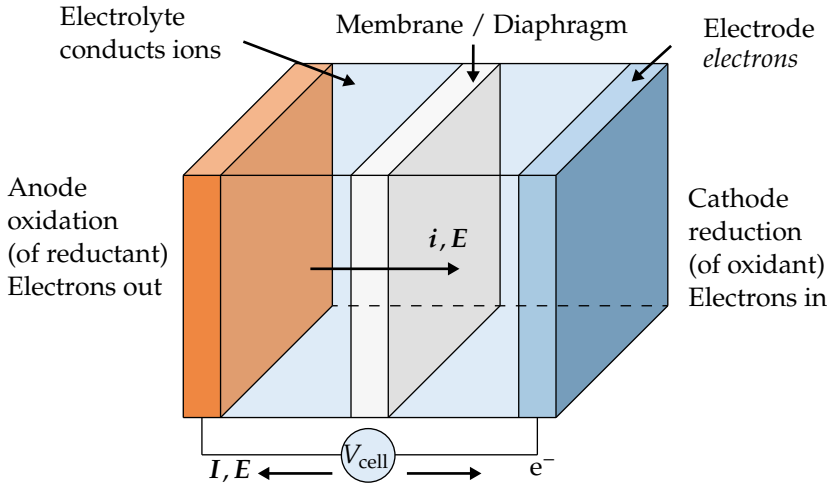

Figure 1.2: *A schematic of a general electrochemical cell. Often, but not always, the anode is depicted on the left and the cathode on the right. Electrons move through a metal from the anode, where the oxidation reaction takes place, to the cathode, where reduction occurs.*

possible. For this reason, electrodes are often directly placed next to a gas-separating membrane, in a *zero-gap* configuration or *membrane-electrode assembly* (MEA).

1.3 An electrochemical cell

A typical electrochemical cell, schematically shown in Figure 1.2, consists of at least the following functional parts:

1. An electric connection ($\kappa = 0$, $\sigma \neq 0$) between the electrodes via a power source or load
2. An *electrolyte*, conducting ions but not electrons ($\kappa \neq 0$, $\sigma = 0$)
3. Two *electrodes*, an anode and a cathode. The function of the electrodes is two-fold: they should conduct electrons *and* be catalytically active for the desired reaction.[2] Only in the case of batteries does the electrode material itself actually participate in the reaction. In this case, the reaction stalls when the electrodes are used up.

1.3.1 Redox reactions

The reactions taking place at electrodes are *redox* (reduction-oxidation) reactions in which electrons are transferred

[2]Sometimes, these functions of an electrode are split, in which case there is a catalyst support and a catalyst layer, for example, in the form of spray-coated catalyst nanoparticles.

1. **Reduction** takes place at the **cathode**[3], where an electron (e^-) is transferred *to an **oxidant*** (O)

2. **Oxidation** takes place at the **anode**, where an electron is transferred *from a **reductant*** (R)[4]

Such a reaction can be schematically depicted as

$$O + ne^- \leftrightarrow R. \tag{1.9}$$

We will consider the stoichiometric coefficient n to be a positive integer and will use it somewhat flexibly to denote the total number of electrons transferred in a redox reaction, or, depending on the context, the number of electrons per reactant or product molecule, respectively.

The reactants may be solids, as in the case of *batteries*. Alternatively, reactants may be dissolved in a liquid electrolyte, or the liquid itself may be the reactant, for example, in a *water electrolyser* or in various redox flow batteries. Finally, gases may also be brought in contact with the electrodes as in the case of *fuel cells*.

Figure 1.2 shows the anode on the left and the cathode on the right, a convention we will adhere to in this book but is not always followed in the literature. Electrons generated in an oxidation reaction at the anode move through the external circuit to the cathode where the reduction reaction takes place. To avoid negative charge accumulation at the cathode, negative ions (*anions*) move back through the electrolyte to the anode. Alternatively, positive ions (*cations*) move from anode to cathode. Either way, an electric field is set up and directed from the anode to the cathode to transport this charge.

1.3.2 Thermodynamics

Electrochemists often use the symbol E to denote the potential of an electrode.[5] We hope that this will cause no confusion with the magnitude of the electric field.

Neglecting ohmic losses in the external circuitry and the electrodes for now, the *cell voltage* V_{cell} reads

$$V_{\text{cell}} = E_{\text{c}} - E_{\text{a}}, \tag{1.10}$$

[3]To avoid renaming an electrode depending on whether a battery is charging or discharging, for a battery this naming convention only holds during discharging. During charging the oxidation reaction takes place at the cathode.

[4]Other terms for an oxidant are oxidiser/oxidising agent/electron acceptor. Other terms for a reductant are reducer/reducing agent/electron donor. Reduction refers to a reduction in charge, so the addition of electrons. Some chemists may insist it is rather the oxidation state or oxidation number that is reduced. This hypothetical charge is usually +1 for hydrogen and -2 for oxygen. The sum of oxidation states of a molecule equals its charge, in units of electron charge, which is called the charge number or valence.

[5]This notation derives from the electromotive force (EMF), a term used to describe the transformation from a different type of energy (like chemical bonding energy) to electrical energy. Electrode potentials are actually voltages since they are measured relative to some reference electrode; see the optional section 1.3.4 for more information. Sometimes the terminology cell potential is used, for which we will consistently use cell voltage.

where the subscripts a stand for anode and c for cathode, respectively. If we switch off the current, the oxidation and reduction reactions proceed at an equal rate at the equilibrium cell voltage $V_{\mathrm{eq}} = V_{\mathrm{c,eq}} - V_{\mathrm{a,eq}}$.[6] From equilibrium thermodynamics, it follows that the amount of useful work that can be done at constant temperature and pressure is given by (minus) the Gibbs free energy [J] of the reaction. Per mole of product [$\mathrm{mol_p}$] we will denote this as $-\Delta G$ [$\mathrm{J/mol_p}$]. Upon slightly opening the circuit, an infinitesimal amount of current will run that does electrical work, given by Eq. (1.3) as qV_{eq} [J].

For one mole of product, we convert a charge $q = nF$, with n [$\mathrm{mol_{e^-}/mol_p}$] here representing the number of moles of electrons per mole of product. Here, $F \approx 96485\ \mathrm{C/mol_{e^-}}$ is Faraday's constant, which gives the charge of a mole of electrons.[7] Combining this gives

$$\Delta G = -nFV_{\mathrm{eq}}. \tag{1.11}$$

1. Spontaneous reactions have $\Delta G < 0$, so such *galvanic* or *voltaic* cells have $V_{\mathrm{eq}} > 0$.[8]

2. Non-spontaneous reactions have $\Delta G > 0$, so such *electrolytic* cells have $V_{\mathrm{eq}} < 0$.

Besides useful work, at a finite current, there are also various types of losses. For example, the collisions of electrons and ions result in resistive heating. In defining energy efficiency, we will compare the total energy consumption by the cell to the amount of useful work.

For a galvanic cell the useful work that can be done per mole of product is $-\Delta G = nFV_{\mathrm{eq}}$, while dissipation lowers the cell voltage to $0 < V_{\mathrm{cell}} < V_{\mathrm{eq}}$, leaving nFV_{cell} for useful work. Hence we define the energy efficiency or voltage efficiency as

$$\varphi_{\mathrm{e}} = \frac{V_{\mathrm{cell}}}{V_{\mathrm{eq}}}. \tag{1.12}$$

For an electrolytic cell, dissipation makes that a more negative cell voltage $V_{\mathrm{cell}} < V_{\mathrm{eq}} < 0$ is needed to drive a current. Hence, the voltage efficiency, in this case, reads

$$\varphi_{\mathrm{e}} = \frac{V_{\mathrm{eq}}}{V_{\mathrm{cell}}}. \tag{1.13}$$

[6] This open-circuit voltage (OCV) may be different when side-reactions like corrosion determine the cell voltage. Here we consider that an equilibrium of the desired reactions prevails.

[7] With $e = 1.602(..) \cdot 10^{-19}$ C the elementary charge and N_{A} Avogadro's number, or the number of particles in a mole, we have $F = eN_{\mathrm{A}}$.

[8] This is a consequence of the second law of thermodynamics that states that the entropy of the universe increases. We have $\Delta G = \Delta H - T\Delta \mathcal{S}$ where $\Delta \mathcal{S} > 0$ is the entropy increase in the reaction and $\Delta H/T > 0$ is entropy *decrease* of the environment due to heat and work. The Gibbs free energy, therefore, gives the total entropy decrease, which is negative for a spontaneous process. For a non-spontaneous process, it can be positive, but this requires an entropy increase elsewhere in the system.

1.3.3 *Example: alkaline water electrolysis **

As an example, we consider in this section the reactions taking place in an *alkaline* water electrolyser producing hydrogen and oxygen. The word alkaline here refers to a pH>7. Note also that this process is named *water* electrolysis for the reactant rather than for the products hydrogen and oxygen. The overall reaction $2H_2O \rightarrow 2H_2 + O_2$, proceeds through two redox reactions. The reduction reaction at the cathode, the hydrogen evolution reaction (HER), reads

$$2H_2O + 2e^- \rightarrow H_2 + 2OH^-. \tag{1.14}$$

The pre-factors for each term in this reaction are called stoichiometric coefficients. The hydrogen gas forms bubbles that leave the electrolyte. Hydroxide ions (OH-) take over the transfer of current from electrodes and move to the anode, where they take part in the oxidation reaction, the oxygen evolution reaction (OER):

$$4OH^- \rightarrow 4e^- + O_2 + 2H_2O. \tag{1.15}$$

At the anode, the current is continued by the transport of electrons in the electrodes. A power source closes the circuit and gives the electrons enough Gibbs free energy to participate in the reactions. Note that water is consumed at the cathode but formed at the anode. However, of course, more water molecules are consumed at the cathode than are produced at the anode so that, overall, water is consumed. The equilibrium voltage of the water electrolysis reactions

$$V_{\text{eq}} = -\frac{\Delta G}{nF} \approx \frac{237\ \text{kJ/mol}}{2 \cdot 9.65 \cdot 10^4\ \text{C/mol}} \approx 1.23\ \text{V}. \tag{1.16}$$

When $V_{\text{cell}} \approx V_{\text{eq}}$ the process will be endothermic, causing local cooling, which is resupplied by heat drawn from the environment. This additional heat is taken into account in the enthalpy of reaction $\Delta H = \Delta G + T\Delta \mathcal{S}$. Here $\Delta \mathcal{S}$ is the entropy of reaction, associated with the higher entropy of the produced gases compared to those of the consumed liquid. The cell voltage at which this additional heat is produced by internal dissipation

$$V_{\text{tn}} = -\frac{\Delta H}{nF} \approx \frac{286\ \text{kJ/mol}}{2 \cdot 9.65 \cdot 10^4\ \text{C/mol}} \approx 1.48\ \text{V}, \tag{1.17}$$

is called the *thermoneutral voltage*. At higher voltages, the process becomes exothermic, as more heat and entropy are produced than is required for the reaction. To create gaseous hydrogen and oxygen bubbles requires a further small heat/enthalpy of vaporisation.

The equilibrium voltage of Eq. (1.16) at standard conditions can be found in tables of standard electrode potentials, like Table. 1.1 in the next section. The energies of reaction ΔG and ΔH are referred to as the lower and higher heating values, respectively. In the combustion of hydrogen, this difference arises due to the additional energy required to vaporize the product water.

Often, instead of ΔG as was used in Eqs. (1.12) and (1.13), ΔH is used to define the energy efficiency of water electrolysis. In this way of bookkeeping, only the electrical energy is used for the minimum required energy, and the required heat is assumed to be freely available. This makes for a maximum efficiency $\frac{\Delta H}{\Delta G} \approx 118\%$, that can be reached for the non-spontaneous reaction, by using heat from the environment. For the spontaneous reactions of hydrogen and oxygen in a fuel cell, the reverse of Eqs. (1.14) and (1.15), on the other hand, a maximum efficiency of $\frac{\Delta G}{\Delta H} \approx 85\%$ can be reached. The generated heat is then discarded as not being useful enough to contribute to energy efficiency. This reasoning has some logic, although so does having 100% as a maximum efficiency.[9]

Note that, however we define it, at low enough current density the reactions can, in theory, be performed back and forth with 100% efficiency in an electrochemical cell. This is in stark contrast with the energy efficiency of producing work from the heat released in burning hydrogen, which is limited by the Carnot efficiency. Therefore, at ambient or moderate temperatures, the energy efficiency of electrochemical cells easily beats their mechanical equivalents.

1.3.4 *Reduction potentials* *

An electrode potential E is defined as the cell voltage $E_{\text{right}} - E_{\text{left,SHE}}$ measured when the left electrode is a reference electrode, often a *standard hydrogen electrode* (SHE). This is a theoretical, idealised, electrode but can be approximated by bubbling pure hydrogen past a platinum electrode in an acidic solution at ambient conditions. The term “standard" here refers to the *standard conditions* of 25°C, 1 atm, 1 M of all reactants, or actually, to account for non-ideal behaviour, an *activity* of 1. Electrode potentials at standard conditions are typically dressed with a superscript 0 (or sometimes $\ominus$) so that a standard hydrogen electrode has $E^0 = 0$ by definition. For other reactions, the *standard electrode potentials* can be looked up in tables.

These potentials are usually given as reduction potentials; for reduction reactions examples are shown in Table 1.1

Rows of Table 1.1 can be combined to give new reactions. For example, the final line follows by subtracting twice the second line from the one before it. Also, the potential follows from subtracting -0.83 from 0.4 to give 1.23 V. However, this is fortuitous, as, in general, we have to realise that Gibbs' free energy can be added in this way and not the potential. By Eq. (1.11), the factor n must be corrected when adding potentials.

[9]The EU in its “harmonized protocols for testing of low temperature water electrolysis” advises a definition also propagated in Ref. [16], which amounts to $\varphi_e = \frac{V_{tn}}{V_{cell}+V_{tn}-V_{eq}}$. Note that in this definition too, the maximum cannot exceed 100 %.

Reduction reaction	E^0 [V]
$Li^+ + e^- \rightarrow Li$	-3.04
$2H_2O + 2e^- \rightarrow H_2 + 2OH^-$	-0.83
$2CO_2 + 2H^+ + 2e^- \rightarrow CO + H_2O$	-0.52
$2H^+ + 2e^- \rightarrow H_2$	0
$O_2 + 2H_2O + 4e^- \rightarrow 4OH^-$	0.4
$O_2 + 4H^+ + 4e^- \rightarrow 2H_2O$	1.229

Table 1.1: *An example list of reduction reactions and their reduction potentials. All values are relative to SHE.*

1.4 Kinetics

We conclude this chapter in section 1.5 with a simple cell model relating the cell voltage V_{cell} to the current density j and various geometrical and material parameters of the cell. Two important elements, the equilibrium voltage V_{eq} and the ohmic losses IR have already been described. In this section, we introduce a final important ingredient, the activation overpotential.

1.4.1 Faraday's law

Consider a redox reaction taking place at an electrode. Such a surface reaction is called a heterogeneous reaction because of the two or more phases involved. We will use a *normal-to* symbol $\perp$ to denote vector components of the molar flux normal to this surface in the direction **away from the surface into the fluid**:

$$N_\perp = \hat{\boldsymbol{n}} \cdot \boldsymbol{N} \tag{1.18}$$

Here $\boldsymbol{N}$ is the molar flux [mol/m^2/s] and $\hat{\boldsymbol{n}}$ is a unit normal vector directed into the electrolyte. Since reactants move towards the electrode surface in the $-\hat{\boldsymbol{n}}$-direction, $N_\perp$ [mol/m^2/s] is negative for reactants. Product fluxes are always positive because products move away from the electrode in the direction of $\hat{\boldsymbol{n}}$.

In the case of the redox reaction of Eq. (1.9), for each mole of products made or reactants consumed, n mole of electrons are used. This proportionality between charge and flux is referred to as *Faraday's law* and can be expressed as

$$j_\perp = nFN_{\perp,\text{O}}, \tag{1.19}$$

This equation relates the molar flux $N_{\perp,\text{O}}$ of oxidants to the charge flux $j_\perp = \hat{\boldsymbol{n}} \cdot \boldsymbol{j}$, or current density. A positive local current density $j_\perp$ is directed from the electrode into the electrolyte. In a reduction reaction, oxidants move towards the electrode so that $N_{\perp,\text{O}} < 0$ and $j_\perp < 0$, so *cathodic currents are negative*. Conversely, in an oxidation reaction oxidants move away from the electrode so that $N_{\perp,\text{O}} > 0$ and $j_\perp > 0$, so *anodic currents are positive*.

Figure 1.3: *The local electronic current density $\boldsymbol{j}_\perp$, product flux $\boldsymbol{N}$, ionic current density $\boldsymbol{i}$, and wall-normal unit vector $\boldsymbol{n}$.*

1.4.2 Activation energy

To have a chemical reaction proceed at a significant rate, an *activation energy* $\mathcal{E}_a$ [J/mol] usually has to be supplied. This additional energy that molecules should have to overcome the reaction energy barrier is schematically depicted in Figure 1.4. This schematic shows a spontaneous reaction, for which the Gibbs free energy of reaction $\Delta G < 0$. The energy of the molecules in their final state is below that of the energy of their initial state.

This activation energy is associated with overcoming repulsive interactions between the reactants before the attractive binding energies can take over. The activation energy can be lowered using a suitable catalytic surface. The right catalyst binds the reactant not too strongly but neither too weakly and may also align the reactants for the reaction to proceed more easily. This results in a lower activation energy barrier, as is illustrated with the dashed blue curve in Figure 1.4.

Consider a reaction at the surface of an electrode, immersed in a liquid electrolyte. For many reactions, the product flux $N_\perp$ [mol/m^2/s] can approximately be written as

$$N_\perp = k c^\nu, \tag{1.20}$$

where c [mol/m^3] is the reactant concentration, k [mol$^{1-\nu}$ s^{-1} m$^{3\nu-2}$] the reaction *rate constant* and ν is the reaction order. For first-order reactions $\nu = 1$ and the reaction rate is proportional to the reactant concentration. The rate constant often approximately satisfies the semi-empirical Arrhenius equation

$$k \propto \mathrm{e}^{-\frac{\mathcal{E}_a}{\mathcal{R}T}}. \tag{1.21}$$

Here, $\frac{\mathcal{E}_a}{\mathcal{R}T}$ is the ratio between the activation energy and the characteristic kinetic energy $\mathcal{R}T$ for a mole of reactants.[10] The higher the temperature, the larger the kinetic energy of the reactants, and the faster the reaction proceeds. This is the reason that chemical reactors typically operate at high temperatures. They often also operate at a high pressure to increase the concentration c of gaseous or dissolved reactants, further increasing the reaction rate. Finally, often a catalyst helps to lower $\mathcal{E}_a$. These are the main means available to accelerate chemical reactions.

[10]The characteristic kinetic energy per particle is $k_B T$, with k_B the Boltzmann constant. The gas constant can be written as $\mathcal{R} = N_A k_B$, with N_A Avogadro's constant.

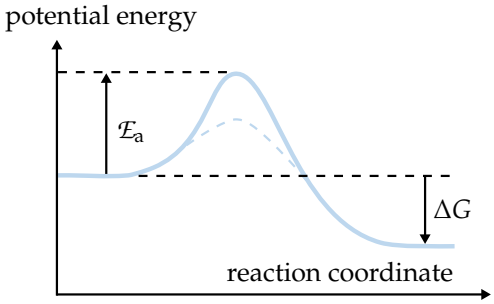

Figure 1.4: *The activation energy $\mathcal{E}_a$ "barrier" for a spontaneous reaction ($\Delta G < 0$) to proceed from left to right along the reaction coordinate, which may be seen as a re-scaled time coordinate. For a chemical reaction, the height of this barrier can be lowered using a better catalyst (dashed curve).*

Electrochemical reactions, however, have an additional "knob" that can be used to speed up a reaction, which allows them to proceed rapidly even at low temperatures $T \ll \mathcal{E}_a/\mathcal{R}$. This has to do with the potential energy of Eq. (1.3). By lowering the potential of the cathode E_c, the potential energy of electrons is increased. The most energetic electrons, at the *Fermi energy*, can then transition to a lower energy state by participating in a reduction reaction.

Similarly, by increasing the anode potential E_a relative to the potential ϕ of the adjacent electrolyte,[11] The potential energy of electrons in the anode is lowered. This facilitates electrons from oxidation reactions near the surface to enter the anode. As argued by a geometrical argument in the caption of Figure 1.5 an increase in electrode potential E, relative to that of the electrolyte, lowers the activation energy for an oxidation reaction by adding $-\alpha_O F\left(E-\phi\right)$.[12]

Here, the charge-transfer coefficient α_O for the oxidation reaction is typically around ½, and adds up to unity when combined with that for the reverse reduction reaction:

$$\alpha_O + \alpha_R = 1. \tag{1.22}$$

We consider a first-order, single-electron transfer oxidation reaction so that $n = r = 1$. As argued above, an increase in the anode potential E will decrease the activation energy $\mathcal{E}_a$ by adding $-\alpha_O F\left(E-\phi\right)$. Inserting into Eqs. (1.19), (1.20) and

[11] We take here the electrostatic potential in the electrolyte, measured using an electrode made of the same material as that used to measure the electrode potential. The measurement position should be very close to the electrode to exclude any ohmic drops or concentration differences over the distance to the electrode. So, it should be well within any diffusion layer thickness, but we consider it outside the electric double layer (EDL). At high electrolyte concentrations, this layer can be as thin as a few molecules, much smaller than the continuum scales considered in this book.

[12] If you have never seen this derivation before, the present exposition may be too short to appreciate the intricacies involved. In that case, you are recommended to study Fig. 1.5 and its caption in detail and/or consult electrochemistry textbooks like [3]. However, the details here will not be crucial to appreciate and apply the final results, so you may also skim over some technicalities.

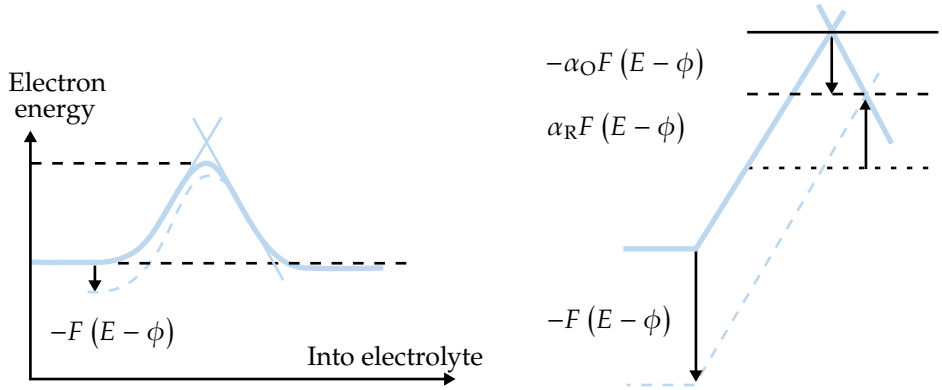

Figure 1.5: *Left: a schematic depiction of the energy landscape for a general single-electron transfer redox reaction* $a\mathrm{A} + \mathrm{e}^- \longrightarrow \mathrm{B}$. *The x-axis is a reaction coordinate, which may be seen as a sequence of reaction steps like adsorption, reorientation of molecules, the breakup of bonds, etcetera. Heuristically, it may also be seen as a re-scaled spatial coordinate from the anode into the electrolyte. The energy barrier of Figure 1.4 is decreased by increasing the potential E of the metal electrode relative to the electrolyte* ϕ. *This would lower the potential energy of electrons, accelerating oxidation reactions. Right: the activation barrier is approximated by two lines under an angle. Lowering the left line while keeping the right one fixed increases the peak by* $\alpha_{\mathrm{R}}F\left(E-\phi\right)$ *as seen from the left but decreases it by* $-\alpha_{\mathrm{O}}F\left(E-\phi\right)$ *as seen from the right. This decrease makes it easier for electrons to move to the left into the electrode, accelerating the oxidation reaction. Since these changes add up to* $-F\left(E-\phi\right)$ *we have* $\alpha_{\mathrm{O}} + \alpha_{\mathrm{R}} = 1$. *The exact values depend on the angle between the two lines, but* $\alpha_{\mathrm{O}} = \alpha_{\mathrm{R}} = 1/2$ *for a symmetric peak.*

Eq. (1.21) gives for the positive anodic current

$$j_\perp = k_O F c e^{\frac{\alpha_O F(E-\phi)}{\mathcal{R}T}}, \tag{1.23}$$

where the oxidation rate constant $k_O \propto e^{-\mathcal{E}_{a,O}/\mathcal{R}T}$. Simultaneously, reduction reactions will also take place at the anode, but at a much lower rate than the oxidation reactions. An increase in anode potential E will increase the activation energy $\mathcal{E}_a$ by adding $\alpha_R F(E-\phi)$. Inserting this into Eqs. (1.19), (1.20) and Eq. (1.21) adds a negative reduction current so that

$$j_\perp = k_O F c_R e^{\frac{\alpha_O F(E-\phi)}{\mathcal{R}T}} - k_R F c_O e^{-\frac{\alpha_R F(E-\phi)}{\mathcal{R}T}}. \tag{1.24}$$

At the anode, the first term will be referred to as the "forward" reaction and will exceed the second "reverse reaction" term so that $j_{\perp a} > 0$. At the cathode a similar expression will hold, although the kinetic parameters k_O, k_R, α_O, and α_R will generally be different when different cathode materials are used. At the cathode, the second term in Eq. (1.23) will dominate giving $j_{\perp c} < 0$. Note that for smooth planar electrodes, by charge conservation $j_{\perp a} = -j_{\perp c} = j$.

1.4.3 Current-overpotential relations

Nernst equation

Under equilibrium conditions $j_\perp = 0$ and Eq. (1.24) gives the single electron transfer Nernst-equation describing the equilibrium electrode potential

$$E_{eq} = E^{0\prime} + \frac{\mathcal{R}T}{nF}\ln\left(\frac{c_{O,eq}}{c_{R,eq}}\right), \tag{1.25}$$

where $E^{0\prime} = \phi_{eq} + \frac{\mathcal{R}T}{F}\ln\left(\frac{k_R}{k_O}\right)$ is the *formal potential* and $n = 1$, since we consider a single-electron transfer reaction. In 1.A, we consider the more general case of several reaction steps, which gives again Eq. (1.25), but now with n, the total number of electrons transferred in the reaction and a different formal potential. If the reaction is extremely fast, we speak of a reversible or Nernstian process for which this equilibrium equation can be used.

Butler-Volmer equation

We define the *activation overpotential* or *surface overpotential*

$$\eta \equiv (E-\phi) - (E-\phi)_{eq} \tag{1.26}$$

as the difference between the potential E in the electrode and the potential ϕ in the electrolyte, relative to that same difference in equilibrium. Therefore, under equilibrium conditions at zero current, the activation overpotential vanishes by definition.

You may wonder where in the electrode and in the electrolyte we take these potentials. At the high electrolyte concentrations used in most applications, the change in electrostatic potential from E inside the metal to ϕ in the electrolyte takes place over a distance of the order of a few molecules: the electric double layer (EDL).[13]

Using Eq. (1.26) in Eq. (1.24), we obtain the Butler-Volmer equation

$$j_\perp = j_*\left(\overbrace{\frac{c_\mathrm{R}}{c_\mathrm{R,eq}}\mathrm{e}^{\frac{\alpha_\mathrm{O}F\eta}{\mathcal{R}T}}}^{\text{oxidation}} - \overbrace{\frac{c_\mathrm{O}}{c_\mathrm{O,eq}}\mathrm{e}^{-\frac{\alpha_\mathrm{R}F\eta}{\mathcal{R}T}}}^{\text{reduction}}\right). \tag{1.27}$$

Here the exchange current density $j_* \equiv nF\left(k_\mathrm{O}c_\mathrm{R,eq}\right)^{\alpha_\mathrm{R}}\left(k_\mathrm{R}c_\mathrm{O,eq}\right)^{\alpha_\mathrm{O}}$.

The Butler-Volmer equation, Eq. (1.27), cannot, in general, be inverted analytically to give an exact expression for the overpotential η as a function of current density $j_\perp$.

Tafel equation

A noteworthy case in which an explicit expression for the overpotential can be obtained is when one of the exponentials dominates. When $j_\perp \gg j_*$ or $\eta \gg \frac{\mathcal{R}T}{F}\ln\left(\frac{c_\mathrm{O}}{c_\mathrm{O,eq}}\frac{c_\mathrm{R,eq}}{c_\mathrm{R}}\right)$, the oxidation reaction dominates over the reduction reaction and we obtain the Tafel equation

$$j_\perp = j_*\frac{c_\mathrm{R}}{c_\mathrm{R,eq}}\mathrm{e}^{\eta_\mathrm{a}/b_\mathrm{a}}. \tag{1.28}$$

Solving for η gives the concentration-dependent Tafel equation

$$\boxed{\eta_\mathrm{a} = b_\mathrm{a}\ln\left(\frac{j_\perp}{j_*}\frac{c_\mathrm{R,eq}}{c_\mathrm{R}}\right).} \tag{1.29}$$

Here the anodic Tafel slope $b_\mathrm{a} \equiv \mathcal{R}T/\alpha_\mathrm{O}F$ is around 0.05 V at ambient temperature when $\alpha_\mathrm{O} = 1/2$. This means that as long as $c_\mathrm{R} \approx c_\mathrm{R,eq}$ we can increase the current by an order of magnitude with an anodic activation overpotential of only $\eta_\mathrm{a} = b_\mathrm{a}\ln(10) \approx 120$ mV[14].

[13] This thin region near any surface in an electrolyte consists of a layer of ions that are chemically adsorbed to the surface and a layer of ions of opposing charge that are attracted to this surface charge. Hence the name electric double layer. This second layer screens the surface charge over the *Debye length* and is at relevant electrolyte concentrations $\lesssim 1$ nm thick. It is also sometimes called the diffuse layer. This is not to be confused with the diffusion layer. This boundary layer where diffusion dominates over advection, typically 10 – 100 μm, is many orders of magnitude thicker.

[14] Tafel slopes are often reported in this way, per decade rather than per e. If this is the case, the value mentioned in the literature has to be divided by $\ln(10) \approx 2.3$ to obtain Tafel slopes as defined here.

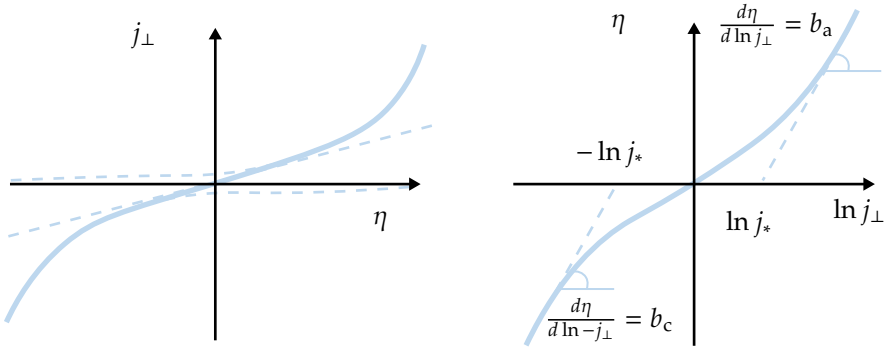

Figure 1.6: *A plot of current density $j_\perp$ versus activation overpotential η as described by the concentration-independent Butler-Volmer equation $j_\perp = j_*\left(\mathrm{e}^{\eta/b_\mathrm{O}} - \mathrm{e}^{-\eta/b_\mathrm{R}}\right)$ on a linear scale (left) and a lin-log plot with the logarithm of the current density on the x-axis (right). From this latter* Tafel plot*, the Tafel slopes $b_\mathrm{O} = \frac{\mathcal{R}T}{\alpha_\mathrm{O}F}$ and $b_\mathrm{R} = \frac{\mathcal{R}T}{\alpha_\mathrm{R}F}$ can be obtained as the slope of the linear sections. The intercept with the horizontal axis gives the exchange current density j_*.*

Concentration overpotential

Using $\ln ab = \ln a + \ln b$ we can write Eq. (1.29) as

$$\eta_\mathrm{a} = \overbrace{b_\mathrm{a}\ln\left(\frac{j_\perp}{j_*}\right)}^{\text{surface overpotential}} + \overbrace{b_\mathrm{a}\ln\left(\frac{c_{\mathrm{R,eq}}}{c_\mathrm{R}}\right)}^{\text{concentration overpotential}} . \tag{1.30}$$

The surface overpotential is independent of concentration and describes purely kinetic activation losses.[15] The second part, the concentration overpotential, increases as the reactant concentration c_R decreases.

Similarly, we obtain for the reverse reduction reaction, in terms of the cathodic Tafel slope $b_\mathrm{c} \equiv \mathcal{R}T/\alpha_\mathrm{R}F$:

$$\eta_\mathrm{c} = -b_\mathrm{c}\ln\left(\frac{-j_\perp}{j_*}\frac{c_{\mathrm{O,eq}}}{c_\mathrm{O}}\right) . \tag{1.31}$$

At the cathode, both $j_\perp$ and η_c are negative quantities.

Concentration-independent symmetric kinetics

When there are no appreciable concentration gradients throughout the cell so that $\frac{c_\mathrm{R}}{c_{\mathrm{R,eq}}} = \frac{c_\mathrm{O}}{c_{\mathrm{O,eq}}} = 1$, we obtain in the concentration-independent Butler-Volmer equation

[15] Sometimes another convention is used in which part of the concentration effect is attributed to the surface overpotential, see the end of 1.B.2.

$$\boxed{j_\perp = j_* \left(e^{\eta/b_a} - e^{-\eta/b_c} \right).} \tag{1.32}$$

Figure 1.6 illustrates the shape of this curve and how to use it to derive b_a, b_c, and j_*. In case of equal charge transfer coefficients $\alpha_O = \alpha_R = 1/2$ we can use the definition $\sinh x \equiv \frac{1}{2}(e^x - e^{-x})$ of the hyperbolic sine, to write Eq. (1.32) as $j_\perp = 2j_* \sinh\left(\frac{\eta}{b}\right)$ using $b = \frac{2\mathcal{R}T}{F}$. This may be referred to as the symmetric concentration-independent Butler-Volmer equation. Inverting it gives[16]

$$\eta = b \operatorname{asinh}\left(\frac{j_\perp}{2j_*}\right). \tag{1.33}$$

At high current densities $j_\perp \gg j_*$ we have $b \operatorname{asinh}(j_\perp/2j_*) \approx b \ln j_\perp/j_*$ so that Eq. (1.33) reduces to the Tafel equation.[17]

Linear kinetics

For most applications $j_\perp \gg j_*$ so that Tafel kinetics is an appropriate approximation. For some particularly facile reactions, like hydrogen oxidation on platinum, the exchange current density j_* is so high that $|j_\perp| < j_*$. Using the first-order Taylor expansion $e^x \approx 1 + x$ for $x \ll 1$, Eqs. (1.32) and (1.22) give the equation for linear kinetics

$$\eta = ARj_\perp \quad \text{with} \quad AR = \frac{\mathcal{R}T}{Fj_*}. \tag{1.34}$$

Here, in analogy with Eq. (1.8), we introduced an area-specific resistance AR. Note that linear kinetics only holds for very low activation overpotentials $\eta \lesssim \mathcal{R}T/F \sim 25$ mV.

1.5 Simplified cell model

In this section, we integrate the various elements discussed in this chapter into a first cell model.

Figure 1.7 shows typical profiles of both the electronic and the electrolyte potentials through an electrochemical cell in equilibrium during electrolysis ($V_{cell} < V_{eq} < 0$) and galvanic operation ($0 < V_{cell} < V_{eq}$), respectively. The figure is slightly complicated by including the increase in potential inside the cables and electrodes in the direction of the electron flow but it does not have to be fully comprehended at this point. In case of negligible electronic resistance, the picture would be slightly simpler.

[16] Here the inverse hyperbolic sine can be written as $\operatorname{asinh}(x) = \ln\left(x + \sqrt{1+x^2}\right)$ so that for $x \gg 1$ we have $\operatorname{asinh}(x) \approx \ln(2x)$

[17] For low current densities $j_\perp \ll j_*$ we have $b \operatorname{asinh}(j_\perp/2j_*) \approx b\, j_\perp/2j_*$, which is consistent with Eq. (1.34).

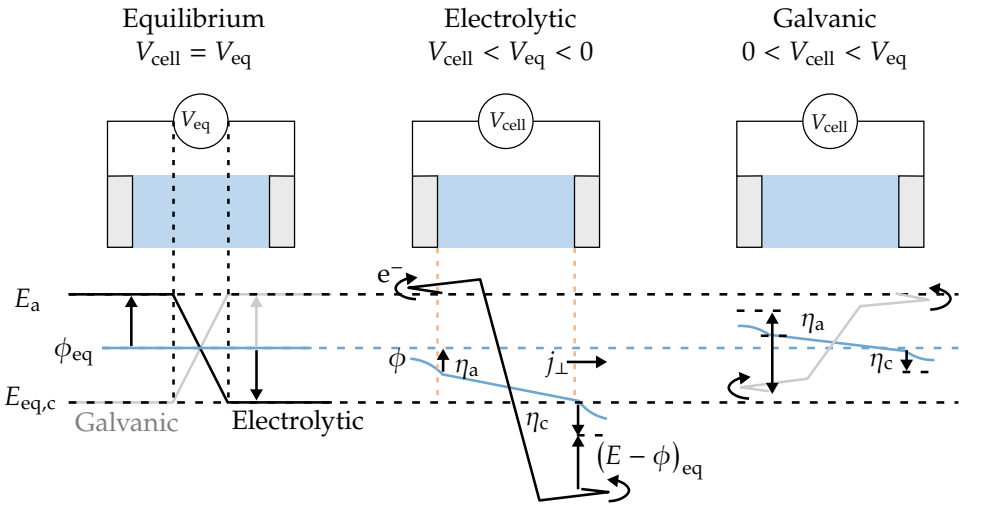

Figure 1.7: *The electronic potential (black for an electrolytic cell, grey for a galvanic cell) and electrolyte potential ϕ (blue) profiles throughout the cell and inside the external circuit. In an electrolytic cell $V_{cell} < V_{eq} < 0$. The electronic potential is locally multi-valued to show both variations inside the porous electrode and the cables. The electrolyte potential ϕ shows a constant slope in the electrolyte, which is assumed to have a constant conductivity. The "entrance" of the porous electrodes is indicated in the middle picture with the orange vertical dashed lines to guide the eye. Beyond this point, a gradually decreasing slope inside the (porous) electrodes can be seen towards the back where the ionic current and hence this slope vanishes.*

For completeness, and to anticipate what lies ahead in chapter 3, we also considered the electrodes to be porous. In this case, the overpotential $\eta = E - \phi - (E-\phi)_{eq}$ is not a constant, but varies throughout the electrode, further complicating the picture.

Often, the electronic conductivity of the electrodes is high enough to assume constant electrode potentials E_a and E_c. However, for generality, we include here an ohmic potential drop ΔV, which receives contributions from electrons moving through the electrode material, current collectors, and cables before arriving at the load or source. Note that in a galvanic cell ΔV decreases the positive cell voltage, while in an electrolytic cell ΔV makes the negative cell voltage more negative. Both efficiencies thus decrease as a result of the electronic ohmic losses ΔV.

We will define the electrolyte potentials ϕ_a and ϕ_c at the electrode-electrolyte interface so that $\Delta\phi \equiv \phi_a - \phi_c > 0$ gives the ohmic drop between the electrodes, which vanishes in equilibrium $\Delta\phi_{eq} = 0$. With the definition of Eq. (1.26) and $V_{eq} = E_{eq,c} - E_{eq,a}$ we can then write

$$\boxed{V_{cell} = V_{eq} + \eta_c - \eta_a - \Delta\phi - \Delta V.} \tag{1.35}$$

This important result gives the cell potential as a sum, or an equivalent series circuit,

of the equilibrium potential. All terms on the right act to reduce V_{eq} and may be referred to as voltage losses, or overpotentials. These losses consist of activation overpotentials $\eta_{\mathrm{a}} > 0$ and $-\eta_{\mathrm{c}} > 0$ as well as ohmic losses due to ions $\Delta\phi$ and electrons ΔV.

We conclude this chapter by inserting expressions for these losses obtained from the previous section, assuming:

1. An electrolyte with constant conductivity between the anode and cathode, so we can insert Eq. (1.6) for the electrolyte potential drop $\Delta\phi = jL/\kappa$.
2. An ohmic resistance R for the electronic circuit, so we can use Eq. (1.8) for the electronic potential drop $\Delta V = jAR$.
3. Concentration-independent Tafel kinetics for the anode, where $j_\perp = j > 0$, so we can use Eq. (1.32) to write $\eta_{\mathrm{a}} = b_{\mathrm{a}} \ln(j/j_{*\mathrm{a}})$.[18]
4. Similarly, at the cathode $j_\perp = -j$, so we can use Eq. (1.31) to write $\eta_{\mathrm{c}} = -b_{\mathrm{c}} \ln(j/j_{*\mathrm{c}})$.

Inserting these expressions into Eq. (1.35) gives

$$V_{\mathrm{cell}} = V_{\mathrm{eq}} - \left(b_{\mathrm{c}} \ln\left(\frac{j}{j_{*\mathrm{c}}}\right) + b_{\mathrm{a}} \ln\left(\frac{j}{j_{*\mathrm{a}}}\right) + \frac{jL}{\kappa} + jAR \right). \tag{1.36}$$

All voltage losses between brackets are positive as they should be. Figure 1.8 illustrates this expression using values that are typical for a common alkaline water electrolyser. For low current densities, the logarithmic activation overpotentials dominate,[19] while for the higher current densities, their contribution increases only very slowly. Therefore, the linear ohmic losses dominate the slope of the cell voltage at higher current densities.

The electrochemical engineer aims to minimise the voltage losses in an electrochemical cell while keeping the system costs to a minimum. Economic viability usually requires the use of high current densities to get as much product as possible for as little cell material as possible. More expensive catalysts may be used to reduce activation and voltage losses, but alternatively, using a larger surface area may be more cost-effective. Therefore, porous electrodes with a large internal surface area are often used. Also, additional phenomena like mass transport and multiphase flow phenomena start to play a role and impact the cell voltage. Creating an understanding of all these factors of influence, providing a mathematical description, and, where possible, providing optimised design parameters will be the main goal of the remainder of this book.

[18] For many applications this is a reasonable approximation for intermediate current densities that are large enough for Tafel kinetics to hold ($j \gtrsim 2j_*$) but small enough for concentration effects to be neglected. When smaller currents $j \lesssim j_*$ should also be included, Eq. (1.33) shows we can replace $\ln\left(\frac{j}{j_*}\right)$ with $\operatorname{asinh}\left(\frac{j_\perp}{2j_*}\right)$. Strictly speaking, this is only exactly valid for symmetric kinetics with $\alpha = 1/2$.

[19] We replaced $\ln x$ with $\operatorname{asinh}\frac{x}{2}$ in Eq. (1.36), as in Eq. (1.33). This gives approximately the same result for $x \gg 1$ but avoids the negative values that arise for $x < 1$ for which the Tafel approximation is invalid.

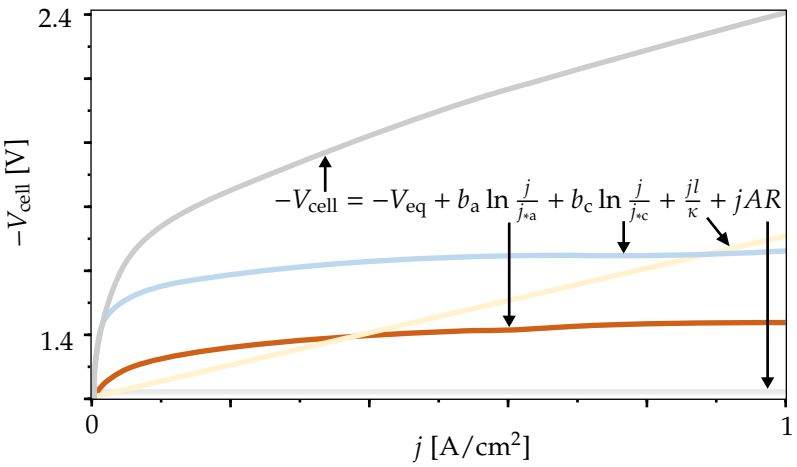

Figure 1.8: *The negative of the cell voltage $-V_{\text{cell}}$ of an electrolytic cell as a function of current density j as described by Eq.* (1.36) *using $V_{\text{eq}} = -1.23$ V, $b_{\text{a}} \approx b_{\text{c}} \approx 50$ mV, $j_{*\text{c}} = 10^{-2}$ A/cm^2, $j_{*\text{a}} = 10^{-4}$ A/cm^2, an electrolyte area-specific resistance $\kappa/L = 0.5$ Ω cm^2 and electronic area-specific resistance $AR = 0.01$ Ωcm^2. The logarithmic activation overpotentials mostly increase the voltage losses at low current densities but hardly vary for higher values, where the linear ohmic losses dominate the slope.*

1.6 Summary

- The ionic current density in an electrochemical cell often approximately follows Ohm's law $\boldsymbol{i} = \kappa \boldsymbol{E} = -\kappa \nabla \phi$. It is oriented in the direction of the electric field from anode, where the oxidation reaction releases electrons, to cathode, where electrons are consumed in the reduction reaction $\text{O} + n\text{e}^- \leftrightarrow \text{R}$, Eq. (1.9), through a potential drop $\Delta\phi = ARj = jL/\kappa$.
- The cell voltage $V_{\text{cell}} = E_{\text{c}} - E_{\text{a}} = V_{\text{cell}} + \eta_{\text{c}} - \eta_{\text{a}} - \Delta V$ of Eq. (1.10) is positive in a galvanic cell and related to voltage efficiency as $\varphi_{\text{e}} = \frac{V_{\text{cell}}}{V_{\text{eq}}}$, Eq. (1.12). It is negative in an electrolytic cell and related to efficiency as $\varphi_{\text{e}} = \frac{V_{\text{eq}}}{V_{\text{cell}}}$, Eq. (1.13).
- For first-order kinetics, the current density $j_\perp = nFN_\perp$ from anode to cathode can often be described by the Butler-Volmer equation $j_* \left(\frac{c_{\text{R}}}{c_{\text{R,eq}}} \text{e}^{\frac{\alpha_{\text{O}} F\eta}{\mathcal{R}T}} - \frac{c_{\text{O}}}{c_{\text{O,eq}}} \text{e}^{-\frac{\alpha_{\text{R}} F\eta}{\mathcal{R}T}} \right)$, Eq. (1.27), which can be reduced to
  - the Tafel equation, $j_\perp = j_* \frac{c_{\text{R}}}{c_{\text{R,eq}}} \text{e}^{\eta_{\text{a}}/b_{\text{a}}}$, (1.28) for high overpotentials $\eta = (E - \phi) - (E - \phi)_{\text{eq}}$, or $j_\perp \gg j_*$
  - linear kinetics, with an areal resistance $AR = \frac{\mathcal{R}T}{Fj_*}$ for low overpotentials, and

– the Nernst equation $E_{\mathrm{eq}} = E^{0\prime} + \frac{\mathcal{R}T}{nF} \ln\left(\frac{c_{\mathrm{O,eq}}}{c_{\mathrm{R,eq}}}\right)$, where n appears when considering multiple reaction steps near equilibrium (1.C.49).

1.7 Exercises

Exercise 1.1

The exchange current density and charge transfer coefficient of an electrochemical reaction at a cathode are $j_* = 0.01$ mA/cm^2 and $\alpha_R = 0.65$, respectively. Give an approximate value for the activation overpotential on the cathode at ambient conditions, at a current density $j_\perp = -20$ mA/cm^2, assuming $C_O \approx C_{O,eq}$.

Exercise 1.2

Consider the simple cell model

$$V_{cell} = V_{eq} - \eta - jAR$$

. Assume that the current density j is high enough for the activation overpotential η to be approximately independent of current density. The useful power output of a galvanic cell is given by $P = jAV_{cell}$. Give an expression for the current density j for which this quantity is maximised.

Exercise 1.3

Consider a cell in which both anode and cathode follow concentration-independent Tafel kinetics, with the anodic and cathodic activation overpotentials given by

$$\eta_a = b_a \ln\left(\frac{j}{j_{*a}}\right) \text{ and } \eta_c = -b_c \ln\left(\frac{j}{j_{*c}}\right). \tag{1.37}$$

Combine both overpotentials in a single expression for the total activation overpotential $\eta_a - \eta_c = b \ln(j/j_*)$.

a. What is the combined Tafel slope b?

b. If $b_a = \mathcal{R}T/\alpha_a F$ and $b_c = \mathcal{R}T/\alpha_c F$ give the combined charge transfer coefficient $\alpha = \mathcal{R}T/bF$ in terms of α_a and α_c

c. What is the combined exchange current density j_*?

Exercise 1.4

A consortium of companies is developing a new wind park integrated with water electrolysers. The combined nominal electrolyser power is chosen to be 50 MW. As the available space is important, the electrolysers have to be as small as possible. We assume a distance between the electrodes of 500 µm with an effective electrolyte conductivity 20 S/m, with $b_c = b_a = 0.05$ V, $j_{*a} = 10^2$ A/m^2 and $j_{*c} = 1$ A/m^2. We neglect any ohmic losses in the electrical connections and electrodes and any effect of bubbles.

a. If a voltage efficiency of 60% with respect to 1.23 V is required, how much anode plus cathode electrode area do you need? **Hint**: You might need to use a numerical solver to get to the solution.
b. Someone in your company finds out that heating the electrolyte to 100 °C increases the ionic conductivity to 70 S/m. With the same electrode area and electrolyser power, what will the new efficiency be?

Exercises 1.5-1.9

Fill in the missing steps in the main text, indicated by the symbol  .

*Appendices **

1.A *Multiple reaction steps*

Often, electrochemical reactions involve several subsequent steps, including mass transfer, adsorption, desorption, redox reactions, and sometimes chemical reactions. Usually one of the steps is much slower than the rest,[20] which is then referred to as the rate-determining step (rds). Parsons [20] considered how to deal with multi-step reactions in a rather general way. Considering a process consisting of n_{preO} electron-transfer steps before a rate-determining oxidation step and n_{postO} after, he found that the effective charge transfer coefficients becomes $\alpha_{\mathrm{effO}} = n_{\mathrm{preO}} + n_{\mathrm{rdsO}}\alpha_{\mathrm{O}}$, and similarly $\alpha_{\mathrm{effR}} = n_{\mathrm{postO}} + n_{\mathrm{rdsO}}\alpha_{\mathrm{R}}$. Inserting these effective values in Eq. (1.27) gives

$$j_{\perp} = j_{*}\left(\frac{c_{\mathrm{R}}}{c_{\mathrm{R,eq}}}\mathrm{e}^{(n_{\mathrm{preO}}+n_{\mathrm{rds}}\alpha_{\mathrm{O}})\frac{F\eta}{\mathcal{R}T}} - \frac{c_{\mathrm{O}}}{c_{\mathrm{O,eq}}}\mathrm{e}^{-(n_{\mathrm{postO}}+n_{\mathrm{rds}}\alpha_{\mathrm{R}})\frac{F\eta}{\mathcal{R}T}}\right). \tag{1.A.38}$$

Here $n_{\mathrm{rdsO}} = 1$ since the rate-determining step almost always involves the transfer of a single electron [3] or $n_{\mathrm{rdsO}} = 0$ when the rate-determining step is not a charge-transfer step. The sum of the rate-determining step charge transfer coefficients $\alpha_{\mathrm{O}}+\alpha_{\mathrm{R}} = 1$ as indicated in Eq. (1.22) so that $\alpha_{\mathrm{effO}} + \alpha_{\mathrm{effR}} = n_{\mathrm{preO}} + n_{\mathrm{postO}} + n_{\mathrm{rdsO}}(\alpha_{\mathrm{O}}+\alpha_{\mathrm{R}}) = n$, the total number of electrons transferred

Note that the rate-determining step for the reverse reduction reaction does not have to be the same as that of the forward oxidation reaction. In this case we have $\alpha_{\mathrm{effR}} = n_{\mathrm{preR}} + n_{\mathrm{rds}}\alpha_{\mathrm{R}}$ and $\alpha_{\mathrm{effO}} = n_{\mathrm{postR}} + n_{\mathrm{rds}}\alpha_{\mathrm{O}}$ where n_{preR} is not necessarily equal to n_{postO} and n_{postR} is not necessarily equal to n_{preO}, unless the rate-determining step is the same.

Electron-transfer steps preceding the rate-determining step thus act to increase the effective transfer coefficient and reduce the Tafel slope. When the rate-determining step is the first single-electron transfer step $\alpha_{\mathrm{eff}} = \alpha \approx 1/2$, while if there is a preceding electron transfer step $\alpha_{\mathrm{eff}} = 1 + \alpha \approx 3/2$, or there are two preceding electron transfer steps and the rsd does not involve an electron transfer $\alpha_{\mathrm{eff}} = 2 + 0 = 2$. The latter is thus beneficial in the sense that it gives a lower Tafel slope, and measurement of the Tafel slope under controlled conditions gives insight into the reaction mechanism.

[20] As all steps take place subsequently, they must all proceed at the same rate. What is meant here is that the step has a much lower rate constant. In the case of an electrochemical reaction, it requires much more overpotential than the others to proceed at the same rate.

Take, for example, the hydrogen evolution reaction in which, according to the Volmer mechanism, the rate-determining step can be the first electron transfer step. With $\alpha_R = 1/2$ this gives at room temperature a Tafel slope $b_c = \mathcal{R}T/\alpha_R F \approx 50$ mV, or $\ln 10 b_c \approx 2.3 b_c \approx 120$ mV per decade. In case the *Heyrovski step* is rate-determining, $\alpha_{\text{effR}} = 3/2$ and the Tafel slope becomes 40 mV per decade. Finally, a Tafel step involving the desorption of oxygen or hydrogen but no electron transfer can be rate-determining, in which case $\alpha_{\text{effR}} = 2$ and the Tafel slope reduces further to only 30 mV. The oxygen evolution reaction involves more electron transfer steps so even smaller Tafel slopes can be observed. Note that a Tafel slope of 120 mV does not automatically imply the Volmer mechanism [23]. Also, transport phenomena can significantly influence the Tafel slope, which we will consider in Chapter 3.

1.B *Alternative Butler-Volmer formulations*

1.B.1 *Changing reference concentrations*

Eq. (1.27) uses the equilibrium concentrations of the oxidants and reductants. These are the concentrations associated with a zero current density. Sometimes, it can be convenient to use different reference concentrations $c_{R,\text{ref}}$ and $c_{O,\text{ref}}$. In terms of these we can rewrite Eq. (1.27), after some algebra, as

$$j_\perp = j_{*\text{ref}} \left(\frac{c_R}{c_{R,\text{ref}}} e^{\frac{\alpha_O F}{\mathcal{R}T}(E - E_{\text{ref}})} - \frac{c_O}{c_{O,\text{ref}}} e^{-\frac{\alpha_R F}{\mathcal{R}T}(E - E_{\text{ref}})} \right). \tag{1.B.39}$$

Here $E - E_{\text{ref}} = \eta + \ln\left(\frac{c_{R,\text{ref}}}{c_{R,\text{eq}}}\right) - \frac{\alpha_R}{\alpha_O}\ln\left(\frac{c_{O,\text{ref}}}{c_{O,\text{eq}}}\right)$ and $j_{*\text{ref}} = j_* \left(\frac{c_{R,\text{ref}}}{c_{R,\text{eq}}}\right)^{\alpha_R} \left(\frac{c_{O,\text{ref}}}{c_{O,\text{eq}}}\right)^{\alpha_O}$, as can be verified by inserting Eq. (1.22). Choosing $c_{R,\text{ref}} = c_{O,\text{ref}} = 1$ M we can write

$$j_\perp = nFk^0 \left(c_R e^{\frac{\alpha_O F}{\mathcal{R}T}(E - E^{0\prime})} - c_O e^{-\frac{\alpha_R F}{\mathcal{R}T}(E - E^{0\prime})} \right), \tag{1.B.40}$$

in terms of the intrinsic or *standard rate-constant* k^0 and *formal potential* $E^{0\prime}$ as is done in, for example, Ref. [3]. The associated Nernst equation obtained for $j_\perp = 0$ reads $E = E^{0\prime} + \frac{\mathcal{R}T}{F}\ln\frac{c_{O,\text{eq}}}{c_{R,\text{eq}}}$. The exchange current density follows, inserting this back in Eq. (1.27) as $j_* = nFk^0 c_{R,\text{eq}}^{\alpha_R} c_{O,\text{eq}}^{\alpha_O}$.

1.B.2 *Changing overpotentials*

The overpotential $\eta = (E - \phi) - (E - \phi)_{\text{eq}}$ in Eqs. (1.27) and (1.B.39) is relative to different but fixed reference concentrations. When the current is switched on these concentrations will change: the reactant concentration will decrease while the product concentration increases. Both effects will increase the overpotential required to sustain the current. To quantify this effect we transform Eq. (1.A.38), with some

algebra, into the following form

$$j_\perp = j_{*\mathrm{s}} \left(\mathrm{e}^{\frac{\alpha_{\mathrm{effO}} F \eta_\mathrm{s}}{\mathcal{R}T}} - \mathrm{e}^{-\frac{\alpha_{\mathrm{effR}} F \eta_\mathrm{s}}{\mathcal{R}T}} \right), \tag{1.B.41}$$

where the effective exchange current density $j_{*\mathrm{s}}$ depends on the concentration according to

$$j_{*\mathrm{s}} = j_* \left(\frac{c_\mathrm{R}}{c_{\mathrm{R,eq}}} \right)^{\frac{\alpha_{\mathrm{effR}}}{n}} \left(\frac{c_\mathrm{O}}{c_{\mathrm{O,eq}}} \right)^{\frac{\alpha_{\mathrm{effO}}}{n}} \tag{1.B.42}$$

and $\eta_\mathrm{s} \equiv \eta - \eta_\mathrm{c}$ where the *concentration overpotential*

$$\eta_\mathrm{c} = \frac{\mathcal{R}T}{nF} \left[\ln\left(\frac{c_\mathrm{O}}{c_{\mathrm{O,eq}}} \right) + \ln\left(\frac{c_{\mathrm{R,eq}}}{c_\mathrm{R}} \right) \right] \tag{1.B.43}$$

At the anode, the reactant C_R will decrease, making a positive contribution to the concentration overpotential. The product C_O increases, also making a positive contribution. So both effects increase the total overpotential η, and similarly for a cathode.

In this new formulation, the Butler-Volmer equation (1.B.41) has seemingly become concentration-independent. The concentration-dependence has now entered the new exchange current density $j_{*\mathrm{s}}$ and the associated surface overpotential η_s is now only one component of the full overpotential $\eta = \eta_\mathrm{s} + \eta_\mathrm{c}$, with the other part being the concentration overpotential. This makes it possible to determine which part of the overpotential should be attributed to concentration and which part is due to kinetics, where we note that the kinetics is furthermore influenced by the concentration through the new exchange current density $j_{*\mathrm{s}}$.

In case of a symmetric reaction with $\alpha_\mathrm{O} = \alpha_\mathrm{R}$ we can solve Eq. (1.B.41) analytically as in Eq. (1.33) to give

$$\eta = \overbrace{b \operatorname{asinh}\left(\frac{j_\perp}{2 j_{*\mathrm{s}}} \right)}^{\text{surface overpotential}} + \overbrace{\frac{\mathcal{R}T}{F} \ln\left(\frac{c_\mathrm{O}}{c_{\mathrm{O,eq}}} \frac{c_{\mathrm{R,eq}}}{c_\mathrm{R}} \right)}^{\text{concentration overpotential}} \tag{1.B.44}$$

where $b = \frac{2\mathcal{R}T}{F}$.

We may further simplify by assuming an anode where the reactant concentration c_R changes significantly while the product concentration $c_\mathrm{O} \approx c_{\mathrm{o,eq}}$ remains fairly constant. An example is the anode in alkaline water electrolysis at low electrolyte concentrations where the reactant is hydroxide and the product is water. In this case

$$\eta = \frac{\mathcal{R}T}{F} \left[2 \operatorname{asinh}\left(\frac{j_\perp}{2 j_{*\mathrm{s}}} \right) + \ln\left(\frac{c_{\mathrm{R,eq}}}{c_\mathrm{R}} \right) \right]. \tag{1.B.45}$$

Another relevant limit is the Tafel limit, in which one of the terms in the Butler-Volmer equation (1.27) dominates over the other. For definiteness let us assume an anode, in which case Eq. (1.B.41) can be solved to give

$$\eta_\mathrm{s} = b_\mathrm{a} \ln\left(\frac{j_\perp}{j_{*\mathrm{s}}} \right) = b_\mathrm{a} \ln\left(\frac{j_\perp}{j_*} \right) - \frac{\mathcal{R}T}{F} \left[\frac{\alpha_\mathrm{R}}{\alpha_\mathrm{O}} \ln\left(\frac{c_\mathrm{R}}{c_{\mathrm{R,eq}}} \right) + \ln\left(\frac{c_\mathrm{O}}{c_{\mathrm{O,eq}}} \right) \right] \tag{1.B.46}$$

where $b_a = \mathcal{R}T/\alpha_O F$ and we inserted Eq. (1.B.42). The final term exactly cancels with the first term of Eq. (1.B.43). The first term between the square brackets combines with the second term of Eq. (1.B.43), using $1 - \alpha_R = \alpha_O$ to give $\frac{\mathcal{R}T}{F} \ln\left(\frac{c_R}{c_{R,eq}}\right)$.

1.C *The Nernst equation*

Next, we aim to derive the Nernst equation for the equilibrium potential. For this purpose, we use the form of the Butler-Volmer equation of Eq. (1.B.39), which in equilibrium gives

$$\frac{c_{rdsO,eq}}{c_{rdsR,eq}} = e^{\frac{F n_{rdsO}}{\mathcal{R}T}\left(E_{eq} - E^{0\prime}_{rds}\right)}. \tag{1.C.47}$$

The non-rate-determining steps will usually be fast enough compared to the rate-determining step, so they can be considered in equilibrium [1]. When the n_{preO} charge-transfer steps before and n_{postO} after the rate-determining step are in equilibrium:

$$\frac{c_{O,eq}}{c_{rdsO,eq}} = e^{\frac{n_{preO} F}{\mathcal{R}T}\left(E_{eq} - E^{0\prime}_{preO}\right)} \text{ and } \frac{c_{rdsR,eq}}{c_{R,eq}} = e^{\frac{n_{postO} F}{\mathcal{R}T}\left(E_{eq} - E^{0\prime}_{postO}\right)}. \tag{1.C.48}$$

This gives $\frac{c_{O,eq}}{c_{R,eq}} = e^{\frac{n_{preO} F}{\mathcal{R}T}\left(E_{eq} - E^{0\prime}_{preO}\right)} e^{\frac{F}{\mathcal{R}T}\left(E_{eq} - E^{0\prime}_{rds}\right)} e^{\frac{n_{postO} F}{\mathcal{R}T}\left(E_{eq} - E^{0\prime}_{postO}\right)} = e^{\frac{nF}{\mathcal{R}T}\left(E_{eq} - E^{0\prime}\right)}$ where $E^{0\prime} = \frac{n_{preO} E^{0\prime}_{preO} + n_{rdsO} E^{0\prime}_{rds} + n_{postO} E^{0\prime}_{postO}}{n}$ when used in Eq. (1.C.47). This leads to the general multi-electron transfer **Nernst equation**

$$E_{eq} = E^{0\prime} + \frac{\mathcal{R}T}{nF} \ln\left(\frac{c_{O,eq}}{c_{R,eq}}\right). \tag{1.C.49}$$

Solving Eq. (1.B.39) for $j_\perp = 0$, with α_O and α_R replaced with α_{effO} and α_{effR}, gives $E = E_{eff} + \frac{\mathcal{R}T}{nF} \ln\left(\frac{c_{O,eq} c_{R,ref}}{c_{O,ref} c_{R,eq}}\right)$, another form of the multi-electron transfer Nernst equation.

Chapter 2

Transport

Starting from a general conservation equation, the conservation of mass, heat, momentum, and charge are described. The mass transport equations are used to calculate the concentration overpotential. The Boltzmann distribution and Einstein relations are used to derive the Nernst-Planck equation, which describes the transport of ions. A mathematical description of a binary electrolyte, with and without a surplus of supporting electrolyte, is provided. Finally, a time-dependent solution to the mass transport equations is used to describe the concentration overpotential and the associated limiting current density as a function of time.

2.1 Conservation equations

A general conservation equation can be written in differential form as

$$\frac{\partial c}{\partial t} = -\nabla \cdot \boldsymbol{N} + S, \tag{2.1}$$

where c is the concentration [something/m^3] of a conserved quantity. This can be for example the mass density ρ [kg/m^3] or the charge density ρ_q [C/m^3]. The final term S is a source, and $\boldsymbol{N}$ [something/m^2/s] is the flux related to c. We will use the symbol c [mol/m^3] to represent the molar concentration of a species in a gas or dissolved in a liquid. If the fluid moves with a velocity $\boldsymbol{u}$, the flux associated with a low concentration c can be approximately written as

$$\boldsymbol{N} = c\boldsymbol{u} - D\nabla c. \tag{2.2}$$

The first term $c\boldsymbol{u}$ is the convective flux. The concentration at a location can increase or decrease because of a higher or lower concentration upstream, respectively. In the absence of flow, $\boldsymbol{N} = -D\nabla c$ is called Fick's law and describes diffusive transport proportional to the diffusivity or diffusion coefficient D [m^2/s].[1] Inserting Eq. (2.2)

[1] In this book we will assume dilute concentrations so we can neglect the impact of mass transport of a species on the flow velocity. See appendix 2.B for a simple 1D example in which this effect is included.

in Eq. (2.1) gives, with $\nabla \cdot (c\boldsymbol{u}) = c\nabla\cdot\boldsymbol{u} + \boldsymbol{u} \cdot \nabla c$ and assuming incompressible flow, $\nabla \cdot \boldsymbol{u} = 0$ as discussed in Appendix 2.A.1, and constant D:

$$\frac{Dc}{Dt} = D\nabla^2 c + S. \tag{2.3}$$

Here $\frac{Dc}{Dt} \equiv \frac{\partial c}{\partial t} + \boldsymbol{u} \cdot \nabla c$ is the *material derivative*. It represents the time variation of c, while moving along a streamline of the flow. Equation (2.3) is referred to as an advection-diffusion-reaction equation, in case S represents a reaction.

Integrating Eq. (2.1) over a fixed volume $\mathcal{V}$ we obtain

$$\frac{d\int c d\mathcal{V}}{dt} = -\int \boldsymbol{N} \cdot d\boldsymbol{A} + \int S d\mathcal{V}, \tag{2.4}$$

where we used the divergence theorem, also known as Gauss' theorem, to write $-\int \nabla \cdot \boldsymbol{N} d\mathcal{V} = -\int \boldsymbol{N} \cdot d\boldsymbol{A}$.[2]

2.1.1 Charge transport

The flux of electric charge is the current density, for which we use the symbols $\boldsymbol{j}$ and $\boldsymbol{i}$ [A/m^2], depending on whether we describe electrons or ions, respectively. Except in the electric double layer, with length scales of the order of a few molecules near a surface, electrolytes contain an equal density of positive and negative ions so that the charge density ρ_q [C/m^3] vanishes. Nonetheless, we can create a conservation equation for charge by replacing c in Eq. (2.1) with ρ_q and $\boldsymbol{N}$ with $\boldsymbol{i}$ to give

$$\frac{\partial \rho_q}{\partial t} = -\nabla \cdot \boldsymbol{i} + S_q, \tag{2.5}$$

where S_q [C/s/m^3] is a volume source of charge. Assuming zero charge density:[3]

[2]The infinitesimal area vector $d\boldsymbol{A}$ is directed outwards of the integration volume. Equation (2.4) shows the change in time by influx ($d\boldsymbol{A} \cdot \boldsymbol{N} < 0$) or outflux ($d\boldsymbol{A} \cdot \boldsymbol{N} > 0$), sources ($S > 0$) or sinks ($S < 0$).

[3]Gauss's law from electrostatics relates the divergence in the electric field to charge density

$$\nabla \cdot \boldsymbol{E} = \rho_q / \varepsilon_\mathrm{r} \varepsilon_0 \tag{2.6}$$

where $\varepsilon_\mathrm{r}\varepsilon_0$ is the electrical permittivity of the material under consideration, with $\varepsilon_0 = 8.85 \cdot 10^{-12}$ C/V/m that of the vacuum and ε_r the relative permittivity. Comparing Eq. (2.6) with Eq. (1.1), we may interpret $\rho_q/\varepsilon_\mathrm{r}\varepsilon_0$ as the source of some constant quantity for which the electric field is the flux. Inserting Ohm's law, Eq. (1.5), into Eq. (2.5) and using Eq. (2.6), assuming constant κ and no sources or sinks, we obtain

$$\frac{\partial \rho_q}{\partial t} = -\frac{\kappa}{\varepsilon_\mathrm{r}\varepsilon_0}\rho_q. \tag{2.7}$$

The solution to Eq. (2.7) will be $\rho_q(t) = \rho_q(0)\mathrm{e}^{-\frac{t}{\varepsilon_\mathrm{r}\varepsilon_0/\kappa}}$. In the previous chapter, we argued that good performance of electrochemical devices requires high conductivity, usually $\kappa \gtrsim 1$ S/m. The resulting characteristic time-scale, $\varepsilon_0/\kappa \ll 10^{-11}$ s, is extremely small. This implies that any small charge imbalance will be restored almost instantaneously to give $\rho_q = 0$. Therefore, we can safely assume electroneutrality.

$$\rho_q = 0, \tag{2.8}$$

equation (2.5) gives:

$$\nabla \cdot \boldsymbol{i} = S. \tag{2.9}$$

Thus, in the absence of charge sources, the current is divergence-free. In Appendix 2.A, three more examples of conservation equations for mass, heat, and momentum are provided for readers needing more practice or familiarity.

2.2 Concentration overpotential

In the previous chapter we considered the concentration-dependent Tafel equations (1.29) and (1.31) for an oxidation and reduction reaction respectively. To avoid having to specify whether we describe an anode or a cathode we will use a general reactant concentration c and the current density magnitude j.[4] We can then write Eqs. (1.29) and (1.31) as

$$\eta = b\ln\left(\frac{j}{j_*}\frac{c_{\mathrm{eq}}}{c}\right) = b\ln\left(\frac{j}{j_*}\right) + b\ln\left(\frac{c_{\mathrm{eq}}}{c}\right). \tag{2.10}$$

The final term, the *concentration overpotential* introduced already in Eq. (1.30), increases when the concentration c at the surface of the electrode drops below the equilibrium concentration c_{eq}. This will generally happen as the reaction proceeds and the reactant concentration c locally decreases. The concentration difference with the unaltered bulk concentration, $c_{\mathrm{eq}} - c$, will drive the supply of fresh reactants to the electrode by diffusion.

Consider a steady-state without a concentration volume source, $S = 0$, so that Eq. (2.1) becomes $0 = -\nabla \cdot \boldsymbol{N}$. Here $\boldsymbol{N}$ is the molar flux of reactant with concentration c that is consumed at the electrode surface. Close to this electrode we can consider a one-dimensional approximation and introduce an x-coordinate normal to an electrode, with the electrode surface at $x = 0$, and positive values for x extending into the the electrolyte as shown in Fig. 2.1, so

$$\frac{\mathrm{d}N}{\mathrm{d}x} = 0. \tag{2.11}$$

Equation (2.2) in the x-direction, in the absence of flow, gives $N = -D\frac{\mathrm{d}c}{\mathrm{d}x}$. Inserting this into Eq. (2.11) shows that for constant diffusivity D, the concentration gradient $\mathrm{d}c/\mathrm{d}x$ is a constant, as depicted in Figure 2.1. Usually, at some distance from an electrode, the fluid flows can no longer be neglected due to intentional stirring, forced flow, gas bubbles, or natural convection due to concentration or temperature

[4] In case of a catalyst-coated or rough surface there may be a difference between the local current density $j_\perp$ and the overall current density magnitude j. We can take this into account by redefining or measuring the exchange current density j_* with respect to the macroscopic surface area.

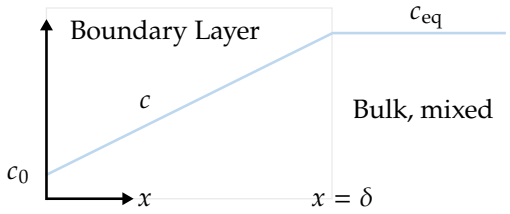

Figure 2.1: *A schematic of an idealised boundary layer concentration profile near an electrode. Within a distance $x < \delta$ no flow is assumed, giving a constant concentration gradient. Beyond $x > \delta$ exists a perfectly mixed bulk solution with reactant concentration c_{eq}.*

gradients. Beyond this distance, mixing will ensure a more or less constant bulk concentration. We will assume this to be equal to the concentration before the current was switched on so that we can use the equilibrium concentration c_{eq}.

Figure 2.1 depicts the often-used boundary layer idealisation that results from our assumptions, in which the domain is split into a no-flow region close to the electrode surface and a perfectly mixed bulk at a distance $x = \delta$ from the electrode. This is sometimes referred to as a Nernst layer, Nernst diffusion layer, or simply diffusion layer. This should not be confused with the electric double layer (EDL), which is typically several orders of magnitude thinner.

With this idealisation, the constant concentration gradient can be written as $\frac{dc}{dx} = \frac{c_{eq}-c_0}{\delta}$, with c_0 the concentration at the position of the electrode at $x = 0$. Faraday's law (1.19) gives for the electric current density magnitude $j = nF|N|$ or

$$j = nF\frac{D(c_{eq} - c_0)}{\delta} = j_{lim}\left(1 - \frac{c_0}{c_{eq}}\right). \tag{2.12}$$

Here the *limiting current density*

$$j_{lim} \equiv nF\frac{Dc_{eq}}{\delta}, \tag{2.13}$$

represents the maximum possible current, corresponding to the situation where $c_0 = 0$. A higher current density will not be possible with this boundary layer thickness δ, since diffusion cannot supply reactants at a higher rate. Inserting Eq. (2.12) into Eq. (2.10) gives

$$\boxed{\eta = b\ln\left(\frac{j/j_*}{1 - j/j_{lim}}\right) = b\ln\left(\frac{j}{j_*}\right) + b\ln\left(\frac{1}{1 - j/j_{lim}}\right).} \tag{2.14}$$

As j approaches the limiting current density j_{lim}, the concentration overpotential, represented by the last term in Eq. (2.14), diverges. As long as $j \ll j_{lim}$ the concentration at the electrode surface will remain relatively close to the equilibrium

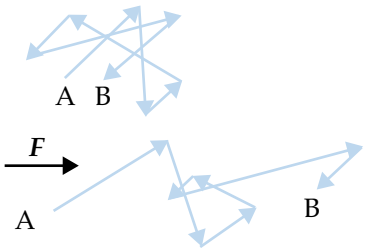

Figure 2.2: *Some particle trajectories of a molecule from A to B, where the changes in direction are due to collisions with other molecules, without a net force acting (top) and with a net force (bottom). An average drift velocity $\boldsymbol{u}_\mathrm{d} = \mathcal{M}\boldsymbol{F}$ can be associated with the force $\boldsymbol{F}$.*

concentration. In this case, the concentration overpotential will be well below the Tafel slope (typically of the order $b \sim 50$ mV) and can often be neglected.

In case the reactant is an ion, we will have to consider the effect of the electric force, which will be the topic of the next section.

2.3 Transport of charged species

Transport of ions is governed by the Nernst-Planck equation, which is a slight generalisation of the conservation equation (2.1) with the flux expression (2.2). By Newton's second law, the force on a charged particle in an electric field leads to a constant acceleration. In an electrolyte, these accelerating charged particles undergo frequent collisions with each other or other species, as illustrated in Figure 2.2. The combined effect of the acceleration in the direction of the electrical force $\boldsymbol{F}$ and these frequent collisions is a constant effective *drift velocity* in the direction of the force:

$$\boldsymbol{u}_\mathrm{d} = \mathcal{M}\boldsymbol{F}. \tag{2.15}$$

The constant of proportionality is called the mobility $\mathcal{M}$ [m/s/N]=[s/kg]. Also, macroscopic particles can have a mobility. This results from collisions with molecules observed as friction. This is considered, for the interested reader, in more detail in Appendix 2.C.

2.3.1 Boltzmann distribution

Not all molecules in a gas or a liquid move with the same velocity. In equilibrium thermodynamics, the probability of finding a particle with potential energy $\mathcal{U}$ is proportional to the Boltzmann factor $\mathrm{e}^{-\frac{\mathcal{U}}{k_\mathrm{B}T}}$, where the thermal energy $k_\mathrm{B}T$ is a measure of the average kinetic energy per particle.[5]

[5]The probability of finding a molecule with an energy between E and $E + dE$ is given by $f(E)dE$ with the probability density distribution $f(E)$ given by Boltzmann distribution $f(E) = \mathrm{e}^{-E/k_\mathrm{B}T}/k_\mathrm{B}T$,

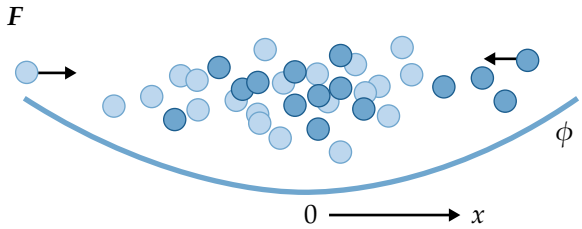

Figure 2.3: *Positively charged particles in thermal equilibrium near a minimum $\phi = 0$ in the electrical potential are distributed according to a Boltzmann distribution $\mathrm{e}^{-z\bar{\phi}}$. Exponentially fewer particles have sufficient kinetic energy to be found far away from the location where ϕ is a minimum, for example, near $x = 0$ when $\phi \propto x^2$.*

The Boltzmann constant can be expressed as $k_\mathrm{B} = \mathcal{R}/N_\mathrm{A}$, with N_A Avogadro's number and $\mathcal{R}$ the gas constant. The average kinetic energy of a mole of particles is therefore $N_\mathrm{A} k_\mathrm{B} T = \mathcal{R}T$. In the previous chapter, we encountered the Boltzmann distribution in the Arrhenius expression (1.21). The reaction rate is thus proportional to the chance that particles have a thermal energy per mole $\mathcal{R}T$ that exceeds the activation energy $\mathcal{E}_\mathrm{a}$. In Eq. (1.3) we introduced the potential energy $\mathcal{U} = q\phi$ of a charged particle in a electric potential field ϕ. We can write the charge q of a particle as a multiple, the charge number $\varkappa$, of the elementary charge (of a proton) $e = 1.602176634 \cdot 10^{-19}$ C as

$$q = \varkappa e. \tag{2.16}$$

In thermodynamic equilibrium, the concentration c of charged particles will be given by the Boltzmann distribution as

$$\boxed{c \propto \mathrm{e}^{-\frac{\mathcal{U}}{k_\mathrm{B}T}} = \mathrm{e}^{-\frac{q\phi}{k_\mathrm{B}T}} = \mathrm{e}^{-\varkappa\bar{\phi}}.} \tag{2.17}$$

In the second expression, we inserted Eq. (1.3) and in the third, we introduced the dimensionless electrostatic potential

$$\bar{\phi} = \frac{e\phi}{k_\mathrm{B}T} = \frac{F\phi}{\mathcal{R}T}. \tag{2.18}$$

Figure 2.3 schematically illustrates the Boltzmann distribution of Eq. (2.17) for positively charged particles in thermal equilibrium distributed around a minimum in the electrostatic potential.

---

which is normalised such that the probability of finding a particle at all $\int_0^1 f(E)dE = 1$. The average energy $\int_0^\infty Ef(E)dE$, is the thermal energy $k_\mathrm{B}T$. This exponential relation is the only function for which $f(E_1)f(E_2)$ is a function of $E_1 + E_2$. This should hold since the probability of finding two particles with energy E_1 and E_2 can only depend on the sum of their energies.

Symbol	Value	Unit	Description
$\mathcal{R}T/F = k_\mathrm{B}T/e$	≈ 0.025	V	Thermal potential
$\varkappa$	..-2,-1,0,1,2,...	-	Charge number, q/e
$\mathcal{R}$	8.314	J/mol/K	Ideal gas constant
e	$1.602 \cdot 10^{-19}$	C	Elementary charge
k_B	$1.38 \cdot 10^{-23}$	J/K	Boltzmann constant
F	96485.332	C/mol	Faraday constant

Table 2.1: *Constants and notation used throughout the book. The dimensionless ionic potential $\bar{\phi} = F\phi/\mathcal{R}T$ is obtained by dividing the ionic potential by the thermal potential, whose numerical value is provided for room temperature.*

Another example of the Boltzmann distribution can be found in how molecules of an ideal gas distribute themselves in the presence of gravity in an isothermal atmosphere, as discussed in Appendix 2.E.

2.3.2 Einstein relation

As discussed in the previous chapter, charged particles will experience an electric force given by Eqs. (1.1), (1.2), and (2.16) as

$$\boldsymbol{F} = -\varkappa e \nabla\phi. \tag{2.19}$$

This force will cause a drift velocity given by Eq. (2.15) as $\boldsymbol{u}_\mathrm{d} = -\varkappa e \mathcal{M} \nabla\phi$. For a dilute concentration c, so that the particle drift does not influence the flow velocity, we can simply add this drift velocity to the flow velocity in Eq. (2.2) to give

$$\boldsymbol{N} = \left(\boldsymbol{u} - \varkappa e \mathcal{M} \nabla\phi\right) c - D\nabla c. \tag{2.20}$$

In thermodynamic equilibrium, without any flux and fluid flow, the concentration c will satisfy the Boltzmann distribution Eq. (2.17). Differentiating Eq. (2.17) using the chain rule gives $\nabla c = -\varkappa c \nabla\bar{\phi}$, which upon insertion into Eq. (2.20) with $\boldsymbol{N} = \boldsymbol{u} = 0$ gives

$$\mathcal{M} = \frac{D}{k_\mathrm{B}T}. \tag{2.21}$$

This proportionality between the mobility and the diffusivity is called the Einstein-Smoluchowski equation.[6] Because the mobility and diffusion coefficient are determined by the same collision rate, this linear relation may also be appreciated intuitively.

[6] Although Smoluchowski and Sutherland derived the same relation independently around the same time, Albert Einstein published it in 1905. We derived it here for the case of an electrical force, but there are more *Einstein relations*. With Eq. (2.C.72), the Stokes-Einstein relation $D = \frac{k_\mathrm{B}T}{3\pi\mu d}$ results, which was used by Einstein to support the molecule hypothesis using observation of the diffusive Brownian motion of tiny dust particles. The mobility $\mathcal{M}$ is the ratio between drift velocity and force, while sometimes the *electrical mobility* $\mathcal{M}_q = \boldsymbol{u}_\mathrm{d}/\boldsymbol{E} = q\mathcal{M}$ is used so that the Einstein-Smoluchowski relation reads $D = k_\mathrm{B}T\mathcal{M}_q/q$.

2.3.3 Nernst-Planck flux

Inserting the Einstein relation (2.21) into Eq. (2.20) gives, using Eq. (2.18)

$$\boldsymbol{N} = c\boldsymbol{u} - D\left(\nabla c + \varkappa c \nabla\bar{\phi}\right). \tag{2.22}$$

This expression for the flux of charged particles is referred to as the Nernst-Planck flux. For neutral particles with $z = 0$, or in the absence of an electric field $\boldsymbol{E} = -\nabla\phi$, Eq. (2.22) reduces to Eq. (2.2). In the absence of flow and concentration gradients the flux

$$\boldsymbol{N}^{\text{mig}} = \frac{\varkappa F D c}{\mathcal{R}T}\boldsymbol{E}, \tag{2.23}$$

is solely due to the drift of charged particles constantly accelerating and colliding, a process sometimes referred to also as *migration* or *conduction*. We will sometimes use a superscript "mig" or "diff" to denote those parts of the flux that can be attributed to migration or diffusion, respectively. In this case, the concentration gradients and flow are negligible and a flux of charged particles leads to a current density that is proportional to the electric field. The proportionality constant, the conductivity κ, follows as

$$\boldsymbol{i} = \varkappa F \boldsymbol{N}^{\text{mig}} = \kappa \boldsymbol{E} \quad \text{where } \kappa = \frac{\varkappa^2 F^2 D c}{\mathcal{R}T}. \tag{2.24}$$

So we see that Ohm's law Eq. (1.5) also holds for charged particles in a well-mixed but otherwise stationary fluid.

We note that the Einstein relation, Eq. (2.21), with constant diffusivity, only holds for **dilute** mixtures, typically for concentrations well below 1 M. However, taking into account the concentration-dependence of the diffusivity D, the Nernst-Planck equation (2.22) can often be used as a reasonable approximation also at higher concentrations.

2.3.4 Multicomponent transport equations

As discussed in section 2.1.1, the charge density of an electrolyte can usually be considered to vanish, a condition referred to as electroneutrality or quasi-neutrality. Therefore, there have to be at least two charged species with opposite charges. We will label the different species[7] by an index i, not to be confused with the magnitude of the ionic current density, so that the Nernst-Planck flux of Eq. (2.22) becomes

$$\boxed{\boldsymbol{N}_i = c_i\boldsymbol{u} - D_i\left(\nabla c_i + \varkappa_i c_i \nabla\bar{\phi}\right).} \tag{2.25}$$

Each species diffuses with its own diffusivity D_i and migrates with its own mobility $D_i/k_{\text{B}}T$ but all share the same advection velocity $\boldsymbol{u}$ and potential ϕ. Each species individually satisfies a conservation equation Eq. (2.1)

[7] An example is the commonly used electrolyte sulphuric acid $H_2^+SO_4^{2-}$ dissolved in water. There will be a concentration c_1 with charge number $\varkappa_1 = 1$ of H^+ and a concentration c_2 with charge number $\varkappa_2 = -2$ of SO_4^{2-}. The charge density $\rho_q = \varkappa_1 c_1 + \varkappa_2 c_2 = 0$ so that $c_1 = 2c_2$, so there are twice as many H^+ compared to SO_4^{2-}.

$$\boxed{\frac{\partial c_i}{\partial t} = -\nabla \cdot \boldsymbol{N}_i + S_i.} \tag{2.26}$$

Eqs. (2.25) and (2.26) together are called the Nernst-Planck equation or equations.[8]

The charge flux, or species current density, associated with $\boldsymbol{N}_i$ is $\varkappa_i F \boldsymbol{N}_i$ so that the total current density reads

$$\boxed{\boldsymbol{i} = \sum \varkappa_i F \boldsymbol{N}_i,} \tag{2.28}$$

where the summations here and below are understood to be over the index i. Inserting Eq. (2.25) into Eq. (2.28) gives

$$\boxed{\boldsymbol{i} = \rho_q \boldsymbol{u} - F \sum \varkappa_i D_i \nabla c_i + \kappa \boldsymbol{E},} \tag{2.29}$$

where the charge density can be usually assumed to be zero in accordance with Eq. (2.8):

$$\rho_q = F \sum \varkappa_i c_i = 0, \tag{2.30}$$

and the ionic conductivity follows as

$$\boxed{\kappa = \frac{F^2}{\mathcal{R}T} \sum \varkappa_i^2 D_i c_i.} \tag{2.31}$$

Note from Eqs. (2.29) and Eq. (2.30) that the fluid velocity $\boldsymbol{u}$ does not influence the current of a quasi-neutral electrolyte, since anions and cations are advected equally. The linear dependence of conductivity on electrolyte concentration in Eq. (2.31) only holds for dilute electrolytes. Often, there is a maximum conductivity so that at higher concentrations, the electrolyte conductivity again decreases with increasing electrolyte concentrations.

In the **absence of concentration gradients**, Eq. (2.29) gives Ohm's law $\boldsymbol{i} = \kappa \boldsymbol{E}$, introduced in Eq. (1.5). Equation (2.31) generalises Eq. (2.24) to include the effect of several ions. The relative contribution of each species to the conductivity is expressed by the ion transport number or **transference number**

$$t_i = \left.\frac{\varkappa_i F N_i}{i}\right|_{\substack{u=0 \\ \nabla c=0}} = \frac{\varkappa_i^2 D_i c_i}{\sum \varkappa_i^2 D_i c_i}. \tag{2.32}$$

[8] Inserting (2.25) and assuming incompressible flow Eq. (2.A.61) and a divergence-free electric field by Eq. (2.6) and constant D_i gives

$$\frac{\partial c_i}{\partial t} + \left(\boldsymbol{u} + \boldsymbol{u}_{\mathrm{d},i}\right) \cdot \nabla c_i = D_i \nabla^2 c_i + S_i, \tag{2.27}$$

an advection-diffusion-reaction equation like Eq. (2.A.62) but with an additional drift velocity $\boldsymbol{u}_{\mathrm{d},i} = -D_i \varkappa_i \nabla \tilde{\phi}$.

In the absence of concentration gradients $\nabla c = 0$ this number expresses the fraction of the flux that is carried by a species.[9] By construction, they add up to unity $\sum t_i = 1$.

2.4 Binary electrolytes

2.4.1 General binary electrolytes

An important class of electrolytes is the binary electrolyte, which contains only two ions, one anion A and one cation C. Strong acids and bases show complete dissociation of their salts upon dissolving in water

$$\mathrm{AC} \rightarrow \nu_- \mathrm{A}^{z_-} + \nu_+ \mathrm{C}^{z_+}. \tag{2.33}$$

Here z_- and z_+ represent the ion valencies and ν_- and ν_+ are the stoichiometric coefficients of the ions in the salt. For those in need of more practice with ion transport, appendix 2.F considers two examples of monovalent binary electrolytes, the acidic $\mathrm{H^+Br^-}$ used in redox flow batteries, and the alkaline $\mathrm{K^+OH^-}$ used in water electrolysis. Footnote 7 considers the divalent electrolyte $\mathrm{H_2SO_4}$, which has $z_+ = 1$ and $z_- = -2$ and $\nu_+ = 2$ and $\nu_- = 1$ since it dissociates into two $\mathrm{H^+}$ and one $\mathrm{SO_4^{2-}}$ ion. $\mathrm{CuSO_4}$ on the other hand has $z_+ = -z_- = 2$ and $\nu_- = \nu_+ = 1$, because it dissociates into one $\mathrm{Cu^{2+}}$ and one $\mathrm{SO_4^{2-}}$ ion. In general, charge conservation requires

$$\nu_+ z_+ + \nu_- z_- = 0. \tag{2.34}$$

Therefore, we can define the salt concentration as

$$c \equiv \frac{c_+}{\nu_+} = \frac{c_-}{\nu_-}, \tag{2.35}$$

equal to the number of moles of dissolved salt AC per unit volume. Note that the salt concentration may not be equal to the ion concentration.

2.4.2 Monovalent binary electrolytes

Here we will outline the equations describing a monovalent binary electrolyte, $z_+ = -z_- = \nu_+ = \nu_- = 1$, reserving the general case of arbitrary valencies and stoichiometries for Appendix 2.G. We will assume that the ion diffusivities D_- and D_+ are constant. The electroneutrality condition (2.30) for a monovalent binary electrolyte gives $c_+ - c_- = 0$, which is automatically satisfied using a single salt concentration $c \equiv c_+ = c_-$. Equation (2.32) gives

[9] Sometimes in literature, this additional restriction of zero concentration gradient is not added. In this case, instead of a material parameter, the transference number becomes dependent on the particulars of the situation considered and which species reacts for example.

$$t_+ = \frac{D_+}{D_+ + D_-} \text{ and } t_- = \frac{D_-}{D_+ + D_-}, \tag{2.36}$$

satisfying $t_+ + t_- = 1$. Equation (2.25) gives

$$\boldsymbol{N}_+ = c\boldsymbol{u} - D_+ \left(\nabla c + c\nabla\bar{\phi}\right), \tag{2.37}$$

$$\boldsymbol{N}_- = c\boldsymbol{u} - D_- \left(\nabla c - c\nabla\bar{\phi}\right). \tag{2.38}$$

Equation (2.26) allows us to write

$$t_- \left(\frac{\partial c}{\partial t} + \nabla\cdot\boldsymbol{N}_+ - S_+\right) + t_+ \left(\frac{\partial c}{\partial t} + \nabla\cdot\boldsymbol{N}_- - S_-\right) = 0, \tag{2.39}$$

because the expressions between brackets vanish individually.

Using $t_+ + t_- = 1$

$$\frac{\partial c}{\partial t} + \nabla\cdot\boldsymbol{N} = S, \tag{2.40}$$

where $S \equiv t_-S_+ + t_+S_-$ and the *salt flux*

$$\boldsymbol{N} \equiv t_-\boldsymbol{N}_+ + t_+\boldsymbol{N}_- = c\boldsymbol{u} - D_\mathrm{a}\nabla c. \tag{2.41}$$

The *ambipolar diffusivity* or *salt diffusivity* D_a is defined as

$$\boxed{D_\mathrm{a} \equiv t_-D_+ + t_+D_- = \frac{2D_+D_-}{D_+ + D_-}.} \tag{2.42}$$

For an incompressible flow $\nabla\cdot\boldsymbol{u} = 0$ and Eq. (2.40) can be further simplified to

$$\boxed{\frac{Dc}{Dt} = D_\mathrm{a}\nabla^2 c.} \tag{2.43}$$

Note that the potential has disappeared from Eqs. (2.40) and (2.43) because $t_-\boldsymbol{N}_+^{\mathrm{mig}} + t_+\boldsymbol{N}_-^{\mathrm{mig}} = 0$ and. Remarkably, we have obtained an advection diffusion equation, similar to that of a neutral species. However, through the boundary conditions, the electric field may still affect the solution. The influence of the electric field may also be seen in the definition of the effective diffusion coefficient, Eq. (2.42). Due to electro-neutrality, there is an electrostatic connection between the ions, and together they can only move as fast as the slowest ion. The faster ions are held back by slower ions by electrostatic forces, and the slower ions are pulled along by the faster ones. If the ionic diffusivities are very different, D_a is about twice the lowest value.[10] The reason for this doubling is that the transport by migration is effectively included

[10] If $D_+ \gg D_-$ we have $D_\mathrm{a} \approx 2D_-$ while if $D_- \gg D_+$ we have $D_\mathrm{a} \approx 2D_+$

in the diffusivity. If the ion diffusivities are equal, there is no electrostatic tethering between ions and the ambipolar diffusivity becomes equal to the ion diffusivity.

The current density of Eq. (2.29) gives with $c_+ = c_- \equiv c$

$$\boldsymbol{i} = F\left(D_- - D_+\right)\nabla c + \kappa \boldsymbol{E}, \tag{2.44}$$

The first part gives the *diffusion current density*, proportional to the difference in ion diffusivities. In agreement with Eq. (2.31), the conductivity reads

$$\kappa = \frac{F^2}{\mathcal{R}T}\left(D_+ + D_-\right)c. \tag{2.45}$$

Note that, while the diffusion current is proportional to the difference in ion diffusivities, the conduction current is proportional to their sum. Using Eq. (2.45), Eq. (2.44) can alternatively be written as

$$\boldsymbol{i} = -\kappa\left(\chi\frac{\nabla c}{c} + \nabla\phi\right), \tag{2.46}$$

where $\chi \equiv \frac{\mathcal{R}T}{F}\frac{D_+ - D_-}{D_+ + D_-}$. This characteristic diffusion potential is rarely much larger than around 10 mV, so that often, but not always, the diffusion current can be neglected. In this case, the current in a binary electrolyte can be approximately described by Ohm's law $\boldsymbol{i} = -\kappa\nabla\phi$, where the conductivity depends on the ion concentration c through Eq. (2.45).

In case of a constant current boundary condition, we see from Eq. (2.44) that the electric field determines the concentration gradient boundary condition to Eq. (2.40) or (2.43).

2.4.3 Zero-flux ion

An often-encountered case in which we can analytically solve for the concentration profile is when only one of the ions in the binary electrolyte has a non-zero flux. The other ion has a zero flux.[11]

This happens, for example, when only one of the ions in a binary electrolyte participates in a steady-state reaction. In alkaline water electrolysis, for example, the cation K^+ does not react. It will have a net average zero flux in a steady state.

Let us consider the case of *a monovalent binary electrolyte with a zero-flux cation* for definiteness. The opposite case of a zero-flux anion is readily obtained by switching all + and − signs. We consider the case of a stagnant layer of thickness δ. This may be, for example, inside a microporous diaphragm with small enough pores to avoid fluid flow. It may also serve as a crude description of a hydrodynamic boundary layer.

[11] This happens, for example, near an ion exchange membrane, which only allows cations (PEM, proton exchange membrane) or anions (AEM, anion exchange membrane) to pass through. Such ions are 'blocked' while the term 'immobile' or 'fixed' ions is typically reserved for ions in a membrane.

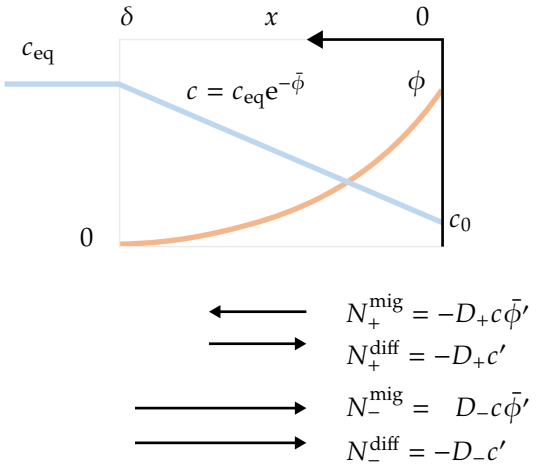

Figure 2.4: *The concentration and potential profiles in a stagnant layer between $x = \delta$, where the concentration is at its bulk value c_{eq} and $x = 0$, where the concentration c is lower. A zero-flux-cation's migration and diffusion fluxes cancel each other, which means they add for the anion. Note that the arrow sizes indicate that $D_- > D_+$.*

In the wall-normal direction, the assumption of a cation with zero flux in a stagnant layer allows us to write Eq. (2.37), for the cation flux, as

$$N_+ = -D_+ \left(c' + c\bar{\phi}'\right) = 0. \tag{2.47}$$

Here N_+ is used to denote the vector component of $\boldsymbol{N}_+$ in the x-direction, presently under consideration, so that it can also be negative. A prime indicates a derivative with respect to x, so $c' = \mathrm{d}c/\mathrm{d}x$.

Eq. (2.47) is solved by the Boltzmann distribution $c = c_{eq}e^{-\bar{\phi}}$. This is expected, actually by construction, since the cations with zero flux are in thermodynamic equilibrium.[12] Here c_{eq} is the equilibrium bulk at $x = \delta$, where we take $\bar{\phi} = 0$, as illustrated in Figure 2.4.

Equation (2.38) gives the anionic flux in the x-direction as

$$N_- = -D_- \left(c' - c\bar{\phi}'\right). \tag{2.48}$$

This flux is now solely responsible for the ionic current density[13] $i = -FN_-$. Equation (2.47) gives $c' = -c\bar{\phi}'$, which inserted into Eq. (2.48) allows $i = D_- F \left(c'_- - c\bar{\phi}'\right)$ to be written as

[12] This is by construction, as this solution was actually used to derive the Einstein equation (2.21) used to formulate the Nernst-Planck equations.

[13] We will use i to denote the x-component of the ionic current density so i_x, dropping the sub-script x. This can, therefore, be positive or negative. Note that this contrasts with our use of j, which we use to denote the magnitude of the electronic current density, which is always positive.

$$\boxed{i = -2D_- Fc\bar{\phi}' = 2D_- Fc'_-.} \tag{2.49}$$

The current can thus be described as a pure migration current, proportional to ϕ', or as a pure diffusion current density, proportional to c'. Or, of course, by the combination of both, which it really is. Both diffusion and migration will drive the current, but because these effects contribute in a fixed proportion, we can write the current density using either of the two terms. The reason for this fixed proportion is that the fluxes due to diffusion and migration have to be equal and opposite for the cation with zero flux, as described by Eq. (2.47). As a consequence, the diffusion and migration fluxes are equal and of the same sign for the other ion. This is schematically depicted by the arrows at the bottom of Fig. 2.4. In the case of a monovalent binary electrolyte, exactly half the current is transported by diffusion and the other half by migration. In Appendix 2.G.2 a general binary electrolyte is considered.

Note that we can reuse the analysis of section 2.2 concerning the concentration overpotential, where we also considered a Nernst boundary layer. Comparing Eq. (2.49) with Eq. (2.12), we see that we have to replace D with $2D_-$. The limiting current density of Eq. (2.13) then becomes

$$j_{\text{lim}} \equiv nF\frac{2D_- c_{\text{eq}}}{\delta}. \tag{2.50}$$

Here n denotes the number of electrons per reactant molecule. In the case of a redox reaction involving a monovalent binary electrolyte, generally $n = 1$. Using Eqs. (2.36) and (2.42)

$$2D_- = \frac{D_{\text{a}}}{1 - t_-}. \tag{2.51}$$

The equations in this section are often found in the literature with the expression on the right-hand side instead of the left-hand side of Eq. (2.51).[14]

2.5 Supporting electrolyte

In the previous section we found that for a steady-state monovalent binary electrolyte without flow, half the current is carried by diffusion and half by migration. To reduce the ohmic losses associated with migration, sometimes a *supporting electrolyte* is added. This electrolyte is not involved in the reaction, but the additional ions do increase the conductivity through Eq. (2.31) and, therefore, reduce the potential gradient required for migration. It may seem somewhat strange at first that a species that does not contribute to the transport can do this, so the sceptical reader is referred

[14] One reason may be because of its natural generalisation to multi-component electrolytes. In case of a single ion i with a net flux we have $\boldsymbol{i} = \varkappa_i F\boldsymbol{N}_i = -\varkappa_i FD_i\left(\nabla c_i + \varkappa_i c_i \nabla\bar{\phi}\right) = -\varkappa_i FD_i \nabla c_i - t_i\kappa\nabla\phi$. When concentration gradients are small we can substitute the bulk relation $\boldsymbol{i} = -\kappa\nabla\phi$ to give $\boldsymbol{i} = \varkappa_i F\boldsymbol{N}_i \approx -\frac{\varkappa_i FD_i}{1-t_i}\nabla c_i$. This approximate relation looks similar to the exact Eq. (2.49) that can, with Eq. (2.51), be written as $i = -\frac{D_{\text{a}}\varkappa_- F}{1-t_-}c'_-$.

to the derivation in Appendix 2.G.3. The main outcome of this analysis is that *when the supporting electrolyte concentration far exceeds the reactant concentration, the electric field and its effect through migration can be neglected*. Adding a supporting electrolyte essentially has the same effect as adding more of the reactant ion species. Equations (2.G.104) and (2.G.106) give, with the index i for the reacting ion and c_{supp} the concentration of the supporting electrolyte,

$$\frac{i}{\nu_i F} = 2D_i c_{\text{supp}} \bar{\phi}' = -D_i c_i'. \tag{2.52}$$

As in the case of a binary electrolyte, Eq. (2.49), the current density can be written in terms of a pure diffusion current or a migration current, or a combination, because they are proportional. The first relation in Eq. (2.52) is similar to the first of Eq. (2.49) for a binary electrolyte. The difference is, however, that the concentration in Eq. (2.52) is not that of the reacting ion, but the concentration of the supporting electrolyte. Therefore, the supporting electrolyte concentration can be increased to reduce the potential gradient $\bar{\phi}'$. The second expression in Eq. (2.52) differs from that in Eq. (2.49) in that the additional factor two is missing.

The reason is that the potential gradient is strongly reduced due to the presence of the supporting electrolyte. Therefore, there can be little migration and the current is determined solely by diffusion. This reduces the limiting current density to

$$j_{\text{lim}} \equiv nF \frac{D_i c_{\text{eq}}}{\delta}, \tag{2.53}$$

so without the additional factor two of Eq. (2.50) due to migration. A small downside of adding a supporting electrolyte is thus a reduced limiting current density.

Note that the negligible electric field strength allows the reacting ion concentration to be described by an advection-diffusion equation. Equation (2.27) without the effect of migration becomes (2.3). The difference with the advection-diffusion equation derived for a binary electrolyte, Eq. (2.43), is the diffusion coefficient. Instead of the ambipolar diffusion coefficient, in the presence of a supporting electrolyte, it is the ion with a non-zero flux whose diffusivity appears. Also, the boundary conditions will be different. We summarise the differences between the case of a single ion with a non-zero flux in a binary electrolyte and a supporting electrolyte in Table 2.2.

2.6 Transient diffusion, constant current, Sand's analysis

We end this chapter by considering our first transient case. Shortly after a current is switched on, a growing boundary layer will arise in a stagnant electrolyte as illustrated in Figure 2.5. An analytical solution can be derived for a semi-infinite domain, as is outlined in Appendix 2.H. However, a more heuristic approach [4] is almost as accurate but arguably more insightful. Consider a neutral reactant or a reacting ion in a supporting electrolyte, with concentration c and diffusion coefficient

	Binary electrolyte	Supporting electrolyte
Diffusion coefficient	D_a	D_i
Conductivity $\lvert i\rvert/\lvert\nabla\phi\rvert$	$2D_i\frac{F^2}{\mathcal{R}T}c_i$	$2D_i\varkappa_i\frac{F^2}{\mathcal{R}T}c_\mathrm{supp}$
Boundary condition for c_i'	$-i/2FD_i\varkappa_i$	$-i/F\varkappa_i D_i$
Limiting current density j_lim	$2nFD_i\lvert c_0'\rvert$	$nFD_i\lvert c_{i,0}'\rvert$

Table 2.2: *The differences between a monovalent binary electrolyte and a supporting electrolyte with concentration c_supp in which a single non-zero-flux-ion with charge number $\varkappa_i$ and a concentration c_i carries the current. In the case of a binary electrolyte, generally, the number of electrons per reactant molecule $n = \lvert\varkappa_i\rvert$.*

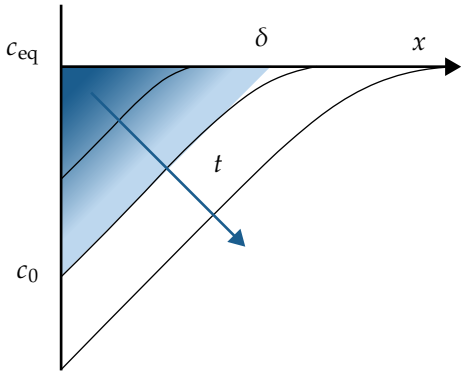

Figure 2.5: *Reactant concentration profiles $c(x,t)$ for various times t due to step change in current over time. The shaded blue triangle graphically depicts the linearisation approximation used Eq.* (2.56).

D. The reactant diffusive flux in the x-direction $N_x = -Dc' < 0$ so that the associated current is given by $j = nF\lvert N_x\rvert$. We consider the case in which the electrode potential is adjusted such that the current density becomes constant. Equation (2.52) gives the following boundary condition

$$c_0' = \frac{j}{nFD}. \tag{2.54}$$

Here a subscript 0 indicates the electrode surface at $x = 0$. Integrating Eq. (2.4) with respect to time t and dividing by the electrode area A gives the number of moles of reactant consumed per unit area as

$$\int \left(c_\mathrm{eq} - c\right)\mathrm{d} = \lvert N_x\rvert t = \frac{jt}{nF}. \tag{2.55}$$

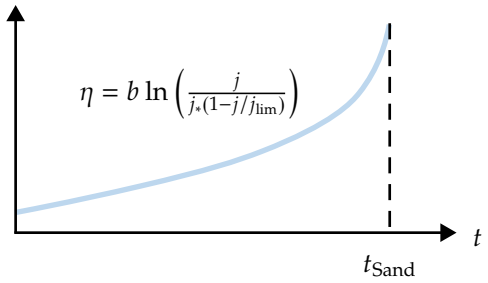

Figure 2.6: *The concentration overpotential increases with time and diverges as the surface concentration drops to zero at $t = t_{\text{Sand}}$.*

The integral can be accurately approximated by the shaded area indicated in Figure 2.5. The area of this triangle is given by half the boundary layer thickness δ times $c_{\text{eq}} - c_0 = c_0'\delta$, so

$$\frac{c_0'\delta^2}{2} \approx \frac{jt}{nF}. \tag{2.56}$$

This gives an expression for the boundary layer thickness $\delta \approx \sqrt{2Dt}$, which is close to the exact result derived in the appendix, Eq. (2.H.109):

$$\boxed{\delta \approx 2\sqrt{Dt/\pi}.} \tag{2.57}$$

The surface concentration $c_0 = c_{\text{eq}} - \delta c_0'$ follows, using Eq. (2.54), as

$$c_0 = c_{\text{eq}}\left(1 - \frac{j}{j_{\text{lim}}}\right), \tag{2.58}$$

where

$$j_{\text{lim}} = \frac{nFDc_{\text{eq}}}{\delta} = \frac{nFDc_{\text{eq}}}{2\sqrt{Dt/\pi}}. \tag{2.59}$$

The surface concentration c_0 decreases in time according to Eq. (2.58). This gives rise to a concentration overpotential that increases in time, as described by Eq. (2.14). When the concentration c_0 approaches zero, the overpotential diverges. This is schematically shown in Figure 2.6.

The requested constant current density can be maintained by increasing the overpotential. However, after some time the electrode concentration $c_0 = 0$ and the current density will have to decrease in time as the boundary layer thickness δ continues to increase while the concentration difference $c_{\text{eq}} = c_0$ cannot be increased

further. These limiting current conditions are reached after a time called Sand's time given by solving $j = j_{\text{lim}}$, using Eq. (2.59) as

$$t_{\text{Sand}} = \frac{\pi D}{4j^2}\left(nFc_{\text{eq}}\right)^2. \tag{2.60}$$

We note that when one of the ions of a binary electrolyte reacts, this same analysis holds using $D = 2D_i$, with D_i the diffusivity of the reacting ion. In this case, the ohmic drop will increase in time in addition to this overpotential activation since the ionic conductivity is proportional to the decreasing electrolyte concentration.

2.7 Summary

- The Nernst-Planck flux $\boldsymbol{N}_i = c_i\boldsymbol{u} - D_i\left(\nabla c_i + \varkappa_i c_i \frac{F}{\mathcal{R}T}\nabla\phi\right)$ (2.25) of a dilute ion concentration accounts for advection, diffusion, and migration, respectively. In the absence of flow and concentration gradients, the conductivity $\kappa = \boldsymbol{i}/\boldsymbol{E} = -\sum \varkappa_i F\boldsymbol{N}_i/\nabla\phi = \frac{F^2}{\mathcal{R}T}\sum \varkappa_i^2 D_i c_i$ (2.31). A zero-flux ion with $\boldsymbol{N}_i = 0$ in the absence of flow satisfies the Boltzmann distribution $c_i \propto \mathrm{e}^{-\frac{\varkappa_i F}{\mathcal{R}T}\phi}$.

- The general conservation equations $\frac{\partial c_i}{\partial t} = -\nabla\cdot\boldsymbol{N}_i$ (2.26) for a *binary* electrolyte and incompressible flow reduce to an advection-diffusion equation $\frac{\partial c}{\partial t} + \boldsymbol{u}\cdot\nabla c = D_{\text{a}}\nabla^2 c$ (2.43) with the ambipolar diffusivity $D_{\text{a}} = \frac{2D_+D_-}{D_+ + D_-}$. Without flow and for a monovalent cation with no flux, the anion flux $\boldsymbol{N}_- = 2D_- c\nabla\frac{F}{\mathcal{R}T}\phi = -2D_-\nabla c$ (2.49) equals twice the diffusion or migration flux since both are equal because $\boldsymbol{N}_+ = 0$. A supporting electrolyte strongly increases the conductivity, suppressing the electric field and associated migration, halving the limiting current density.

- The concentration overpotential $b\ln\left(\frac{c_{\text{eq}}}{c}\right)$ (2.10) diverges as c approaches zero. Without advection or migration, this happens at a limiting current density $j_{\text{lim}} = \frac{nFDc_{\text{eq}}}{\delta}$ (2.13). At constant current, the boundary layer thickness $\delta \approx 2\sqrt{Dt/\pi}$ is obtained after Sand's time $t_{\text{Sand}} = \frac{\pi D}{4j^2}\left(nFc_{\text{eq}}\right)^2$ (2.60).

2.8 Exercises

Exercise 2.1

Consider a fuel cell cathode in which oxygen, with a concentration c in air, reacts with protons to water.

a. What is the number n of electrons consumed per oxygen molecule in this reaction?
b. Give an expression for the limiting current density, assuming the oxygen molecules have to diffuse through an air layer of thickness L with a diffusivity D.
c. Now assume that this 'gas diffusion layer' consists of straight channels with a volume fraction ϵ in a solid. Give an expression for the limiting current density.

Exercise 2.2

Consider the porous separator inside a Li-ion battery, filled with the monovalent binary electrolyte $Li^+PF_6^-$. The electrolyte effective conductivity is $\kappa = 1.3$ S/m. The cathode where Li^+ is reduced is at $x = 0$ on the left, and the anode where it is oxidised is at $x = L$ on the right. Assume: 1D, steady-state, no flow, a temperature of 300 K, and a constant average electrolyte concentration $c = 800$ mol/m^3.

a. Derive an expression for the Li^+ diffusivity D_+ in terms of the ambipolar diffusivity D_a and the transfer coefficient $t_+ \equiv \frac{D_+}{D_+ + D_-}$.
b. Derive the electrolyte concentration profile for a given current density j.
c. Use the given conductivity $\kappa = 1.3$ S/m and cation transfer number $t_+ = 0.4$ to give a numerical value for the ambipolar diffusivity D_a.
d. Assuming $L = 200$ µm, what is the associated characteristic time-scale for diffusion $t \sim L^2/D_a$? Is the assumption of steady-state warranted? Give an expression for the magnitude of the limiting current density

Exercise 2.3

In electrolysers, a concern is hydrogen 'crossing over' through the membrane or separator to the anode, where at sufficiently high concentrations it could reach the 'lower explosion limit' of about 4 vol% hydrogen in oxygen.

a. If hydrogen is present at a concentration c_0 at the cathode and an approximately zero concentration at the anode, calculate the diffusive flux N_0 through a membrane with thickness L and effective diffusivity D
b. Now if there is a small pressure difference, perhaps because after start-up the pressure rises faster at the cathode due to the larger volume of gases produced, there may be a small flow velocity u through the separator from cathode to anode. The hydrogen flux in the x-direction from $x = 0$ at the cathode to $x = L$ at the anode is now given by $N = uc - D\frac{\mathrm{d}c}{\mathrm{d}}$. Assuming a steady state, give the concentration profile through the membrane.

c. Give an expression for the flux N in terms of the Péclet number $\mathrm{Pe} = uL/D$ and the flux N_0 without advection.

d. Considering a typical alkaline water electrolyser separator with an effective oxygen diffusion coefficient $D = 10^{-9}$ m^2/s and thickness $L = 0.5$ mm, at what velocity is diffusive flux doubled due to advection?

Exercises 2.4-2.19

Fill in the missing steps in the main text, indicated by the symbol .

*Appendices **

2.A *Examples of conservation equations*

2.A.1 *Mass*

Eq. (2.1) is a general conservation equation that can describe various conserved quantities, such as mass. Instead of the molar concentration c we can use the density ρ [kg/m^3]. Without diffusion, the mass flux reads $\rho\boldsymbol{u}$ so that without mass sources, $S = 0$, Eq. (2.1) gives $D\rho/Dt = -\rho\nabla\cdot\boldsymbol{u}$. Moving along with the fluid flow, the density of most fluids stays approximately constant so that $D\rho/Dt = 0$. Even compressible fluids often approximately satisfy this criterion at flow velocities well below the speed of sound. Combining these two equations gives the equation describing *incompressible flow* as

$$\nabla\cdot\boldsymbol{u} = 0. \tag{2.A.61}$$

In this book, generally, divergence-free flow is assumed to hold.

2.A.2 *Heat*

The thermal diffusivity is expressed as $\alpha = \lambda/\rho C_\mathrm{p}$ [m^2/s] with λ the thermal conductivity [W/m/K] and C_p [J/kg/K] the specific heat capacity. Replacing c by the volumetric thermal energy $\rho C_\mathrm{p} T$ [J/m^3] and D by α in Eq. (2.2) gives without flow, $\boldsymbol{u} = 0$, and constant ρC_p

$$\boldsymbol{N} = -\lambda\nabla T, \tag{2.A.62}$$

which is called Fourier's law. Eq. (2.3) becomes, again for constant ρC_p

$$\frac{DT}{Dt} = \alpha\nabla^2 T + \frac{S}{\rho C_\mathrm{p}}. \tag{2.A.63}$$

The heat source S [W/m^3] may include for example viscous heating or a source from an exothermic reaction.

2.A.3 *Momentum*

Equation (2.1) can also be used to describe the conservation of momentum, by replacing c in Equation (2.1) with the momentum density $\rho \boldsymbol{u}$. Because this is a vector, the flux $\boldsymbol{N}$ is replaced by a tensor $\boldsymbol{\tau}$, representing the momentum flux or force per unit area. For *Newtonian fluids* the viscous stress tensor, $\boldsymbol{\tau} = \mu \left(\nabla \boldsymbol{u} + \nabla \boldsymbol{u}^{\mathrm{T}}\right)$, is proportional to the dynamic viscosity μ. An additional force in fluids is due to pressure p, which adds $p\boldsymbol{I}$, with $\boldsymbol{I}$ the unit tensor. Finally adding the convective part $\rho \boldsymbol{u}\boldsymbol{u}$ gives

$$\frac{\partial \rho \boldsymbol{u}}{\partial t} = -\nabla \cdot \left(\mu \left(\nabla \boldsymbol{u} + \nabla \boldsymbol{u}^{\mathrm{T}}\right) + p\boldsymbol{I} + \rho \boldsymbol{u}\boldsymbol{u}\right) + S. \tag{2.A.64}$$

For a constant density and viscosity, assuming the flow is incompressible as described by Eq. (2.A.61), using some vector and tensor relations this can be simplified to the incompressible Navier-Stokes equation

$$\frac{D\boldsymbol{u}}{Dt} = \nu \nabla^2 \boldsymbol{u} - \frac{\nabla p}{\rho} + \frac{S}{\rho}, \tag{2.A.65}$$

where $\nu = \mu/\rho$ is the kinematic viscosity. The source term S/ρ represents any additional force per unit mass, for example, due to gravity $\frac{S}{\rho} = -g\hat{\boldsymbol{z}}$ for a gravitational acceleration g [m/s^2] in the negative z-direction.

2.B *Stefan velocity*

The fickian diffusion flux in Eqs. (2.2) and (2.22) assumes that the concentration of the transported species c is much smaller than the total concentration C of the gas or liquid through which it is transported. If this were not the case, the concentration could influence the density, diffusivity, and other material parameters. Additionally, the flow velocity $\boldsymbol{u}$ cannot be seen as independent and is impacted by the moving species. To illustrate this, we consider the following example of a layer in which a species with a concentration c is transported from $x = 0$ to $x = L$ with constant flux, for example, because it is produced in a reaction and otherwise accumulates. Another species with concentration $\tilde{c}$ is assumed to have zero flux $\tilde{N}_x = u\tilde{c} - D\tilde{c}' = 0$, where D is the mutual diffusion coefficient. Especially in gases, to a good approximation, the total concentration $C = c + \tilde{c}$ is constant. This allows us to write

$$\tilde{N}_x = u\,(C - c) + D\tilde{c}' = 0, \tag{2.B.66}$$

so that the flux of the species with flux reads

$$N_x = uc - Dc' = uC. \tag{2.B.67}$$

We can solve the differential equation (2.B.66) to give

$$c(x) = C - (C - c(0))\,\mathrm{e}^{ux/D}. \tag{2.B.68}$$

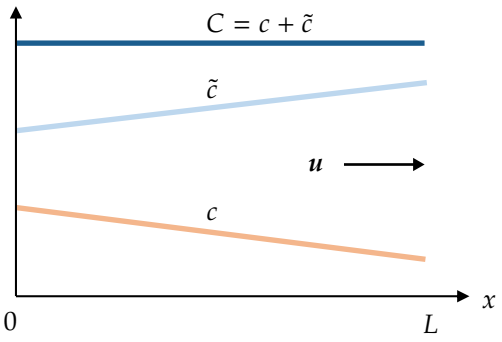

Figure 2.7: *The concentrations c and $\tilde{c}$ of a species, with and without flux, respectively, adding up to a constant concentration C. The mass transport of the finite-flux species to the right introduces a Stefan flow velocity $\boldsymbol{u}$ that counteracts the diffusion flux of the zero-flux species.*

So we see that to maintain a zero flux of one species a velocity is induced, which makes the concentration of the reacting species vary exponentially with x. This velocity arises due to the transport of the mobile species and is called the Stefan velocity. As the concentration $c(x)$ decreases in the x-direction, the concentration $\tilde{c}$ has to increase. The Stefan velocity counteracts the diffusion flux that would otherwise force the zero-flux species to $x = 0$. Solving Eq. (2.B.68) for u and inserting in Eq. (2.B.67) gives, evaluated at $x = L$

$$N_x = \frac{DC}{L} \ln\left(\frac{C - c(L)}{C - c(0)}\right). \tag{2.B.69}$$

For low concentrations $c \ll C$ we can linearise this to give Fick's law $N_x = \frac{D}{L}(c(0) - c(L))$ and Eq. (2.B.68) to give the linear profile $c(x) = c(0) - u\frac{C-c(0)}{D}x$.

2.C *Mobility of a macroscopic particle*

For a mass moving with a velocity u relative to a fluid in rest, in response to a force $\boldsymbol{F}$, we can write Newton's second law as follows:

$$m\frac{d\boldsymbol{u}}{dt} = \boldsymbol{F} + \boldsymbol{F}_\mathrm{d}. \tag{2.C.70}$$

Here $\boldsymbol{F}_\mathrm{d}$ is a frictional force or a drag force. Larger objects will experience a drag force approximately proportional to their velocity squared, due to inertial forces. For smaller particles viscous forces dominate. For small spherical particles, their velocity magnitude u relative to the fluid velocity and diameter d may be small enough that their particle Reynolds number $\mathrm{Re}_\mathrm{p} = \frac{\rho u d}{\mu} \ll 1$. In this case, the flow around them,

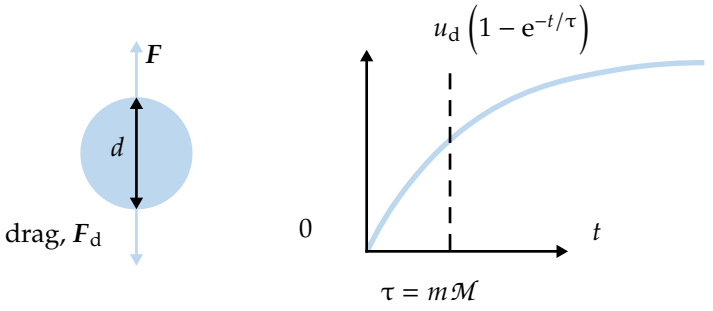

Figure 2.8: *An example particle with diameter d moving upwards due to a force $\boldsymbol{F}$. A drag force $\boldsymbol{F}_d = -\boldsymbol{u}_d/\mathcal{M}$ acts to decelerate the particle, resulting in the shown velocity profile.*

called Stokes flow, can be solved analytically neglecting fluid inertia. The resulting Stokes drag force is given by

$$\boldsymbol{F}_d = -3\pi\mu d\boldsymbol{u}. \tag{2.C.71}$$

This drag force is opposite and proportional to the particle velocity $\boldsymbol{u}$ relative to the fluid, which we assume here to have a vanishing or at least constant velocity. In steady state $d\boldsymbol{u}/dt = 0$ and Eq. (2.C.70) gives $\boldsymbol{F} = -\boldsymbol{F}_d = 3\pi\mu d\boldsymbol{u}_d$ where $\boldsymbol{u}_d$ is the steady-state velocity. The subscript d here stands for drag, or for drift considered in the next section. Comparing with Eq. (2.15) we see that

$$\mathcal{M} = \frac{1}{3\pi\mu d}. \tag{2.C.72}$$

So the mobility of a small spherical particle is inversely proportional to its size and the liquid viscosity.

Solving Eq. (2.C.70) with initial condition $\boldsymbol{u} = 0$ at $t = 0$ gives

$$\boldsymbol{u}(t) = \boldsymbol{u}_d\left(1 - e^{-\frac{t}{\tau}}\right), \tag{2.C.73}$$

where $\boldsymbol{u}_d = \mathcal{M}\boldsymbol{F}$ is the final steady-state velocity and the relaxation time $\tau = m\mathcal{M}$ is proportional to both the object's mass and mobility. With $m = \rho_p\pi d^3/6$ the product of the particle density ρ_p and its volume, and Eq. (2.C.72) we obtain $\tau = \frac{\rho_p d^2}{18\mu}$. With a typical $\mu/\rho_p = 10^{-6}$ m^2/s a particle with a diameter of $d = 1$ µm gives $\tau \approx 6 \cdot 10^{-8}$ s and a particle with a diameter of $d = 1$ mm has a relaxation time of $\tau \approx 0.06$ s. Therefore, for small enough particles, the acceleration phase is only very short and assuming a steady-state force equilibrium with a constant particle velocity is a good approximation under many circumstances.

2.D *Simple conductance model*

We consider a constant charge density ρ_c *of charge carriers*, for example, electrons in a wire or transported ions in an electrolyte. An equal and opposite charge density of counterions will usually ensure a zero charge density. From the analysis of a macroscopic particle in the previous section 2.C, we found that the mobility $\mathcal{M} = \tau/m$ is proportional to the force equilibration time τ and inversely proportional to the particle mass. This will also hold for electrons or ions if we re-interpret τ as the characteristic time between collisions. By Eq. (2.C.71), a particle experiencing an electric force $\boldsymbol{F} = q\boldsymbol{E}$, Eq. (1.1), gives a drift velocity $\boldsymbol{u}_\mathrm{d} = \mathcal{M}\boldsymbol{F} = \frac{q\tau}{m}\boldsymbol{E}$. The charge flux or the current density reads $\boldsymbol{i} = \rho_c \boldsymbol{u}_d$ in agreement with the general Eq. (2.2). We thus naturally recover Ohm's law $\boldsymbol{i} = \kappa\boldsymbol{E}$ which states a proportionality between current density and electric field. The conductivity

$$\kappa = \frac{\rho_c q \tau}{m}. \tag{2.D.74}$$

In this model, a simplification of the model proposed in 1900 by Paul Drude, the conductivity is proportional to the density of charge carriers and their charge squared, since also ρ_c is proportional to the carrier charge. This is in agreement with the result of Eq. (2.31), derived from the Nernst-Planck equation.

2.E *Boltzmann atmosphere*

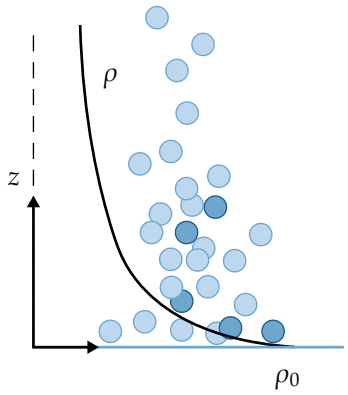

Figure 2.9: *Density distribution $\rho(z)$ as a function of the height of an ideal isothermal atmosphere satisfying the Boltzmann distribution.*

For those readers seeking to get more familiar with the Boltzmann distribution, we consider here the example of an isothermal atmosphere satisfying the ideal gas law. The electric force $\boldsymbol{F} = -q\nabla\phi$ has a strong resemblance to the gravitational force, which is also a conservative force. The gravitational force is also proportional to the

gradient of a scalar, the gravitational potential. An obvious difference is of course that mass, unlike charge, can only be positive.

First, we obtain the hydrostatic force balance assuming zero flow velocity $\boldsymbol{u} = 0$ in the Navier-Stokes Equation (2.A.65) and considering only the direction of gravity, the z-direction:

$$\frac{dp}{dz} = -\rho g. \tag{2.E.75}$$

The ideal gas law can be written as:

$$p = \frac{\mathcal{R}T}{\mathcal{V}_\mathrm{m}} = \frac{\rho \mathcal{R}T}{M}, \tag{2.E.76}$$

where $\mathcal{V}_\mathrm{m} = M/\rho$ [m^3/mol] is the molar volume, with M [kg/mol] the molarity.

Inserting Eq. (2.E.76) in Eq. (2.E.75) gives

$$\frac{d\rho}{dz} = -\frac{\rho}{H} \rightarrow \rho = \rho_0 \mathrm{e}^{-\frac{z}{H}} \quad \text{with } H = \frac{\mathcal{R}T}{gM}. \tag{2.E.77}$$

The density in an isothermal atmosphere thus satisfies the Boltzmann distribution and decreases exponentially with height z from its value ρ_0 at ground level, $z = 0$. The characteristic atmosphere "height" $H \approx 9$ km, using the molarity of air and $T \approx 300$ K. Although our atmosphere is far from isothermal, most mass is roughly within twice this distance.

The argument of the exponent can be written as $-\frac{z}{H} = -\frac{\mathcal{E}_\mathrm{a}}{\mathcal{R}T} = -\frac{\mathcal{U}}{k_\mathrm{B}T}$ with $\mathcal{E}_\mathrm{a} = gMz$ and $\mathcal{U} = gmz$ the average gravitational potential energy per mole or particle, respectively. Therefore, an isothermal ideal gas under the influence of a conservative force satisfies the Boltzmann distribution. The premise of section 2.3.1 is that ions in an electric field will equally satisfy this distribution.

2.F *Balance sheets*

2.F.1 *Example: hydrogen-bromine redox flow battery*

Consider a membrane-less cell with two electrodes far apart and the liquid electrolyte in between well-mixed. In this case, the electrolyte concentration is fairly constant in the centre, while concentration gradients can arise in thin boundary layers near the electrode, see Figure 2.10. Often only one of the ions in an electrolyte participates in a reaction. As an example, we consider the charging reaction of a hydrogen-bromine (H_2Br_2) redox flow battery:[15]

$$2\mathrm{Br}_- \rightarrow 2\mathrm{e}^- + \mathrm{Br}_2, \tag{2.F.78}$$

$$2\mathrm{e}^- + 2\mathrm{H}^+ \rightarrow \mathrm{H}_2. \tag{2.F.79}$$

[15]Note that in Fig. 2.10 we draw the oxidation reaction on the left and the reduction reaction on the right. In batteries, the electrode at which the oxidation reaction occurs is called the anode during discharging, but the cathode during charging. So, as an exception, we here have the cathode on the left.

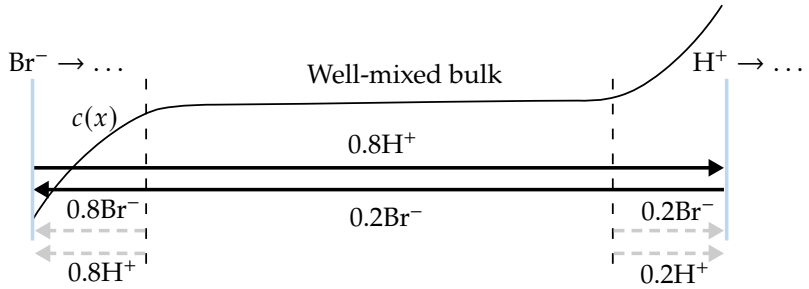

Figure 2.10: *The charging of a H_2-Br_2 flow battery, schematically split into a bulk region with only migration and a boundary layer region with also diffusion. The solid black arrows denote migration fluxes while the grey dashed arrows indicate diffusion fluxes. The difference in transference numbers $t_+ = 0.8$ and $t_- = 0.2$ is compensated by diffusion in the boundary layers near the electrodes.*

Because of its smaller size, the diffusivity of H^+ is substantially higher than that of Br^- so that the H^+ ions (protons) have an approximate transference number of $t_+ \approx 0.8$. In the well-mixed bulk, the electrolyte concentration is approximately constant, and diffusion does not play a role. As shown in Eq. (2.32), transference numbers can be used to indicate the fraction of the current carried by a particular ion in the absence of concentration gradients. Therefore, migration transports about four times as much H^+ in the direction of the electric field, to the right in Figure 2.10, as it transports Br^- in the opposite direction. However, by the reactions of Eqs. (2.F.78) and (2.F.79), equal amounts of H^+ and Br^- are consumed, so how can this be?

At the electrodes, there will be no fluid flow possible so the well-mixed condition cannot extend all the way to the electrode and there will be a diffusion boundary layer close to the electrodes. Here, diffusion will have to make up for the difference in transference number. Near the left Br^--consuming electrode a concentration gradient will arise that will aid the transport of Br^- but oppose the transport of H^+, cancelling the migration flux of H^+. Similarly, at the right H^+-consuming electrode, this concentration gradient will be much smaller since a smaller migration flux of Br^- has to be cancelled.

Note that in these reactions the electrolyte is consumed so that, to obtain a steady charging reaction, fresh electrolyte has to be supplied by advection. A flow velocity parallel to the electrodes will add additional fluxes, but since these will not contribute to the current, they do not impact the general picture of Fig. 2.10.

2.F.2 *Example: alkaline water electrolysis*

A typical electrolyte used in alkaline water electrolysis is potassium hydroxide, which dissociates into K^+ ions and OH^- ions. The diffusivity of K^+ ions is about three times smaller than that of OH^- so that $t_+ \approx 0.25$ and $t_- \approx 0.75$. In the reactions given by Eqs. (1.14) and (1.15), the potassium ion does not participate, so in steady-state and

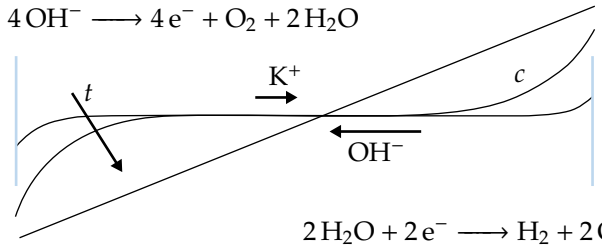

Figure 2.11: *The evolution from an initial concentration profile c to a steady state in alkaline water electrolysis. Initially, the situation is similar to that in Fig. 2.10: in the bulk, there are no concentration gradients and there is only migration. The transported K^+ does not participate in the reaction but moves from the anode on the left, where OH^- is consumed, to the cathode on the right where it is produced, to maintain charge neutrality. In the boundary layers, a concentration gradient arises in which diffusion and migration cancel for K^+, but add for OH^-. In the final steady state, this holds throughout the electrolyte.*

in the absence of flow, it has zero flux. Therefore, a concentration gradient arises that assists the transport of OH^- and completely cancels that of K^+. Figure 2.11 schematically shows the evolution of the concentration profile over time in an unstirred electrolyte, inside a porous diaphragm for example. Initially, diffusion will only play a role in very thin boundary layers near the electrodes. Eventually, the concentration profile will be fully developed and the concentration gradient will be constant. In this steady state, the diffusion flux exactly cancels the migration flux of K^+ so that the net flux is zero. For the OH^- ion, the diffusion and migration fluxes add, as is considered in more detail in section 2.4.3.

2.G *General binary electrolytes*

2.G.1 *General equations*

Here we consider the case of a general binary electrolyte

$$AC \rightarrow \nu_- A^{z_-} + \nu_+ C^{z_+}, \tag{2.G.80}$$

with arbitrary ion charge numbers z_+ and z_- and stoichiometries ν_+ and ν_-. Charge conservation requires

$$\nu_+ z_+ + \nu_- z_- = 0. \tag{2.G.81}$$

We can define the salt concentration as

$$c \equiv \frac{c_+}{\nu_+} = \frac{c_-}{\nu_-}. \tag{2.G.82}$$

Electroneutrality requires $\rho_q = F \sum z_i c_i$ or with $i = +, -$

$$\varkappa_+ c_+ + \varkappa_- c_- = 0. \tag{2.G.83}$$

Using this in in Eq. (2.32) gives

$$t_\pm = \frac{\varkappa_\pm^2 D_\pm c_\pm}{\varkappa_+^2 D_+ c_+ + \varkappa_-^2 D_- c_-} = \frac{|z_\pm| D_\pm}{\varkappa_+ D_+ - \varkappa_- D_-}. \tag{2.G.84}$$

The conservation equations for the cations and anions read, respectively:

$$\frac{\partial c_+}{\partial t} + \nabla \cdot \boldsymbol{N}_+ - S_+ = \frac{\partial c_-}{\partial t} + \nabla \cdot \boldsymbol{N}_- - S_- = 0, \tag{2.G.85}$$

where, from Eq. (2.25)

$$\boldsymbol{N_+} = c_+ \boldsymbol{u} - D_+ \left(\nabla c_+ + \varkappa_+ c_+ \nabla \bar{\phi} \right), \tag{2.G.86}$$

$$\boldsymbol{N_-} = c_- \boldsymbol{u} - D_- \left(\nabla c_- + \varkappa_- c_- \nabla \bar{\phi} \right). \tag{2.G.87}$$

Therefore,

$$\frac{t_-}{\nu_+} \left(\frac{\partial c_+}{\partial t} + \nabla \cdot \boldsymbol{N}_+ - S_+ \right) + \frac{t_+}{\nu_-} \left(\frac{\partial c_-}{\partial t} + \nabla \cdot \boldsymbol{N}_- - S_- \right) = 0. \tag{2.G.88}$$

With $t_+ + t_- = 1$ and some vector algebra this gives

$$\frac{\partial c}{\partial t} + \nabla \cdot \boldsymbol{N} + \boldsymbol{i} \cdot \frac{\nabla t_+}{F} = S, \tag{2.G.89}$$

where $S \equiv \frac{t_- S_+}{\nu_-} + \frac{t_+ S_-}{\nu_+}$ and

$$\boldsymbol{N} \equiv \frac{t_- \boldsymbol{N}_+}{\nu_+} + \frac{t_+ \boldsymbol{N}_-}{\nu_-} = c\boldsymbol{u} - D_\mathrm{a} \nabla c, \tag{2.G.90}$$

and the ambipolar diffusivity D_a is defined as:

$$D_\mathrm{a} \equiv t_- D_+ + t_+ D_- = \frac{(\varkappa_+ - \varkappa_-) D_+ D_-}{\varkappa_+ D_+ - \varkappa_- D_-}. \tag{2.G.91}$$

The current density of Eq. (2.29) gives, with $c_- = \varkappa_+ c_+ / \varkappa_-$ from Eq. (2.34),

$$\boldsymbol{i} = F (D_- - D_+) \varkappa_+ \nabla c_+ + \kappa \boldsymbol{E}, \tag{2.G.92}$$

where, from Eq. (2.31), the conductivity reads

$$\kappa = \frac{F^2}{\mathcal{R}T} (\varkappa_+ D_+ - \varkappa_- D_-) \varkappa_+ c_+. \tag{2.G.93}$$

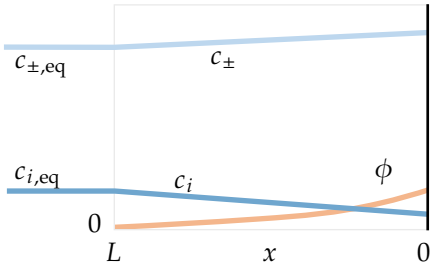

Figure 2.12: *The nernstian layer configuration we consider for the description of a ternary electrolyte. An ion i reacts at $x = 0$, while the supporting electrolyte with concentration $c_\pm$ has zero flux.*

2.G.2 *Nernstian boundary layer with a cation with zero flux*

Without flow, Eq. (2.G.86) for a zero-flux cation gives

$$\frac{N_+}{\nu_+} = -D_+\left(c' + \varkappa_+ c\bar{\phi}'\right) = 0. \tag{2.G.94}$$

The solution is a Boltzmann distribution $c = c_{\mathrm{eq}}\mathrm{e}^{-\varkappa_+\bar{\phi}}$, with c_{eq} the concentration at $x = \delta$, where we take $\bar{\phi} = 0$, as illustrated in Figure 2.4. The anionic flux

$$\frac{N_-}{\nu_-} = -D_-\left(c' + \varkappa_- c\bar{\phi}'\right), \tag{2.G.95}$$

determines $i = \varkappa_- F N_-$. The Boltzmann distribution gives $c' = -\varkappa_+ c\bar{\phi}'$ so

$$-\frac{i}{D_- z_- \nu_- F} = c' + \varkappa_- c\bar{\phi}' = c'\left(1 - \frac{\varkappa_-}{\varkappa_+}\right) = \left(\varkappa_- - \varkappa_+\right) c\bar{\phi}', \tag{2.G.96}$$

or

$$i = -D_-\varkappa_- F\left(\varkappa_- - \varkappa_+\right) c_-\bar{\phi}' = -D_-\left(1 - \frac{\varkappa_-}{\varkappa_+}\right)\varkappa_- F c'_-. \tag{2.G.97}$$

The additional factor $1 - \varkappa_-/\varkappa_+$ represents the additional transport due to migration. This becomes the factor two used for a monovalent binary electrolyte as obtained in Eq. (2.49). The limiting current of Eq. (2.13) is thus also proportionally larger

$$j_{\mathrm{lim}} \equiv nF\frac{\left(1 - \frac{\varkappa_-}{\varkappa_+}\right) D_- c_{\mathrm{eq}}}{L}. \tag{2.G.98}$$

2.G.3 *Ternary electrolyte*

We now consider what happens if we add a third species. In this *ternary electrolyte*, we assume that only one species, with concentration c_i, is transported; for example, because it reacts at $x = 0$. The remaining binary electrolyte with concentrations c_+ and c_- is assumed to satisfy $N_+ = N_- = 0$. This gives a Boltzmann distribution for the zero-flux cations

$$c_+ = c_{+0}\mathrm{e}^{-\varkappa_+\bar{\phi}}, \tag{2.G.99}$$

and the zero-flux anions

$$c_- = c_{-0}\mathrm{e}^{-\varkappa_+\bar{\phi}}. \tag{2.G.100}$$

According to electroneutrality

$$c_i = -\frac{\varkappa_+ c_+ + \varkappa_- c_-}{\varkappa_i}. \tag{2.G.101}$$

Since the i-th species is the only one contributing to the current, we have $j = \varkappa_i F N_i$. The Nernst-Planck equation (2.25) in the absence of advection ($\boldsymbol{u} = 0$) gives $N_i = -D_i\left(c_i' + \varkappa_i c_i \bar{\phi}'\right)$ so that

$$\frac{i}{-\varkappa_i F D_i} = c_i' + c_i\varkappa_i\bar{\phi}' = \left(\frac{\mathrm{d}c_i}{\mathrm{d}\bar{\phi}} + c_i\varkappa_i\right)\bar{\phi}' \tag{2.G.102}$$

$$= \left(\varkappa_+ c_+\left(\frac{\varkappa_+}{\varkappa_i} - 1\right) + \varkappa_- c_-\left(\frac{\varkappa_-}{\varkappa_i} - 1\right)\right)\bar{\phi}'. \tag{2.G.103}$$

In the second step, we used that c_i through Eqs. (2.G.99), (2.G.100), and (2.G.101) is a function of $\bar{\phi}$ so we can use the chain rule to write $\frac{\mathrm{d}c_i}{\mathrm{d}x} = \frac{\mathrm{d}c_i}{\mathrm{d}\bar{\phi}}\frac{\mathrm{d}\bar{\phi}}{\mathrm{d}x}$. In the final step we used Eqs. (2.G.99) and (2.G.100), which give $\frac{\mathrm{d}\bar{\phi}}{\mathrm{d}\bar{\phi}} = -\varkappa_+ c_+$ and $\frac{\mathrm{d}c_-}{\mathrm{d}\bar{\phi}} = -\varkappa_- c_-$, respectively.

For example, in case of a monovalent electrolyte with a reacting anion we have $\varkappa_i = \varkappa_- = -\varkappa_+ = -1$ so that $\varkappa_-/\varkappa_i = 1$, and $\varkappa_+/\varkappa_i = -1$. In this case Eq. (2.G.103) simplifies to

$$i = -2FD_i c_+ \bar{\phi}'. \tag{2.G.104}$$

The current is proportional to the ion diffusivity D_i as expected. However, interestingly and importantly, the current is proportional to the supporting binary electrolyte concentration $c_+ = c_-$ rather than the concentration c_i. Equation (2.G.103) gives

$$\frac{i}{FD_i} = c_i' - c_i\bar{\phi}' = c_i'\left(1 + \frac{c_i}{2c_+ - c_i}\right), \tag{2.G.105}$$

where, in the second step we compared with Eq. (2.G.104) to give $c_i' = (c_i - 2c_+)\,\bar{\phi}'$ or $\bar{\phi}' = \frac{c_i'}{c_i - 2c_+}$. Sometimes a large surplus of binary electrolyte, a supporting electrolyte, is added to a reacting species. In this case $\frac{c_i}{2c_+ - c_i} \approx \frac{c_i}{2c_+} \ll 1$, and Eq. (2.G.105) can be further simplified into:

$$i = FD_i c_i'. \tag{2.G.106}$$

As in the case of a binary electrolyte, we can again write the current density in terms of only diffusion, now with only the properties of the reacting ion playing a role. We have $\bar{\phi}' = \frac{c_i'}{c_i - 2c_+} \approx \frac{c_i'}{-2c_+}$ so that with $c_+ \gg c_i$ the variation in $\bar{\phi}$ is much small smaller than one and the potential variations are small compared to the thermal potential $\frac{\mathcal{R}T}{F} \sim 25$ mV. The large conductivity introduced by the supporting electrolyte ensures the electric field is small, even though the supporting electrolyte ions do not move. The small electric field makes that migration can be neglected with respect to diffusion, resulting in Eq. (2.G.106).

2.H *Transient diffusion: Sand's solution*

The one-dimensional diffusion equation (2.3) in the absence of flow, $\boldsymbol{u} = 0$, and sources $S = 0$ reads

$$\frac{\partial c}{\partial t} = D\frac{\partial^2 c}{\partial x^2}. \tag{2.H.107}$$

The analytical solution with boundary condition (2.54) and $c(x \to \infty) = c_{\mathrm{eq}}$ reads

$$c(x,t) = c_{\mathrm{eq}} - c_0'\left\{\frac{\Delta x}{\sqrt{\pi}}\mathrm{e}^{-\left(\frac{x}{\Delta x}\right)^2} - x\left[1 - \mathrm{erf}\left(\frac{\Delta x}{x}\right)\right]\right\}, \tag{2.H.108}$$

where $\Delta x = 2\sqrt{Dt}$. For $x \to 0$ this gives

$$c_0 = c_{\mathrm{eq}} - \frac{c_0'\Delta x}{\sqrt{\pi}}. \tag{2.H.109}$$

Chapter 3

Porous electrodes

Using porous electrodes, the area available for redox reactions can be increased by many orders of magnitude, strongly reducing the activation overpotentials. However, a porous electrode that is too thick will reduce the "electrode effectiveness factor". This concept will be very useful in describing electrolysers, fuel cells and batteries in the subsequent chapters.

3.1 Porous structure

Porous electrodes are characterised by a large number of voids or *pores* inside the electrode volume. As a result, the total *internal* surface area can be much higher than its *external* surface area. Electrolyte ions, reactants, and products can diffuse or sometimes flow through the pores of the electrode. Figure 3.1 illustrates flow streamlines through a polydisperse spherical arrangement. Electrons can flow through the *matrix*, or the solid part, of the material.

When the porous material is not sufficiently reactive, a thin layer of small (nano-)particles can be used as a coating to create a large number of active sites. In this case, the porous material is just a support or substrate for the catalyst and additionally provides conductivity for electrons. Sometimes, binder materials or solid polymer electrolytes are also added to provide ionic conductivity.

3.1.1 Porosity

Most porous electrodes do not have a regular repeating structure, but their pore geometry is stochastic. Instead, these media are characterised by spatially averaged properties like porosity and tortuosity. The porosity can be defined by either volume fraction or area fraction:

$$\epsilon = \frac{\mathcal{V}_{\text{pore}}}{\mathcal{V}} = \frac{A_{\text{pore}}}{A}, \tag{3.1}$$

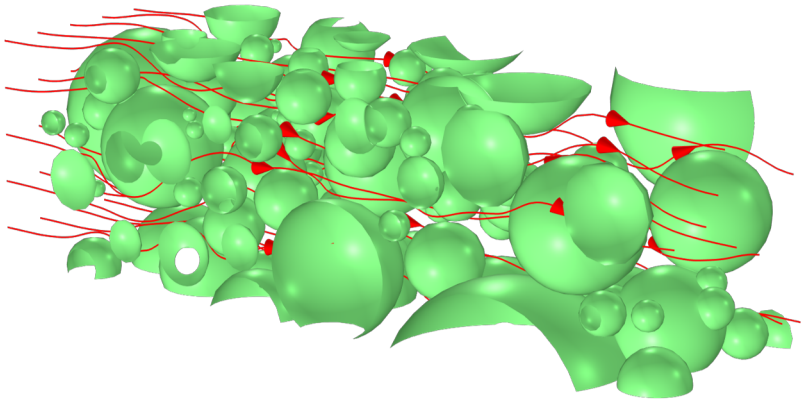

Figure 3.1: *A visualisation of the flow streamlines or ion trajectories inside a porous medium consisting of a polydisperse arrangement of spheres. Image made using the COMSOL Multiphysics® software; provided courtesy of COMSOL.*

$\mathcal{V}_{\text{pore}}$ is the void volume and A_{pore} is the average void area of the cross-section. In general, the volume and area ratios in Eq. (3.1) may be different and vary in space. However, these two definitions can be shown to give the same result for the random isotropic materials considered here.

3.1.2 Tortuosity

The English word tortuous is the antonym of straight: full of bends and twists. For a porous medium, we may define the tortuosity loosely as

$$\tau = \frac{l_{||}}{l}. \tag{3.2}$$

In Figure 3.1, the streamlines travel a longer distance, $l_{||}$, than the shortest path l, which is a straight line. By construction, the tortuosity τ is always equal to or larger than one. Since not all particles will traverse the same distance $l_{||}$, this definition is mathematically not very rigorous. However, this should not bother us here. A high tortuosity is usually not desired because longer path lengths increase resistance and pressure drops and decrease diffusion rates.

3.1.3 Volumetric surface area

The *volumetric surface area*[1] is the combined total external surface area A_{s} per unit of total volume $\mathcal{V}$

[1]The quantity a is often referred to as *specific surface area*specific surface area, although this term should, strictly speaking, perhaps be reserved for the amount of surface area per unit mass.

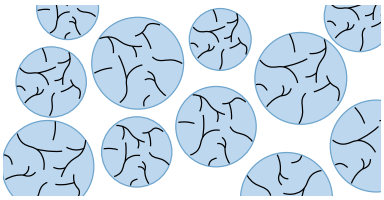

Figure 3.2: *A doubly porous medium with pores in between spherical particles which are themselves also porous.*

$$a \equiv \frac{A_\mathrm{s}}{\mathcal{V}}. \tag{3.3}$$

Often, porous electrodes consist of a collection of solid particles.[2] If these particles are all of similar size, we can write

$$\boxed{a = (1-\epsilon)\, a_\mathrm{s},} \tag{3.4}$$

where $a_\mathrm{s} \equiv A_\mathrm{s}/\mathcal{V}_\mathrm{s}$ is the volumetric surface area of a single particle: the ratio of its area A_s and volume $\mathcal{V}_\mathrm{s}$. The subscript 's' here stands for surface, but for electrodes consisting of solid particles, it also stands for solid. For spherical particles of diameter d

$$a = \frac{6\,(1-\epsilon)}{\mathrm{d}}. \tag{3.5}$$

An inverse relationship between particle size and volumetric surface area generally holds for any shape. Rescaling all particles making up a porous electrode to half their geometrical size doubles the surface area without requiring any additional material. This is particularly important when the catalyst is very precious, for example, platinum or iridium. It explains why in fuel cells, for example, preferably Pt nanoparticles are used. These provide maximum surface area per unit weight.[3]
Note that in case the particles making up the porous medium themselves are also porous, as illustrated in Figure 3.2, Eq. (3.4) may still be used. In this case, a_s should include both internal and external particle surface area.

3.1.4 Superficial, interstitial, and local velocity

When a fluid flows through a porous medium, we can define its velocity in several ways. In this section, we will only consider velocity magnitudes, but in general, these

[2]Particles can be coalesced using heating or sintered so that they form a solid electrode. In pocket electrodes, fine particles are kept within a metallic perforated metal sock. With A_i and $\mathcal{V}_i$ the surface area and volume of the individual particles, $\sum_i \mathcal{V}_i$ gives the total particle volume and, since $1-\epsilon$ is the fraction of particles, $V = \sum_i \mathcal{V}_i/(1-\epsilon)$. With $A_\mathrm{s} = \sum_i A_i$, Eq. (3.3) gives $a = (1-\epsilon)\,\frac{\sum_i A_i}{\sum_i \mathcal{V}_i}$.

[3]Below several nanometres, more subtle molecular quantum effects start to play a role, and fabricating even smaller particles is not necessarily worthwhile.

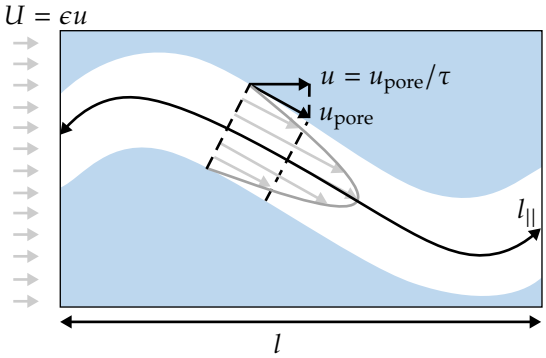

Figure 3.3: *An idealisation of a porous medium as a bundle of capillaries of which one is shown. The superficial velocity U that enters moves faster inside the pores where there is less space to give an interstitial velocity $u = U/\epsilon$. Because only part of the velocity is in the main flow direction, the average pore velocity $u_{\text{pore}} = u\tau$ is even faster. The peak velocities inside the pore can still be faster. Here the porosity and tortuosity $\epsilon = \mathcal{V}_{\text{pore}}/\mathcal{V}$ and $\tau = l_{||}/l$.*

will be vectors which have a direction.

Pore velocity

The first, perhaps most obvious, velocity we can define is by looking inside a pore and measuring the velocity. This varies locally in magnitude and direction; for example, it becomes zero at the solid surface due to the no-slip condition. Therefore, we will average the velocity over the pore's cross-section to obtain the velocity magnitude, u_{pore}. An idealisation that is often made especially for hydraulic calculations is replacing the porous medium with a bundle of capillaries. Fig. 3.3 illustrates one such a capillary. This approach has many conceptual difficulties, but the didactic benefits arguably outweigh them. In this picture, the average pore velocity is an average over a single pore, which should then be representative of the entire porous medium.

Interstitial velocity

Because usually, the streamlines are not straight, there will be an average flow direction and magnitude that we will refer to as the *interstitial velocity* u. This is the volume-averaged velocity *in the main flow direction*. Volume-averaging the flow velocity magnitude gives the pore velocity, but averaging the velocity vectors and then taking the magnitude gives the interstitial velocity. In the latter procedure, any component not in the main flow direction averages out to zero.

The difference between pore velocity and interstitial velocity relates to the tortuosity. Consider Fig. 3.3 again. A fluid parcel moving with the average pore velocity u_{pore} takes a time $l_{||}/u_{\text{pore}}$ to move from the entrance to the exit of the indicated region. With u as the average velocity in the main flow direction and l as the shortest

distance of the pore in this direction, this residence time can be equally written as l/u. Therefore, with the tortuosity $\tau = l_{||}/l$ of Eq. (3.2), we obtain

$$u = \frac{u_{\text{pore}}}{\tau}. \tag{3.6}$$

The interstitial velocity is thus lower compared to the pore velocity by a factor given by the tortuosity.

Superficial velocity

A third velocity, the *superficial* velocity U can be defined as the fluid's velocity in the absence of the solid, assuming an equal volumetric flow rate. Alternatively, it is the bulk velocity of the fluid before entering the porous medium or after leaving it, when the total cross-sectional stays constant, see Fig. 3.3. Since the solid takes up part of the flow area, the interstitial flow velocity u inside the porous medium will be higher. Assuming incompressible flow, the flow rate AU equals $A_{\text{pore}}u$. Using Eq. (3.1), we find

$$U = \epsilon u = \epsilon \frac{u_{\text{pore}}}{\tau} \tag{3.7}$$

The superficial velocity U is lower than the average interstitial velocity u due to the reduced volume fraction ϵ available for the flow. In turn, the interstitial velocity is lower than the average pore velocity u_{pore} because it does not include all the deviations from the main flow direction introduced by the tortuosity.

3.1.5 Effective diffusivity in porous materials

When modelling the transport of species through a porous medium, computationally, we may resolve its full concentration in space and time. A two-dimensional example, for a neutral species, is depicted in Figure 3.1. Without a flow and no source, S, Eq. (2.3) becomes

$$\frac{\partial c}{\partial t} = D_{\text{m}} \nabla^2 c. \tag{3.8}$$

Here, we added a subscript m for the *molecular* diffusivity D_{m} in an electrolyte, to distinguish it from the effective diffusion coefficient D that we will introduce in a moment.[4] The local flux inside a pore $\boldsymbol{N}_{\text{pore}} = -D_{\text{m}} \nabla c$. However, often, we are not interested in the detailed concentration profile but rather in the average concentration and superficial flux in the direction of transport. Therefore, we average the partial differential equation (3.8) over all directions except the transport x-direction, to give an ordinary differential equation

[4]Most texts use a subscript "eff" to denote an effective diffusion coefficient D_{eff}. To keep the notation to a minimum, and since D_{m} is a special case of D without a porous medium, we only highlight the difference when otherwise confusion could arise.

$$\frac{\partial \epsilon c}{\partial t} = D \frac{\mathrm{d}^2 c}{\mathrm{d}x^2}. \tag{3.9}$$

We use the same symbol c in both equations but do realise that, while in Eq. (3.8) c depends on x, y, and z, in Eq. (3.9) it is averaged over y and z to become a function only of x. In Eq. (3.9), D is an effective diffusion coefficient that will be proportional to the molecular diffusivity D_m but will also depend on the structure of the porous electrode in a manner we will now investigate.

Consider a concentration difference Δc between two locations in Fig. 3.1 a distance l apart in the x-direction, amounting to a longer distance $l_\parallel$ inside the pores. Similar to Eq. (3.7) we can write the superficial molar flux $N = D\Delta c/l$ as

$$N = \epsilon \frac{N_\mathrm{pore}}{\tau}. \tag{3.10}$$

Since $N = D\Delta c/l$ and $N_\mathrm{pore} = D_\mathrm{m}\Delta c/l_\parallel$ we find

$$\boxed{D = \frac{\epsilon}{\tau^2} D_\mathrm{m}.} \tag{3.11}$$

Compared to Eq. (3.7) there is an additional factor τ, which has been missed by several authors before [11]. It derives from the factor that the local concentration gradients are inversely proportional to $l_\parallel$ instead of l, giving an additional factor $\tau = l_\parallel/l$.[5]

The exact same effects of porosity and tortuosity also play a role for conduction of ions through a porous medium.[6] The local version of Ohm's law reads $i_\mathrm{pore} = \kappa_\mathrm{m} E_\mathrm{pore}$ in terms of the molecular electrolyte conductivity κ_m and local electric field E_pore. This becomes in terms of the superficial current density $i = \kappa_\mathrm{m} E$ in terms of an effective conductivity κ and global electric field E. Therefore, analogous to Eq. (3.11) we will write for the effective conductivity

$$\boxed{\kappa = \frac{\epsilon}{\tau^2} \kappa_\mathrm{m}.} \tag{3.12}$$

3.1.6 Bruggeman approximation

In the case of a random configuration of particles of various sizes, you can perhaps imagine that the lower the porosity ϵ, the higher the tortuosity $\tau = l_\parallel/l$ will be. Transport is unimpeded for very high porosity and can proceed along straight paths

[5] Here, the squared tortuosity τ^2 is sometimes referred to as the *tortuosity factor* but is often erroneously referred to as the tortuosity and is even sometimes given the symbol τ. The combination $\tau^2/\epsilon > 1$ is called the Macmullin number and is often used to characterise porous media. Note that the reasoning used to derive Eq. (3.11) only assumes a flux proportional to the gradient of a concentration. Therefore, it will equally hold for the transport of heat (Fourier's law), current (Ohm's law) or pressure-driven viscous flow (Darcy's law).

[6] And laminar pressure-driven flow, something we will consider in section 5.3.3.

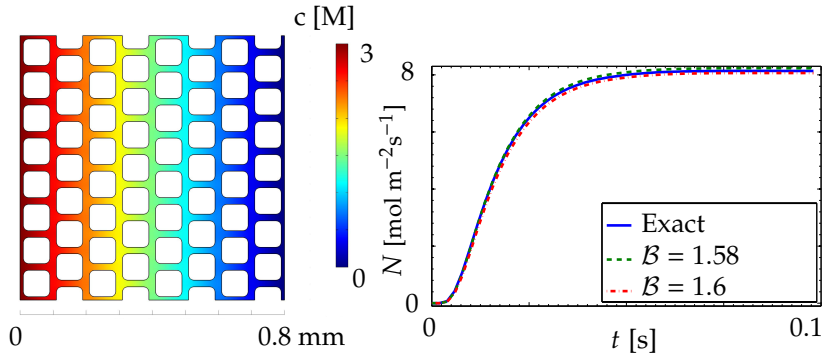

Figure 3.4: *The solution of the transient diffusion equation* (3.8) *in an artificial two-dimensional porous structure 0.1 seconds after a concentration of 3 M is set at the left boundary in a domain with initially zero concentration [9]. The graph on the right shows the evolution of the concentration at the right boundary and compares this with the 1D numerical solution to* $\frac{\partial \epsilon c}{\partial t} = D_{\mathrm{m}} \epsilon^{1+\mathcal{B}} \frac{\mathrm{d}^2 c}{\mathrm{d}x^2}$ *[22]. The images were made using the COMSOL Multiphysics® software and are provided courtesy of COMSOL and Dr. Gregory L. Plett. See his open-access course ECE5710, Modeling, Simulation, and Identification of Battery Dynamics, lecture 11.*

with negligible tortuosity. For a very low porosity, the space is filled with particles, and even the space between particles is filled with smaller particles. In this case, the relative transport path lengths $l_{\parallel}/l$ becomes very large. It can be derived, see for example Ref. [28], that for a random polydisperse packing of spheres in 3D ($\mathcal{B} = 1/2$) or normal to a bundle of parallel cylinders in 2D ($\mathcal{B} = 1$)

$$\boxed{\tau^2 \approx \epsilon^{-\mathcal{B}}.} \tag{3.13}$$

This formula implies a relationship between porosity and tortuosity: the lower the porosity, the higher the tortuosity, following intuition. Inserting this approximation into Eq. (3.11) gives

$$D \approx \epsilon^{1+\mathcal{B}} D_{\mathrm{m}}. \tag{3.14}$$

where D is the effective medium diffusion coefficient and D_{m} is the molecular diffusivity. With $\mathcal{B} = 1/2$ this gives $D \approx \epsilon^{1.5} D_{\mathrm{m}}$, which is often a reasonable approximation for various random porous media, usually referred to as the Bruggeman approximation or correlation[7]

3.2 Macro-homogeneous porous electrode approach

[7] As pointed out in Ref. [28] these simple special cases do not appear in the original German work of Bruggeman from 1935. See, for example, Ref. [30] for application to batteries.

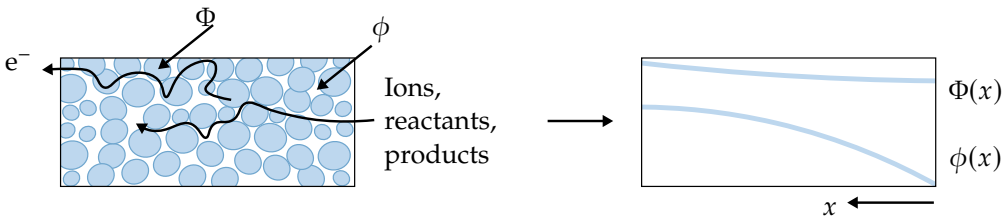

Figure 3.5: *Illustration of the averaging procedure of a porous electrode's ionic and electronic potentials. The electronic potential Φ is relatively flat due to a high metal conductivity, while the electrolyte potential varies more significantly due to ohmic resistance. The inter-electrode gap or membrane is at $x = 0$.*

3.2.1 Macro-homogeneous approach

A porous electrode, by definition, contains more than one phase.[8] The macro-homogeneous approach that we will outline here consists of treating some of these phases as *intertwined* continua—for example, a solid electrode and liquid electrolyte transport electrons and ions throughout the electrode. Even though, in reality, at each location, there will be either solid or liquid present, by mathematically averaging over space, these two phases will co-exist at the same location in the macro-homogeneous approach.

This averaging procedure is schematically depicted in Figure 3.5. On the left, at each location, there is either a solid with a potential Φ or a liquid with a potential ϕ. On the right, these potentials have been averaged over the y- and z-directions to give potentials $\Phi(x)$ and $\phi(x)$ that co-exist for each x. The potential difference $\Phi - \phi$ represents the jump in the potential that exists over the electric double layer in the electrolyte close to the solid.[9]

3.2.2 General porous electrode equations

The volume-average conservation law for a species in the pores of a porous electrode reads *per total unit volume*:

$$\boxed{\frac{\partial \epsilon c}{\partial t} = -\nabla \cdot \boldsymbol{N} + a N_{\perp}.} \tag{3.15}$$

Compared to the general conservation equation Eq. (2.1) the concentration c [mol/m$^3_{\text{pore}}$], which is on a per unit fluid basis, is multiplied with the porosity to

[8] For example, in a *flooded electrode*, there are two phases, a solid and a liquid phase. When one of the reactants or products is gaseous, as is often the case in fuel cells or electrolysers, there is an additional gas phase. In a polymer electrolyte fuel cell, there may even be an additional solid phase to transport the ions.

[9] Relative to its equilibrium value $\eta = \Phi - \phi - (\Phi - \phi)_{\text{eq}}$ is the local activation overpotential. Compared to Eq. (1.26), we allowed here for an electrode potential Φ that varies in space. In case the electrode has a non-negligible resistance, the solid phase potential Φ may vary, and a constant electrode potential E, as assumed in chapter 1, does not suffice.

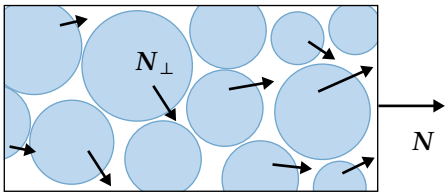

Figure 3.6: *The averaging domain used in Eq.* (3.17)*, showing how the local surface fluxes* $N_\perp$ *add up to a superficial flux* $\boldsymbol{N}$*.*

give ϵc [mol/m$^3_{\text{tot}}$], the number of moles per total unit volume, including both the pores and the solid. The Nernst-Planck equation Eq. (3.16) for the superficial flux N [mol s^{-1}m$^{-2}_{\text{tot}}$] becomes

$$\boldsymbol{N} = \boldsymbol{U}\mathrm{c} - D\left(\nabla c + zc\nabla\bar{\phi}\right). \tag{3.16}$$

Here $\boldsymbol{U}$ is the *superficial* velocity of Eq. (3.7) and D is the *effective* diffusivity, given by Eq. (3.11).

The source term $aN_\perp$ in Eq. (3.15) derives from the general local conservation considering Eq. (2.1) in steady-state $S = \nabla \cdot \boldsymbol{N}_{\text{pore}}$ and volume-averaging so that

$$\frac{1}{\mathcal{V}}\int \nabla \cdot \boldsymbol{N}_{\text{pore}}\mathrm{d}\mathcal{V} = \int \boldsymbol{N}_{\perp,\text{pore}} \cdot \frac{\mathrm{d}\boldsymbol{A}_{\text{s}}}{V} = aN_\perp, \tag{3.17}$$

where in the second step we used the divergence theorem to relate a divergence in the local pore flux $\boldsymbol{N}_{\text{pore}}$ to a local surface flux $\boldsymbol{N}_{\perp,\text{pore}}$ through the solid-fluid interface.

The averaged local surface flux $N_\perp$ is related to the local current density by Faraday's law as

$$N_\perp = \pm\frac{j_\perp}{nF}. \tag{3.18}$$

As discussed in section 1.4.1, the number of transferred electrons $n > 0$ and normal fluxes $N_\perp$ and $j_\perp$ is positive when entering from the solid into the fluid. Therefore, depending on whether our species is a reaction product ($N_\perp > 0$) or a reactant ($N_\perp < 0$) and we are considering an anode ($j_\perp > 0$) or a cathode ($j_\perp < 0$), there is a plus or minus sign in Eq. (3.18).

The charge conservation equation (2.9), after volume-averaging similar to in Eqs. (3.15) and (3.17), reads

$$0 = -\nabla \cdot \boldsymbol{i} + aj_\perp. \tag{3.19}$$

Now, $\boldsymbol{i}$ is a superficial current density per total unit area, even though the ionic current density is confined to the pores. Similarly, we can write a volume-averaged conservation equation for the superficial electronic current density $\boldsymbol{j}$

$$0 = -\nabla \cdot \boldsymbol{j} - aj_\perp. \tag{3.20}$$

Here, the negative sign in the final term arises because we defined $j_\perp$ to be positive when charge enters from the solid into the fluid, which is then a sink for electronic charge.

Adding Eqs. (3.20) and (3.19) gives

$$\nabla \cdot (\boldsymbol{i} + \boldsymbol{j}) = 0. \tag{3.21}$$

The sum of ionic and electronic current densities adds up to a constant current density $\boldsymbol{i} + \boldsymbol{j}$. By charge conservation, any reduction in ionic current density thus has to lead to an increase in electronic current density, and vice versa.

3.2.3 Ohm's law in porous electrodes

Ohm's law often holds to a reasonable degree of accuracy. This holds, for example, in metal electrodes, in solid electrolytes, for binary electrolytes at current densities well below the limiting current density, see section 2.4.3, and in the presence of a supporting electrolyte, see section 2.5. Therefore, to simplify the analysis we will assume Ohm's law to hold and write

$$\boxed{\begin{aligned} \boldsymbol{i} &= -\kappa \nabla \phi, && (3.22)\\ \boldsymbol{j} &= -\sigma \nabla \Phi, && (3.23)\\ \nabla \cdot \boldsymbol{i} &= -\nabla \cdot \boldsymbol{j} = a j_\perp. && (3.24) \end{aligned}}$$

where the final equations are Eq. (3.19) and Eq. (3.20). Here κ and σ are effective ionic and electronic conductivities, respectively, see Eq. (3.12). In the case of a particulate electrode, we may assume the Bruggeman relation (3.11) to hold and write

$$\kappa = \kappa_\mathrm{m} \epsilon^{1.5}, \tag{3.25}$$

$$\sigma = \sigma_\mathrm{m} (1 - \epsilon)^{1.5} \tag{3.26}$$

where κ_m and σ_m are the material conductivities. The electrode volume fraction is one minus the electrolyte volume fraction so $1 - \epsilon$ is used in Eq. (3.26).

To further simplify, we will neglect convection and also the final migration term in Eq. (3.16) and write $\boldsymbol{N} = -D\nabla c$. In the absence of flow, this would, of course, hold for neutral species, but also for a minority species in a supporting electrolyte. In the case of a binary electrolyte, D is replaced by the effective medium ambipolar diffusivity D_a.

With these assumptions Eq. (3.15) can, with Eqs. (3.18) and (3.24), be written as

$$\boxed{\frac{\partial \epsilon c}{\partial t} = \nabla \cdot (D \nabla c) - \frac{\nabla \cdot \boldsymbol{i}}{nF}.} \tag{3.27}$$

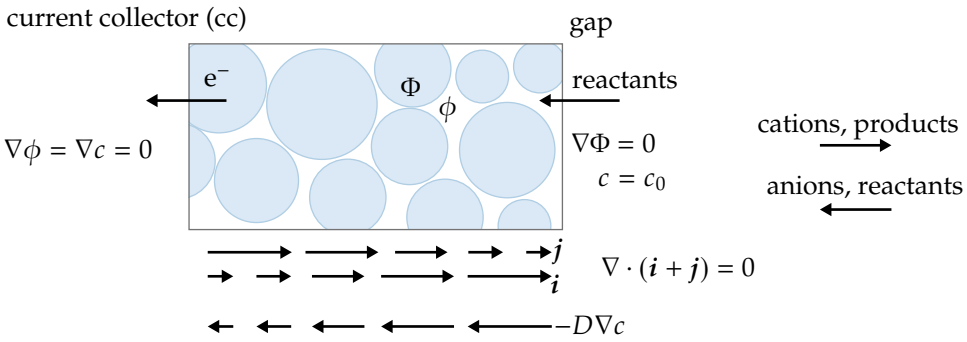

Figure 3.7: *A schematic of a porous anode where electrons and reactants enter from opposite sides so ionic current $\boldsymbol{i}$ is converted into electronic current $\boldsymbol{j}$ as the reactant flux $-D\nabla c$ decreases. The boundary conditions for ionic potential ϕ, electronic potential Φ and reactant concentration c are indicated.*

Here the minus sign in the final term describes a reactant in an anode, for which $N_\perp < 0$ and $\nabla \cdot \boldsymbol{i} = a j_\perp > 0$.[10]

As a boundary condition at a surface that allows no ions to pass through, Eq. (3.22) gives $\nabla\phi = 0$. Similarly, when no electronic current can enter Eq. (3.23) gives $\nabla\Phi = 0$. Finally, we have as a boundary condition $\nabla c = 0$ in case no molecules of the species under consideration can pass. These boundary conditions are illustrated in Fig. 3.7.

3.3 Simplified 1D porous electrode equations

We will further simplify the equations of the previous section, assuming:

- a *reactant* with a volume-averaged concentration $c(x)$ that varies only in a single spatial direction (x) inside an *anode*[10]
- an infinitely high electronic conductivity σ so that the electronic potential $\Phi = E$ is constant throughout.
- steady-state
- constant D

These assumptions simplify the above Eqs. (3.22)- (3.24) and (3.27) to

[10] Alternatively, it equally holds for a product in a cathode for which $N_\perp > 0$ and $\nabla \cdot \boldsymbol{i} = a j_\perp < 0$. For a reactant in a cathode or a product in an anode, the minus sign before the final term in Eqs. (3.27) and (3.30) has to be replaced with a plus sign.

$$i = -\kappa\phi', \tag{3.28}$$

$$i' = aj_{\perp}, \tag{3.29}$$

$$0 = Dc'' - \frac{i'}{nF}. \tag{3.30}$$

where $i = i_x$ is the x-component of the ionic current density. We use a prime to denote a derivative with respect to the x-coordinate so, for example, $i' = \mathrm{d}i/\mathrm{d}x$.

As shown in Figure 3.8, the x-coordinate inside a porous electrode is chosen to run from the inside of the cell outwards, from the gap or separator to the current collector assumed to be at $x = L$. For the anode on the left of Figure 3.8 that is from right to left. so the ionic current density from left to right gives $i < 0$. For the cathode, the x-coordinate would run from left to right. We take the current collector at $x = L$ to be impenetrable for both ions and reactants. The boundary conditions can, therefore, be written as

$$i = -j \qquad (\text{at the separator, } x = 0), \tag{3.31}$$

$$i = 0 \qquad (\text{at the current collector, } x = L). \tag{3.32}$$

Finally, the boundary condition for concentration gives[11]

$$c'(x = L) = 0. \tag{3.33}$$

With these boundary conditions, we can integrate Eq. (3.30) over the spatial coordinate x to give

$$\boxed{0 = Dc' - \frac{i}{nF}.} \tag{3.34}$$

3.3.1 The area multiplier aL

The derivative $i' = \mathrm{d}i/\mathrm{d}x$ is a measure of the local reaction rate since it describes how much ionic current is generated per meter. If it is a constant, we can integrate Eq. (3.29) to give the total current as $j = aLj_{\perp}$. Here

$$aL = \frac{A_{\mathrm{s}}}{\mathcal{V}}\frac{\mathcal{V}}{A} = \frac{A_{\mathrm{s}}}{A}, \tag{3.35}$$

[11] When a neutral reactant is supplied by flow channels engraved into the current collector (*flow field*) from $x = L$ and a membrane avoids these reactants to be transported beyond $x = 0$, Eq. (3.33) may be replaced $c'(x = 0) = 0$. When c describes the concentration of an ionic species supplied or removed through the separator or gap, the boundary condition $c'(x = L) = 0$ will, in case there is also a flow field, only hold exactly where there are no flow channels (*land area*). In the present 1D approximation, however, it will be a reasonable assumption to apply as an averaged condition.

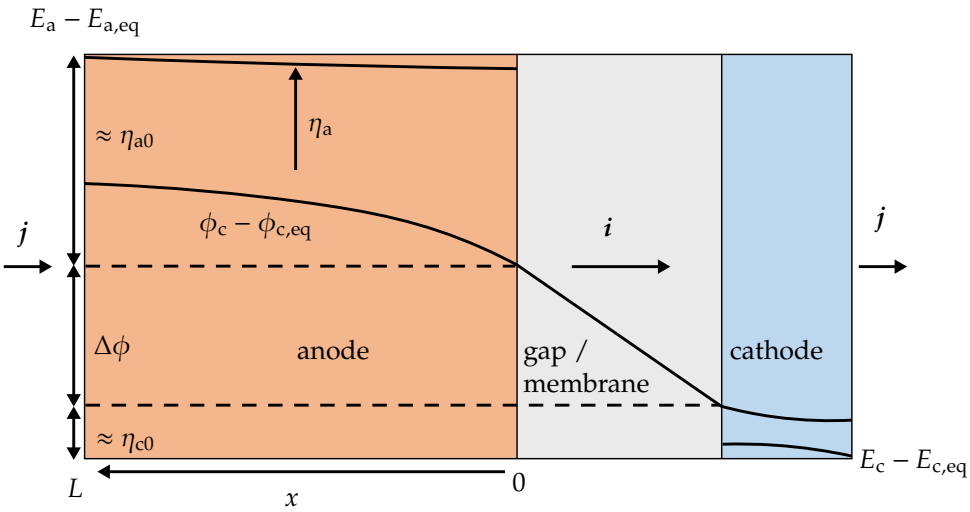

Figure 3.8: *The ionic and electronic potentials ϕ and Φ throughout a cell consisting of, from left to right, a porous anode where electronic current $\boldsymbol{j}$ is converted to ionic current $\boldsymbol{i}$, a gap or separator, and a cathode where the re-conversion to electronic current takes place. When the electronic conductivity σ is much larger than the ionic conductivity κ, the electronic potential drops are much smaller than the ionic potential drop; adding the vertical arrows on the left shows that $E_{\text{cell}} = E_c - E_a \approx E_{\text{eq,c}} - E_{\text{eq,a}} - (\eta_{a0} - \eta_{c0} + \Delta\phi)$.*

is the total electrode surface area A_s as a fraction of the cross-sectional electrode surface area A. It thus describes how much area is inside a porous electrode relative to its outside frontal area. The area multiplier $\frac{j}{j_\perp} = aL$ can be very large[12], and the current j entering or leaving the electrode can be several orders of magnitude larger than the ionic current $j_\perp$ locally entering or leaving the particles (or fibres) making up the porous medium. The much lower local current density $j_\perp$ gives rise to much-reduced activation overpotentials, which is the primary reason why porous electrodes are used.

3.3.2 Activation overpotential

For a reaction that is first order in the concentration c, the concentration-dependent Tafel equation (1.28) can be written as[13]

$$j_\perp = j_* \frac{c}{c_{\text{eq}}} \mathrm{e}^{\eta/b}. \tag{3.36}$$

[12]Non-smooth electrode surfaces can have several times more actual reaction area than geometrical area. A similar multiplier is in this case sometimes referred to as the roughness factor.

[13]For a cathode we would write $j_\perp = -j_* \frac{c}{c_{\text{eq}}} \mathrm{e}^{-\eta/b}$.

Replacing E with the local value Φ the definition of activation overpotential, Eq. (1.26), reads

$$\eta = \Phi - \phi - \left(E_{\text{eq}} - \phi_{\text{eq}}\right) \tag{3.37}$$

visualized in Figure 3.8. Since we assume an large electronic conductivity σ so that $\Phi' \approx 0$, we obtain $\eta' \approx -\phi'$. Inserting Ohm's law, Eq. (3.28), gives

$$\boxed{\eta' = \frac{i}{\kappa}} \tag{3.38}$$

As illustrated in Figure 3.8 the x-coordinate runs from left to right in a cathode, but from right to left in the anode. Therefore, this coordinate always starts at the electrode 'front', as seen from the gap or membrane, or 'entrance' for reactants.

The overpotential η is largest at $x = 0$ where the ionic current enters or leaves. Deeper into the electrode the overpotential decreases due to ohmic losses, leading to lower local current density. Mathematically, in the anode $i < 0$ and $\eta > 0$ so Eq. (3.38) gives $\eta' < 0$ and the overpotential decreases away from $x = 0$. In the cathode $i > 0$ and $\eta < 0$, so Eq. (3.38) gives $\eta' > 0$, and the overpotential becomes less negative the further away from $x = 0$. In either case, the driving force for the reaction, the magnitude of the activation overpotential, is highest where the ions enter and leave the electrode. Since in the Tafel regime the reaction rate is proportional to $e^{|\eta|/b}$, the highest reactivity is at the electrode entrance at $x = 0$. If the current is high and the ionic conductivity is low, it may be that there is very little reactivity near $x = L$.

When we neglect electronic resistance, the voltage losses in the simple cell of Figure 3.8 consists of an ohmic drop over the space between the electrodes and an anodic and cathodic activation overpotential, so

$$V_{\text{cell}} \equiv E_{\text{c}} - E_{\text{a}} = V_{\text{eq}} - (\eta_{\text{a}0} - \eta_{\text{c}0} + \Delta\phi). \tag{3.39}$$

where the activation overpotentials $\eta_0 = \eta(x = 0)$ and are evaluated at the front of the electrode at $x = 0$. This is the main difference with Eq. (1.35), derived previously, in which a planar electrode with a single overpotential was assumed.

From Eq. (3.39) it seems that the potential drops over the electrolyte inside the porous electrodes do not play a role. They do however play an implicit role[14] in determining the activation overpotential η_0 as we will show below. As a result of high electrolyte resistivity, the overpotential can strongly decrease away from $x = 0$, leading to a narrow reaction zone near $x = 0$. This decreases the available reaction area and thereby increases η_0. Due to this implicit influence of ohmic losses, η_0 cannot be seen purely as an activation overpotential. Activation losses and ohmic losses are intrinsically coupled and cannot always be clearly separated. This is because ions arriving at $x = 0$ have the choice to either all react directly, or travel a bit further to where there are fewer ions. The further the ions travel into the electrode, the more the magnitude of the overpotential decreases due to ohmic losses. The current

[14] Alternatively we can write $V_{\text{cell}} = E_{\text{c}} - E_{\text{a}} \approx V_{\text{eq}} - (\eta_{\text{a},x=L} - \eta_{\text{c},x=L} + \Delta\phi + \Delta\phi_{\text{a}} + \Delta\phi_{\text{c}})$ so the electrolyte potential drops $\Delta\phi_{\text{a}}$ and $\Delta\phi_{\text{c}}$ appear explicitly.

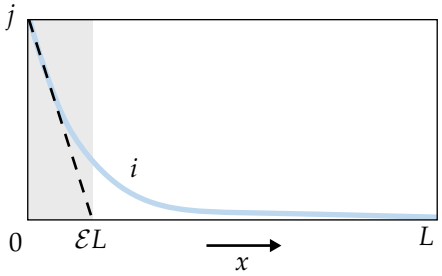

Figure 3.9: *The inhomogeneous ionic current distribution resulting from significant ohmic (or mass transport) resistance.*

distribution resulting from this balance is conveniently described by an effectiveness factor, which we will now introduce.

3.3.3 Electrode effectiveness factor

Inserting $i' = aj_\perp$ from Eq. (3.29) into Eq. (3.36) gives, with $c_0 = c(x = 0)$

$$\boxed{i' = aj_* \frac{c}{c_0} e^{\eta/b}.} \tag{3.40}$$

Here aj_* [A/m^3] is the volumetric exchange current density, which is a measure of how easily the reaction proceeds.[15] The reaction rate i' is here expressed in Coulombs generated or consumed per unit volume and time. Dividing by the number nF of Coulombs per mole of reactant gives the reaction rate in mol/m^3/s.

We define an *electrode effectiveness factor* as the average reaction rate relative to the maximum reaction rate[16], which is at $x = 0$

$$\boxed{\mathcal{E} = \frac{\text{average reaction rate}}{\text{maximum reaction rate}} = \frac{\frac{1}{L}\int_0^L i' \mathrm{d}x}{i'_0} = \frac{-i_0}{Li'_0} = \frac{j}{aLj_* e^{\eta_0/b}},} \tag{3.41}$$

where the current density magnitude $j = |i_0|$ in terms of $i_0 = i(x = 0)$. Equation (3.41) gives $\mathcal{E}L = -i/i'|_0$. As illustrated in Fig. 3.9, the *penetration depth* $\mathcal{E}L$ gives the position where the linearized current density profile $i \approx i_0 + i'_0 x$ vanishes. It follows that when $\mathcal{E} \ll 1$, the effectiveness factor roughly represents the fraction of the electrode that is effectively used. Beyond a fraction $\mathcal{E}$ of the total electrode thickness, the ionic current density has become negligible and this electrode area is ineffectively used.

[15] The combination $i'/nFc = aj_* e^{\eta/b}/nFc_0$ [s^{-1}] is a volumetric reaction rate coefficient, similar to ka_s used in Appendix 3.A.

[16] Using the boundary condition $i_L = 0$ of Eq. (3.32) and using the fundamental theorem of calculus to integrate a derivative, the average value of i' reads $\frac{1}{L}\int_0^L i' \mathrm{d}x = -i_0/L$. In the anode on the left of Figure 3.8 the ionic current is to the right, or in the negative x-direction so that $i_0 < 0$.

Equation (3.41) immediately allows us to write

$$\boxed{\eta_0 = b\ln\left(\frac{j}{J_*\mathcal{E}}\right).} \tag{3.42}$$

Equation (3.42) is very similar to Tafel's equation $\eta = b\ln\left(\frac{j}{j_*}\right)$ for a planar electrode, with two important differences.

Firstly, instead of j_*, what appears is the *superficial exchange current density*

$$J_* \equiv aLj_*. \tag{3.43}$$

As discussed in section 3.3.1, the multiplier aL indicates how much more area is inside the porous electrode relative to its frontal geometrical area. The quantity J_* is, therefore, a measure of the total or superficial exchange current density enhanced by the additional porous electrode surface area.

Secondly, the effectiveness factor $\mathcal{E}$ appears, since, in general, not the entire reactive area is used effectively. Note that $J_*\mathcal{E} = aL\mathcal{E}j_*$, where $L\mathcal{E}$ is the penetration thickness so that only that part of the electrode that is effectively used is counted towards the superficial exchange current density.

Our next goal will be to find out how $\mathcal{E}$ depends on the current density j and transport limitations due to a finite ionic conductivity κ or reactant diffusivity D.

3.3.4 Summary and characteristic dimensionless numbers.

We will consider an anode. Therefore $\eta > 0$ and $i < 0$, and Eqs. (3.34), (3.38), and (3.40) become

$$\boxed{\begin{aligned} c' &= i/nFD. && (3.44)\\ \eta' &= i/\kappa. && (3.45)\\ i' &= aj_*\frac{c}{c_0}e^{\eta/b}. && (3.46)\end{aligned}}$$

Note that $c', \eta' < 0$ and the reactivity $i' > 0$.[17] These are three coupled first-order ordinary differential equations for the concentration c, overpotential η, and i. The boundary conditions at the current collector at $x = L$, from Eqs. (3.33) and (3.48), read

$$\begin{aligned} c'(x=L) &= 0 && && c(x=0) &= c_0, && (3.47)\\ i(x=L) &= 0 && \text{or} && i(x=0) &= -j, && (3.48)\\ \eta'(x=L) &= 0 && && \eta'(x=0) &= -j/\kappa. && (3.49)\end{aligned}$$

[17] For a cathode, where $\eta < 0$, and $i > 0$, the right-hand side of Eqs. (3.44) and (3.46) acquires a minus sign and the argument of the exponent in Eq. (3.46) reads $-\eta/b$. In this case $c', i' < 0$ and $\eta' > 0$. This is equivalent to changing the signs of η and i.

All three of the differential equations (3.44)-(3.46) contain either i or i'. Therefore, associated with these three equations are three characteristic current densities. The first one, J_*, associated with the last equation, Eq. (3.45), we already encountered in Eq. (3.43). The other two are obtained from the first two equations, Eq. (3.44) and (3.45), by inserting the characteristic gradients $\eta' \to -b/L$ and $c' \to -c_0/L$ and solving for $-i$ to give

$$\boxed{J_D = \frac{nFDc_0}{L}} \tag{3.50}$$

$$J_\kappa = \frac{b\kappa}{L} \tag{3.51}$$

$$J_* = aLj_* \tag{3.52}$$

Since the reaction rate in Eq. (3.46) is proportional to $i' \propto ce^{\eta/b}$, the characteristic gradients $\eta' \to -b/L$ and $c' \to -c_0/L$ will give a significant effect on i'. It follows that if the current density is much smaller (larger) than these characteristic values, J_D and J_κ, the gradients will also be much smaller (larger).

- The characteristic diffusional current density J_D is the limiting current density that could be sustained in case the reaction takes place only at $x = L$.
  - If $j \ll J_D$, diffusion limitations can be neglected and *the concentration c is approximately constant*.
- The characteristic ohmic current density J_κ is that which would give an ohmic drop equal to the Tafel slope b over the electrode thickness L.
  - If $j \ll J_\kappa$, ohmic limitations can be neglected and *the overpotential η is approximately spatially constant*.
- The superficial exchange current density J_* is the effective exchange current density that the porous electrode would have in case the electrode is used fully effectively.
  - If $j \ll J_*$, we can assume linear kinetics, while for $j \gg J_*$ the Tafel approximation will be valid.

We note that $J_\kappa/j = b\kappa/jL$ is sometimes referred to as the *Wagner number*. In the following section, we will continue with the example of an anode. It is worth noting that the case of a cathode can be easily obtained by changing the sign of both η and i.

3.4 Transport losses in porous electrodes

3.4.1 No transport limitations, $\mathcal{E} = 1$

We will first consider what happens inside a porous electrode in the absence of transport limitations. When $j \ll J_D$, there are no diffusion limitations and the

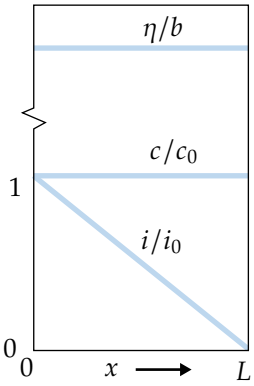

Figure 3.10: *Dimensionless ionic current density i/i_0, concentration c/c_0 and overpotential η/b in the porous electrode for no transport limitation. Note that the Tafel regime requires η/b to be well above 1.*

concentration $c \approx c_0$ throughout. When additionally $j \ll J_\kappa$ there are no ohmic limitations and the overpotential $\eta \approx \eta_0$ throughout.

Solving Eq. (3.46) with $c = c_0$ and $\eta = \eta_0$ and the boundary conditions of Eqs. (3.47)-(3.49) gives the simple linear profile

$$i = J_* e^{\eta_0/b} \left(\frac{x}{L} - 1 \right). \tag{3.53}$$

This situation is illustrated in Figure 3.10. At $x = 0$ we have $i = -j$ so that

$$\eta_0 = b \ln \left(\frac{j}{J_*} \right) = b \ln \left(\frac{j}{j_*} \right) - b \ln (aL). \tag{3.54}$$

This is Tafel's equation with j_* replaced by $J_* = aLj_*$. The larger effective exchange current density J_* is the result of the porous electrode area being a factor aL times larger than that for a planar surface.

In the Tafel regime, the larger area of a porous electrode lowers the overpotential by the second term in Eq. (3.54), $-b \ln (aL)$, compared to the overpotential $b \ln \left(\frac{j}{j_*} \right)$ of a non-porous electrode. This is because the local current density, and thereby the activation overpotential, decreases as the current spreads out over the larger porous electrode area.

3.4.2 Diffusion limitations

Figure 3.11 shows an example where there are diffusion limitations ($j \gg J_D$) but no ohmic limitations ($j \ll J_\kappa$). Without ohmic limitations, the overpotential η will be constant. Due to the finite diffusivity, the concentration decreases inside the

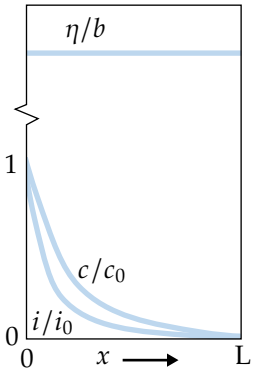

Figure 3.11: *The ionic current distribution i sharply decreases due to the depletion of reactants associated with the diffusion limitations that are a consequence of the high current density $j \gg J_D$. The ionic conductivity is large so that $j \ll J_\kappa$ and the overpotential η is constant.*

porous electrode, causing the reaction rate i' to drop proportionally. These conditions typically arise, for example, in the catalyst layers of fuel cells or CO_2-electrolysers, when they are *flooded* with water. These catalyst layers are usually thin enough to avoid significant ohmic drops, but due to the low solubility and diffusivity in water, the transport of gaseous reactants can be hindered by slow diffusion.

Taking the derivative of Eq. (3.44) and inserting Eq. (3.46), with $\eta = \eta_0$ constant, gives

$$\frac{\mathrm{d}^2 c}{\mathrm{d}\,(x/L)^2} = \mathrm{M}^2 c, \tag{3.55}$$

where the *Thiele modulus* squared reads

$$\mathrm{M}^2 = \frac{J_*}{J_D}\mathrm{e}^{\eta_0/b} = \frac{J_*\mathrm{e}^{\eta_0/b}}{nFDc_0/L}. \tag{3.56}$$

This dimensionless number represents the ratio between the integral reaction rate $J_*\mathrm{e}^{\eta_0/b}$ and the characteristic diffusion rate Dc_0/L.

The limiting solution in case of high or low M reads

$$c = c_0\mathrm{e}^{-\mathrm{M}x/L} \quad (\mathrm{M} \gg 1 \text{ or } \mathrm{M} \ll 1) \tag{3.57}$$

In case $\mathrm{M} \gg 1$ or $\mathrm{M} \ll 1$ this gives $c(x = L) \approx 0$ or $c(x = L) \approx c_0$, respectively[18]. From Eq. (3.46), the reactivity i' is proportional to c so that the effectiveness factor of

[18] In these cases the solution satisfies the boundary condition $c'(x = L) = 0$. For intermediate values, we need to retain also the positive exponent solution $\mathrm{e}^{\mathrm{M}x/L}$ and make a linear combination that satisfies the boundary condition, as is done in the appendix 3.A.3 to derive the full exact solution Eq. (3.A.85).

Eq. (3.41) reads[19]

$$\mathcal{E} = \frac{1}{L}\int_0^L \frac{c}{c_0}\mathrm{d}x \approx \begin{cases} 1 & \mathrm{M} \ll 1 \\ 1/\mathrm{M} & \mathrm{M} \gg 1. \end{cases} \tag{3.58}$$

In the latter case of strong diffusion limitations (M ≫ 1), with Eqs. (3.41) and (3.56), this gives[20]

$$\boxed{\mathcal{E} = \frac{j}{J_* \mathrm{e}^{\eta_0/b}} = \frac{1}{\mathrm{M}} = \frac{j/J_D}{\mathrm{M}^2} = \frac{J_D}{j} \ll 1.} \tag{3.59}$$

We thus find that in the presence of strong diffusion limitations the electrode effectiveness factor is given by the ratio of the characteristic current density J_D and the current density j. The lower the diffusion current density J_D, or the higher the current density, the lower the effectiveness factor. This is a simple but very useful result of the above analysis.

Inserting $\mathcal{E} = J_D/j$ in Eq. (3.42), using Eqs. (3.50) and (3.52), gives

$$\boxed{\eta_0 = b\ln\left(\frac{j^2}{a j_* n F D c_0}\right) = 2b\ln\left(\frac{j}{\sqrt{a j_* n F D c_0}}\right).} \tag{3.60}$$

In the second equation, we see Tafel's equation, but with a doubled Tafel slope $2b$ and a modified effective exchange current density

$$\sqrt{J_* J_D} = \sqrt{a j_* n F D c_0}. \tag{3.61}$$

This effective exchange current density is the geometrical mean of the original $J_* = aLj_*$ and the characteristic diffusion current density $J_D = nFDc_0/L$. A doubling in Tafel slope is bad news, as it means that reaching higher current densities comes at an increasingly large cell voltage. It arises because the higher the current density, the smaller the area inside the electrode that can be effectively used: the penetration thickness $\mathcal{E}L$ becomes inversely proportional to j. Note that the overpotential of Eq. (3.60) is independent of the electrode thickness L. This happens because in the considered case of strong diffusion limitations, the porous electrode is used very ineffectively. Because in the part beyond the penetration depth, virtually no reaction takes place, the electrode thickness does not matter.

3.4.3 Ohmic limitations

Next, we assume a sufficiently high diffusivity and reactant concentration, so $J_D \gg j$. In this case, no diffusion limitations arise and the concentration c is approximately

[19] Evaluating gives $\int_0^1 \mathrm{e}^{-\mathrm{M}x/L} d\left(\frac{x}{L}\right) = \frac{1-\mathrm{e}^{-\mathrm{M}}}{\mathrm{M}}$ which evaluates to 1/M for M ≫ 1. For M ≪ 1 a series expansion $\mathrm{e}^{-\mathrm{M}} \approx 1 - \mathrm{M}$ gives that $\mathcal{E} \approx 1$.

[20] Using the exact solution $\mathcal{E} = \frac{\tanh \mathrm{M}}{\mathrm{M}}$ of Eq. (3.A.87) we see that to find M in terms of j requires solving $j/J_D = \mathrm{M}\tanh(\mathrm{M})$, which has no general analytical solution for M.

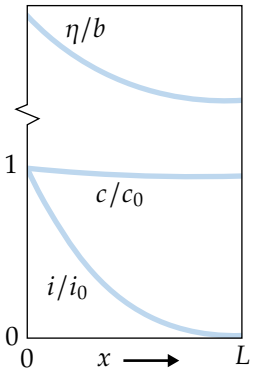

Figure 3.12: *The ionic current distribution i decreasing due to a decrease in activation overpotential associated with $j \gg J_\kappa$. The diffusivity is sufficiently large that $J_D \gg j$ and concentration profile c is approximately flat.*

constant. Nonetheless, when $j \gg J_\kappa = b\kappa/L$, a localised reaction zone appears near $x = 0$ due to ohmic limitations. Because the characteristic ohmic potential drop jL/κ is much larger than the Tafel slope b the reaction rate, proportional to $e^{\eta/b}$, is strongly impacted by ionic resistance. Deeper into the porous electrode, the overpotential η, and therefore the reaction rate, strongly decreases.

Combining Eqs. (3.45) and (3.46) with $c = c_0$ gives

$$e^{\eta/b} = \frac{\kappa}{a j_*}\eta''. \tag{3.62}$$

Using the chain rule $\frac{\mathrm{d}}{\mathrm{d}x} = \frac{\mathrm{d}\eta}{\mathrm{d}x}\frac{\mathrm{d}}{\mathrm{d}\eta}$, so

$$\eta'' = \eta'\frac{\mathrm{d}\eta'}{\mathrm{d}\eta} = \frac{1}{2}\frac{\mathrm{d}\eta'^2}{\mathrm{d}\eta}. \tag{3.63}$$

Inserting in Eq. (3.62) gives upon integration from η_0 at $x = 0$ to η_L at $x = L$

$$e^{\eta_L/b} - e^{\eta_0/b} = \frac{\kappa}{2aj_*b}\left(\eta_L'^2 - \eta_0'^2\right). \tag{3.64}$$

Inserting the boundary conditions of Eqs.(3.47)-(3.49) and assuming strong ohmic limitations $j \gg J_\kappa$ so that $e^{\eta_0/b} \gg e^{\eta_L/b}$ we obtain $e^{\eta_0/b} = j^2/2aj_*\kappa b$ or

$$\eta_0 = 2b\ln\left(\frac{j}{\sqrt{2aj_*\kappa b}}\right). \tag{3.65}$$

The associated effectiveness factor $\mathcal{E} \equiv j/J_* e^{\eta_0/b}$ reads

$$\boxed{\mathcal{E} = \frac{2J_\kappa}{j} \ll 1.} \tag{3.66}$$

This simple expression is very similar to the result $\mathcal{E} = J_D/j$ of Eq. (3.59). Analogously, the ohmic Thiele modulus $M_\kappa = 1/\mathcal{E}_{\to 0} = j/2J_\kappa$ in this case. Again, the effectiveness factor is given by the ratio of a characteristic current density $2J_\kappa$ and the current density j. The lower J_κ, or thheb e higher the current density, the lower the effectiveness factor. Similar to Eq. (3.60), the overpotential of Eq. (3.65) does not depend on the electrode thickness L. Also in the case of strong ohmic limitations, the reaction is limited to a region near $x = 0$. Beyond a penetration depth $\mathcal{E}L$ the electrode volume is ineffectively used and does not help to further reduce the overpotential.

3.4.4 Combined ohmic and diffusion limitations - approximation

In the case of simultaneous diffusion and ohmic limitations, we can approximately add the Thiele moduli and obtain $\frac{1}{\mathcal{E}} \approx \mathrm{M} + \mathrm{M}_\kappa = \frac{j}{J_D} + \frac{j}{2J_\kappa} \gg 1$.[21] In the absence of transport limitations $\mathcal{E} \approx 1$ when $\mathrm{M} + \mathrm{M}_\kappa \ll 1$. An approximate expression that tends to both limits is

$$\boxed{\mathcal{E} \approx \frac{1}{1 + j/J_D + j/2J_\kappa}.} \tag{3.67}$$

This result will be accurate in case the combined Thiele modulus $\mathrm{M} + \mathrm{M}_\kappa$ is either much smaller or much larger than 1. It can only be expected to give a rough approximation for intermediate values. When $\mathrm{M} + \mathrm{M}_\kappa$ is large, the effectiveness factor is small. To make good use of the entire volume of the porous electrode, this regime should be avoided. Since the Thiele moduli $\mathrm{M} = \frac{jL}{nFDc_0}$ and $\mathrm{M}_\kappa = \frac{jL}{2\kappa b}$ are both proportional to the current density and the electrode thickness L, this implies that operation at high current density will require relatively thin electrodes. This will be the case, for example, in fuel cells or advanced electrolysers, where catalyst layers of sometimes only a few micrometres thick are used. Conversely, operating at low current densities allows for thicker electrodes. This will be the case, for example, in some batteries, that can have electrodes of several millimetre thick. These arguments thus go some way to explain the differences in electrode designs between various applications.

Having an electrode effectiveness factor value close to 1 sounds ideal, but it means that a thicker electrode could have been used to increase the reaction area. A very small effectiveness factor, on the other hand, means that most of the electrode area is unused and makes ineffective use of materials. Therefore, an optimal electrode effectiveness factor $\mathcal{E}_{\mathrm{opt}}$ exists. In terms of this parameter, we find the optimal electrode

[21] In Appendix 3.C we derive the exact result and show that this simple addition gives a maximum relative error in the effectiveness factor of 12 %, making it a fairly accurate approximation.

thickness from Eq. (3.67) as

$$L_{\text{opt}} = \frac{1-\mathcal{E}_{\text{opt}}}{\mathcal{E}_{\text{opt}}} \frac{nFDc_0 + 2\kappa b}{j}. \tag{3.68}$$

An often reasonable value [13] is $\mathcal{E}_{\text{opt}} \approx 1/3$, so that the pre-factor in Eq. (3.68) becomes $\frac{1-\mathcal{E}_{\text{opt}}}{\mathcal{E}_{\text{opt}}} \approx 2$.

Inserting Eq. (3.67) in $\eta_0 = b\ln(j/J_*\mathcal{E})$ gives, when $\mathcal{E} \ll 1$:

$$\eta_0 \approx 2b\ln\left(\frac{j}{\sqrt{\frac{aj_*}{\frac{1}{2\kappa b}+\frac{1}{nFDc_0}}}}\right). \tag{3.69}$$

Compared to Eq. (3.54) the inverse electrode thickness $1/L$ is replaced by a sum of the inverse penetration depths $2\kappa b/j$ and $nFDc_0/j$. The shortest of the penetration depths thus dominates. This is to be expected since beyond the shortest of the two penetration depths, the reactivity decreases strongly, and the rest of the electrode helps very little in decreasing the overpotentials.

3.5 Summary

- The effective diffusivity, similar to other transport parameters like conductivity, can be described by $D = \frac{\epsilon}{\tau^2} D_{\text{m}}$ (3.11) with tortuosity squared $\tau^2 \approx \epsilon^{-\mathcal{B}}$. Factor $\mathcal{B} = 1/2$ for a porous medium consisting of spheres and $\mathcal{B} = 1$ for long cylinders.

- Per total unit volume, the conservation equation for a reactant $\frac{\partial \epsilon c}{\partial t} = \nabla\cdot(D\nabla c) - \frac{\nabla\cdot\boldsymbol{i}}{nF}$ (3.27) becomes in 1D, steady-state, and assuming first-order Tafel kinetics:

$$i' = nFDc'' = aj_*\frac{c}{c_0}\mathrm{e}^{\eta/b} \tag{3.70}$$

  viz. Eqs. (3.44) and (3.46). For negligible electrode resistance, the overpotential satisfies $\eta' = i/\kappa$ when $\sigma \gg \kappa$ (3.45).

- The occurrence of diffusion limitations $j \gg J_D = nFDc_0/L$ and/or ohmic limitations $j \gg J_\kappa = b\kappa/L$ can be described by the electrode effectiveness factor $\mathcal{E} \sim \frac{1}{L}\frac{\int i'\mathrm{d}x}{i'_0} \approx \frac{1}{1+M} = \frac{1}{1+j/J_D+j/2J_\kappa}$. When only the electrode region within the penetration depth $\mathcal{E}L \ll L$ is effectively used, the activation overpotential $\eta_0 = b\ln\left(\frac{j}{J_*\mathcal{E}}\right) = 2b\ln\left(\frac{j}{\sqrt{aj_*}}\sqrt{\frac{1}{2\kappa b}+\frac{1}{nFDc_0}}\right)$, (3.42) and (3.69), attains a doubled Tafel slope.

Exercise 3.1

As an engineer at an electrode manufacturer, you performed several tests on a new porous electrode material consisting of sintered spherical particles.

a. You find the effective diffusivity to be one-fourth of the molecular diffusivity. Give an approximation for the porosity ϵ.

b. Estimate the diameter of the spherical particles in case you measure the specific interfacial surface area to be a=3.6·10^5 m^{-1}.

Exercise 3.2

In an air-fed PEM fuel cell cathode, oxygen has to diffuse from the flow channel to the catalyst layer through a diffusion layer of 0.5 mm thick. This layer has an apparent density of 1260 kg/m^3 and is made from a solid material with an intrinsic density of 2100 kg/m^3. The bulk diffusivity of oxygen is D_{O_2}= 20 mm^2/s and the concentration at the flow channel interface is 5·10^{-3} M. Calculate the limiting current density associated with this diffusion layer.

Exercise 3.3

Consider a cathodic reaction in a porous electrode. Assume concentration-independent Butler-Volmer kinetics

$$i' = a j_* \left(\mathrm{e}^{\alpha \frac{F\eta}{\mathcal{R}T}} - \mathrm{e}^{-(1-\alpha)\frac{F\eta}{\mathcal{R}T}} \right), \tag{3.71}$$

and Ohm's law $\Phi' = -i/\kappa$.

a. Under what conditions can we write $i' \approx \frac{\eta}{ARL}$?

b. Write an expression for area-specific resistance AR in terms of exchange current density j_*, volumetric interfacial surface area a, and thickness of electrode L.

c. Under the condition derived at a., find the expression for current density i using boundary condition $i(0) = j$ and $i(L) = 0$ in terms of $\nu \equiv L\sqrt{\frac{a j_* F}{\mathcal{R}T\kappa}}$.

d. Derive an expression for the linear electrode effectiveness factor $\mathcal{E}_{\text{lin}} \equiv \frac{j/L}{-i'(0)}$.

Exercise 3.4

The exchange current density and charge transfer coefficient of an electrochemical reaction at a planar cathode are $j_{*c} = 0.01$ mA/cm^2 and $\alpha_R = 0.65$, respectively. We coat the cathode with a 1 μm thick, catalytically active layer with a volumetric surface area of 10^8 m^{-1}. By approximately how much will the cathode activation overpotential be reduced? Assume an electrode effectiveness factor $\mathcal{E} = 1$ and $T = 300$ K.

Exercises 3.5-3.25

Fill in the missing steps in the main text, indicated by the symbol .

*Appendices **

3.A *Pore versus effective medium*

There are two distinct ways to model a porous electrode: by using an effective medium approach as in the main text, or by studying a single pore. There has been somewhat of a divide in the literature on porous electrodes with, for example, de Levie studying single pores and Newman using effective medium equations. These approaches can give equivalent information when tortuosity and porosity are included properly. The pore perspective may be more intuitive for some, so we work out the simultaneous diffusion and reaction in a single pore.

Consider the idealised cylindrical pore in Figure 3.13. We will only consider transport in the axial direction, so the general steady-state conservation law in 1D reads

$$0 = -\frac{\mathrm{d}N}{\mathrm{d}x} + S, \tag{3.A.72}$$

where $N = -D\frac{\mathrm{d}c}{\mathrm{d}x}$. The reaction takes place only at the pore surface, not at the inlet on the left, nor at the end of the pore on the right. For a first-order reaction in the concentration c, with reaction rate constant k, the surface flux $N_\perp$ reads

$$N_\perp = -kc. \tag{3.A.73}$$

Since we are considering reactants, not products, this radial flux is in the direction from fluid to solid, hence the negative sign.
In a small axial segment with volume $\mathcal{V}_\mathrm{s}$ and surface area A_s the surface reaction subtracts $N_\perp A_\mathrm{s}$ moles of reactant per unit time. This gives a sink $S = N_\perp A_\mathrm{s}/\mathcal{V}_\mathrm{s} = a_\mathrm{s} N_\perp$ per unit volume.[22] We can, therefore, write $S = -ka_\mathrm{s}c$. The volumetric rate constant ka_s allows us to make an effective one-dimensional description of a two-dimensional pore.

[22] The volumetric surface area for a cylinder with diameter d without its two ends is $a_\mathrm{s} = \frac{A_\mathrm{s}}{\mathcal{V}_\mathrm{s}} = \frac{\pi d}{\pi d^2/4} = \frac{4}{\mathrm{d}}$, but we keep it as a general parameter to allow for arbitrary cross-sectional shapes.

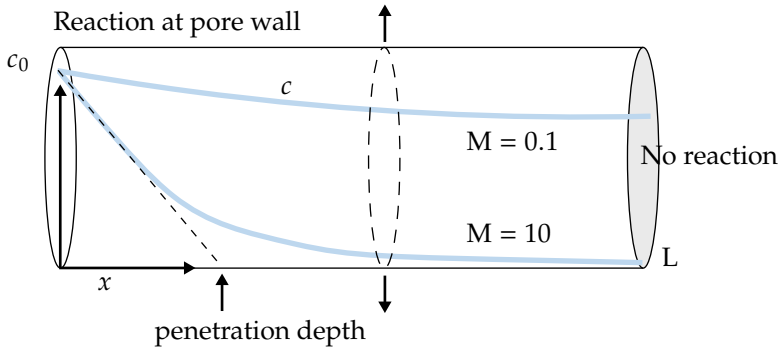

Figure 3.13: *Schematic representation of possible concentration profiles for different Thiele moduli* M *in a single pore, in which a reaction takes place at the pore wall and reactants diffuse inwards from* $x = 0$.

3.A.1 *Effectiveness factor*

The reaction at the pore wall will lead to an axial concentration gradient, bringing in new reactants by diffusion. For higher reaction rates, strong concentration gradients arise, and most of the pore volume can be deprived of reactants, as diffusion is not fast enough to meet the demand for reactants in the reaction.
To quantify this, we define the effectiveness factor as follows:

$$\mathcal{E} = \frac{\text{average reaction rate}}{\text{maximum reaction rate}} = \frac{\frac{1}{\mathcal{V}}\int k a_s c \mathrm{d}\mathcal{V}}{k a_s c_0} = \frac{\langle c \rangle}{c_0}, \tag{3.A.74}$$

where we assumed a reaction rate $S = -k a_s c$ with constant $k a_s$. The notation $\langle c \rangle = \frac{1}{\mathcal{V}}\int c d\mathcal{V}$ denotes a volume average. In the one-dimensional approximation we are after, c becomes only a function of x, and $\langle c \rangle = \frac{1}{L}\int_0^L c \mathrm{d}x$. For a first-order reaction, the effectiveness factor is thus simply the average concentration relative to the entrance concentration. Next, we set out to find an expression for $\mathcal{E}$ as a function of the pore geometry, diffusion coefficient, and reaction rate.

3.A.2 *Thiele modulus*

Equation (3.A.72) becomes:

$$0 = D\frac{\mathrm{d}^2 c}{\mathrm{d}x^2} - k a_s c. \tag{3.A.75}$$

To solve this second-order differential equation for the concentration profile, two boundary conditions are required as follows:

$$c\,(x=0)=c_0, \tag{3.A.76}$$
$$c'\,(x=L)=0. \tag{3.A.77}$$

Introducing the following dimensionless variables

$$\bar{x}=\frac{x}{L},\quad \bar{c}=\frac{c}{c_0}, \tag{3.A.78}$$

Eqs. (3.A.75), (3.A.76) and (3.A.77) can be written in dimensionless form as

$$\bar{c}''=\mathrm{M}^2\bar{c} \tag{3.A.79}$$
$$\bar{c}\,(\bar{x}=0)=1 \tag{3.A.80}$$
$$\bar{c}'\,(\bar{x}=1)=0 \tag{3.A.81}$$

Note that we use prime to denote a derivative with respect to $\bar{x}$ when considering $\bar{c}$, but a derivative with respect to x when considering c. The Thiele modulus squared is defined as:

$$\mathrm{M}^2=\frac{ka_sL^2}{D}. \tag{3.A.82}$$

Writing $\mathrm{M}^2=\frac{ka_sc_0L}{Dc_0/L}$ we clearly see that it is a characteristic dimensionless number representing the ratio between reaction rate and diffusion rate.

3.A.3 *Analytical solution*

The general solution to Eq. (3.A.79) reads

$$\bar{c}=A\mathrm{e}^{M\bar{x}}+B\mathrm{e}^{-M\bar{x}}. \tag{3.A.83}$$

The boundary conditions, Eq. (3.A.76) and Eq. (3.A.77) give

$$A=\frac{\mathrm{e}^{-\mathrm{M}}}{\mathrm{e}^{\mathrm{M}}+\mathrm{e}^{-\mathrm{M}}},\qquad B=\frac{\mathrm{e}^{\mathrm{M}}}{\mathrm{e}^{\mathrm{M}}+\mathrm{e}^{-\mathrm{M}}}, \tag{3.A.84}$$

so

$$\bar{c}\,(\bar{x})=\frac{\mathrm{e}^{\mathrm{M}(1-\bar{x})}+\mathrm{e}^{-\mathrm{M}(1-\bar{x})}}{\mathrm{e}^{\mathrm{M}}+\mathrm{e}^{-\mathrm{M}}}=\frac{\cosh\left(\mathrm{M}\left(1-\bar{x}\right)\right)}{\cosh\left(\mathrm{M}\right)}. \tag{3.A.85}$$

The hyperbolic cosine is defined as $\cosh(x)=\frac{1}{2}\left(\mathrm{e}^{x}+\mathrm{e}^{-x}\right)$.

We can now obtain $\langle\bar{c}\rangle=\int_0^1\bar{c}d\bar{x}$ by directly averaging Eq. (3.A.85). Instead, we integrate Eq. (3.A.79) from $x=0$ to $x=L$ and divide by L to give

$$-\bar{c}_0'=\mathrm{M}^2\langle\bar{c}\rangle, \tag{3.A.86}$$

where we used the boundary condition Eq. (3.A.81). This allows the effectiveness factor to be written as

$$\mathcal{E} = \langle \bar{c} \rangle = -\frac{\bar{c}_0'}{\mathrm{M}^2} = \frac{\tanh(\mathrm{M})}{\mathrm{M}}. \tag{3.A.87}$$

The final result can be obtained either by integration or differentiation of Eq. (3.A.85).

Performing a series expansion around $\mathrm{M} = 0$ we have $\tanh(\mathrm{M}) \approx \mathrm{M}$ for small values $\mathrm{M} \lesssim 0.4$ of the Thiele modulus. So when the reaction rate is low compared to the maximum diffusion rate, inserting this result into Eq. (3.A.87), the effectiveness factor is close to one:

$$\mathcal{E} \approx 1 \qquad (\mathrm{M} \lesssim 0.4)\,. \tag{3.A.88}$$

In this case, the concentration is approximately constant and equal to the inlet concentration throughout the pore, and the reaction rate is high throughout. See the $\mathrm{M} = 0.1$ curve of Figure 3.13 for an illustration.

For roughly $\mathrm{M} \gtrsim 4$ we have $\tanh(\mathrm{M}) \approx 1$, so that

$$\mathcal{E} \approx \frac{1}{\mathrm{M}} \qquad (\mathrm{M} \gtrsim 4)\,. \tag{3.A.89}$$

In this case, the maximum diffusion flux is insufficient to supply material to the end of the pore. This is illustrated by the curve in Figure 3.13, corresponding to $\mathrm{M} = 10$. As the reactivity increases, less volume in the pore can be reached by diffusion, resulting in a smaller fraction of the pore length being used, hence a lower effectiveness factor. The inverse dependence on the Thiele modulus in Eq. (3.A.89) can be understood as follows. Doubling the reaction rate in this regime doubles the required diffusive flux at the entrance. This results in a concentration gradient that is twice as steep so that a near-zero concentration is reached at half the distance from the pore entrance, resulting in a halving of the effectiveness factor.

To quantify this, we define a penetration depth by linearising the concentration profile near $x = 0$ and seeing at which pore depth this linearised concentration profile reaches zero. The result is a distance $-\frac{c}{c'}\big|_{x=0}$. In dimensionless notation, dividing by L, the associated active fraction of the total pore is

$$-\frac{1}{\bar{c}_0'} \approx \frac{1}{\mathrm{M}\tanh(\mathrm{M})} \xrightarrow{\mathrm{M}\gg 1} \frac{1}{\mathrm{M}}, \tag{3.A.90}$$

where we used Eq. (3.A.87). So for large M, similar to the effectiveness factor, the penetration depth also becomes inversely proportional to M. As is illustrated in Figure 3.13 the reaction rate does not immediately vanish beyond the penetration depth. It does give a rough idea of the length of the pore over which the reaction rate is significant.

3.B *Dimensionless porous electrode equations*

The governing equations, Eqs. (3.44), (3.45) and (3.46), the boundary conditions, Eqs. (3.31) and (3.32), and Eq. (3.33) are made dimensionless using the following definitions:

$$\bar{x} = \frac{x}{L},\ \bar{c} = \frac{c}{c_0},\ \bar{\eta} = \frac{|\eta|}{b},\ \bar{\imath} = \frac{i}{i_0},\ \bar{\jmath} = \frac{j_x}{j_{xL}}. \tag{3.B.91}$$

The dimensionless coordinate $\bar{x}$ and concentration $\bar{c}$ we have used already in section 3.A.3. We will again use a prime to denote a derivative with respect to $\bar{x}$, not x as in the case of dimensional quantities. Note that the non-dimensionalization of the overpotential $\bar{\eta}$ deviates from our previous use of the dimensionless potential $\bar{\phi} = F\phi/\mathcal{R}T$ since $b = \mathcal{R}T/\alpha F$, with α the charge transfer coefficient, is used as the reference potential instead of the thermal potential $\mathcal{R}T/F$.

Finally, i and j_x are the x-components of the ionic and electronic current density. We introduced dimensionless ionic and electronic current densities $\bar{\imath}$ and $\bar{\jmath}$ by dividing their extremal value $j_{xL} = i_0$, equal in magnitude to the current density of the cell j. Charge conservation $i + j_x = j_{xL}$ then becomes

$$\bar{\imath} + \bar{\jmath} = 1. \tag{3.B.92}$$

Note that, by dividing with a quantity with the same sign, $\bar{\imath}$ and $\bar{\jmath}$ both vary between 0 and 1. At the electrode front $x = 0$ there is only ionic current, so $\bar{\imath} = 1$ and $\bar{\jmath} = 0$. At the back of the electrode $x = L$ all current is converted to electronic current so that $\bar{\jmath} = 1$ and $\bar{\imath} = 0$. Additionally, at $\bar{x} = 1$ reactants cannot leave or enter so that concentration gradients vanish, resulting in the following boundary conditions:

$$\bar{\jmath} = 0 \text{ or } \bar{\imath} = 1 \qquad (x = 0), \tag{3.B.93}$$

$$\bar{\jmath} = 1 \text{ or } \bar{\imath} = 0 \text{ and } \bar{c}' = 0 \qquad (x = L). \tag{3.B.94}$$

In dimensionless notation, Ohm's law (3.45), the diffusion equation (3.44), and Tafel's equation (3.46) become, respectively

$$\bar{\eta}' = -\bar{j}_\kappa \bar{\imath} \tag{3.B.95}$$

$$\bar{c}' = -\bar{j}_D \bar{\imath} \tag{3.B.96}$$

$$\bar{j}_* \bar{\imath}' = -\bar{c} e^{\bar{\eta}} \tag{3.B.97}$$

where we introduced the following dimensionless current density magnitudes

$$\bar{j}_\kappa = \frac{j}{J_\kappa} \tag{3.B.98}$$

$$\bar{j}_D = \frac{j}{J_D} \tag{3.B.99}$$

$$\bar{j}_* = \frac{j}{J_*}. \tag{3.B.100}$$

Compared to the dimensional Eqs. (3.44)-(3.46) the right-hand side of each of these equations has a minus sign and holds not only for the anode but also for the cathode.

Instead of a dimensionless current density, we can also interpret $\bar{j}_\kappa$ as the ratio between the characteristic ohmic voltage drop jL/κ and the Tafel slope b. The inverse is sometimes referred to as the Wagner number $\mathrm{Wa} = 1/\bar{j}_\kappa = \kappa b/jL$. The number $\bar{j}_D$ divides the current density j with the current $J_D = \frac{nFDc_0}{L}$ that could be sustained by diffusion alone over a distance L.

The boundary conditions of Eq. (3.B.93) and Eq. (3.B.94), applied to Eq. (3.B.95), can equivalently be written as

$$\bar{\eta}_0' = -\bar{j}_\kappa, \tag{3.B.101}$$

$$\bar{\eta}_1' = 0. \tag{3.B.102}$$

Here, we again use a subscript 0 or 1 to denote the position $x = 0$ or 1. In the next few sections, we will consider various cases in which a simple analytical solution to this set of equations can be found. The goal will be to use these to find the relation between current density and potential losses.

In dimensionless notation Eq. (3.41) becomes

$$\mathcal{E} = \frac{1}{\bar{\imath}_0'} = \frac{\bar{j}_*}{\mathrm{e}^{\bar{\eta}_0}}, \tag{3.B.103}$$

so that

$$\bar{\eta}_0 = \ln\left(\frac{\bar{j}_*}{\mathcal{E}}\right). \tag{3.B.104}$$

3.C *Combined ohmic and diffusion limitations - exact*

We will here define $\chi \equiv \frac{\bar{j}_\kappa}{\bar{j}_D} = \frac{J_D}{J_\kappa} = \frac{nFDc_0}{b\kappa}$, which is a characteristic ratio of ohmic and diffusive effects, and is independent of current density. In case $\chi \gg 1$, ohmic limitations are much stronger than diffusive limitations. When $\chi \ll 1$, ohmic effects

can be neglected relative to diffusive effects. This number only says something about the ratio of the two effects, not their magnitudes, which are given by $\bar{j}_\kappa$ and $\bar{j}_D$, respectively.
We can combine equations (3.B.95) and (3.B.96) to give $\eta' = \chi \bar{c}'$. Integrating, using $\bar{c}_0 = 1$ gives

$$\bar{c} = 1 + \frac{\bar{\eta} - \bar{\eta}_0}{\chi}. \tag{3.C.105}$$

Differentiating Eq. (3.B.95) and eliminating $\bar{i}'$ using Eq. (3.B.97), we get

$$\frac{\bar{j}_*}{\bar{j}_\kappa} \bar{\eta}'' = \bar{c} \mathrm{e}^{\bar{\eta}}. \tag{3.C.106}$$

Using $\bar{\eta}'' = \frac{1}{2} \frac{\mathrm{d}\bar{\eta}'^2}{\mathrm{d}\bar{\eta}}$ from Eq. (3.63), we can integrate Eq. (3.C.107) over $\bar{\eta}$ from $\bar{\eta}_0$ to $\bar{\eta}_1$ to give

$$\frac{\bar{j}_*}{2\bar{j}_\kappa} \left(\bar{\eta}_1'^2 - \bar{\eta}_0'^2 \right) = \left(1 + \frac{\bar{\eta} - \bar{\eta}_0 - 1}{\chi} \right) \mathrm{e}^{\bar{\eta}} \Big|_{\bar{\eta}_0}^{\bar{\eta}_1} \to \left(\frac{-1}{\chi} \right) \mathrm{e}^{\bar{\eta}_1} - \left(1 - \frac{1}{\chi} \right) \mathrm{e}^{\bar{\eta}_0}. \tag{3.C.107}$$

In the final expression, we assumed that $\bar{c}_1 = 1 + \frac{\bar{\eta}_1 - \bar{\eta}_0}{\chi} \approx 0$. This gives $\bar{\eta}_0 - \bar{\eta}_1 \approx \chi$, which we use to write the right-hand side of Eq. (3.C.107) as $\left(-\frac{1}{\chi} \mathrm{e}^{-\chi} + \left(1 - \frac{1}{\chi} \right) \right) \mathrm{e}^{\bar{\eta}_0} = \frac{\chi - 1 - \mathrm{e}^{-\chi}}{\chi} \mathrm{e}^{\bar{\eta}_0}$. Finally, we use the boundary conditions (3.B.101) to write the left-hand side as $\frac{\bar{j}_* \bar{j}_\kappa}{2}$ to give

$$\mathrm{e}^{\bar{\eta}_0} = \frac{\chi \bar{j}_\kappa \bar{j}_* / 2}{\chi - 1 - \mathrm{e}^{-\chi}} \approx \begin{cases} \frac{\bar{j}_\kappa \bar{j}_*}{2} = \frac{j^2}{2 a j_* \kappa b} & (\chi \gg 1) \\ \bar{j}_D \bar{j}_* = \frac{j^2}{a j_* n F D c_0} & (\chi \ll 1). \end{cases} \tag{3.C.108}$$

The final expression in Eq. (3.C.108) is obtained by making a Taylor expansion $\mathrm{e}^{-\chi} \approx 1 - \chi + \chi^2/2$ to second order in $\chi \ll 1$. This result was first obtained in Ref. [2].

The physical interpretation of these results is that a proportionally smaller part of the electrode is used as the current increases. In case of diffusion limitations, the reactants will be depleted within a fraction of the electrode thickness. In the case of ohmic limitations, the ionic resistance decreases the overpotential so much that the reaction rate strongly decreases. The electrode thickness that is effectively used, therefore, shrinks. Thinner electrodes have a smaller total area and thus a smaller exchange current density ($J_* = aLj_*$). So when the current density is increased, not only does the numerator in the logarithm of Eq. (3.54) increase, but the denominator decreases as well. This gives rise to twice the normal activation losses or a doubled Tafel slope.
Inserting the polarisation relation of Eq. (3.C.108) we obtain, when $\mathcal{E} \ll 1$:

$$\mathcal{E} = 2\frac{\chi - 1 + \mathrm{e}^{-\chi}}{\chi \bar{j}_\kappa} \approx \begin{cases} 2/\bar{j}_\kappa & (\chi \gg 1) \\ 1/\bar{j}_D & (\chi \ll 1)\,. \end{cases} \tag{3.C.109}$$

In case $\chi \ll 1$, ohmic limitations can be neglected, and only diffusion limitations are considered. One of the assumptions behind Eq. (3.C.108) was that $\bar{c}_1 \ll 1$, so that Eq. (3.C.109) is valid only in case of severe diffusion limitations.

The approximation of simply adding Thiele moduli to give $1/\mathcal{E} \sim \bar{j}_D + \bar{j}_\kappa/2$, as done in section 3.4.4, is quite accurate. The relative error in the effectiveness factor compared to the exact result of Eq. (3.C.109) is only 12 % and occurs when $\chi \approx 2.7$.

Chapter 4

Batteries

This chapter introduces several fully analytical battery models. At high charge or discharge rates, the reaction zone model considers a steep reaction front that slowly moves through the battery electrode. At low discharge rates, slow diffusion into the solid active material can allow using a single particle model. We briefly consider the general structure of modern battery models, which contain both the reaction zone and single particle model as its limits. Finally, we consider a solution to the porous electrode equations for a binary electrolyte.

4.1 Introduction

For short-term storage of electricity, for example in electronics and electric vehicles, batteries are a popular choice. With the advent of renewable energy, they may also play a role in mitigating the problem of intermittency of renewable sources, which requires highly efficient storage of electricity over the scale of hours or shorter.

4.1.1 *Types of batteries **

Historically, the word battery refers to a series of at least a few electrochemical cells, typically put in series to obtain large voltages. While some batteries still contain several cells, the word presently can also refer to a single electrochemical cell. For example, common 1.5 V batteries usually consist of a single cell, while a nine-volt *block battery* consists of six such batteries in series.

1. **Primary batteries**: These batteries are for one-time use. They are not rechargeable. In other words, the electrochemical reactions involved are not reversible. An example is the ubiquitous AA *alkaline battery*.
2. **Secondary batteries:** These are rechargeable and can be used for many cycles. An example is the *lithium-ion battery*, commonly used in mobile phones and laptops.